

NOAA Technical Report NESDIS 119

Calibration and Validation of NOAA-18 Instruments



Washington, D.C.
August 2005

U.S. DEPARTMENT OF COMMERCE
National Oceanic and Atmospheric Administration
National Environmental Satellite, Data, and Information Service

NOAA TECHNICAL REPORTS

National Environmental Satellite, Data, and Information Service

The National Environmental Satellite, Data, and Information Service (NESDIS) manages the Nation's civil Earth-observing satellite systems, as well as global national data bases for meteorology, oceanography, geophysics, and solar-terrestrial sciences. From these sources, it develops and disseminates environmental data and information products critical to the protection of life and property, national defense, the national economy, energy development and distribution, global food supplies, and the development of natural resources.

Publication in the NOAA Technical Report series does not preclude later publication in scientific journals in expanded or modified form. The NESDIS series of NOAA Technical Reports is a continuation of the former NESS and EDIS series of NOAA Technical Reports and the NESC and EDS series of Environmental Science Services Administration (ESSA) Technical Reports.

A limited number of copies are available by contacting Jessica Pejsa, NOAA/NESDIS, E/RA3, 5200 Auth Road, Room 601, Camp Springs, Maryland 20746, (301) 763-8184 x115. Copies can also be ordered from the National Technical Information Service (NTIS), U.S. Department of Commerce, Sills Bldg., 5285 Port Royal Road, Springfield, VA 22161, (703) 487-4650 (prices on request for paper copies or microfiche, please refer to PB number when ordering). A partial listing of more recent reports appear below:

- NESDIS 88 Analytical Model of Refraction in a Moist Polytrropic Atmosphere for Space and Ground-Based GPS Applications. Simon Rosenfeld, April 1997.
- NESDIS 89 A GOES Image Quality Analysis System for the NOAA/NESDIS Satellite Operations Control Center. Donald H. Hillger and Peter J. Celone, December 1997.
- NESDIS 90 Automated Satellite-Based Estimates of Precipitation: An Assessment of Accuracy. Michael A. Fortune, June 1998.
- NESDIS 91 Aliasing of Satellite Altimeter Data in Exact-Repeat Sampling Mode: Analytic Formulas for the Mid-Point Grid. Chang-Kou Tai, March 1999.
- NESDIS 92 Calibration of the Advanced Microwave Sounding Unit-A Radiometers for NOAA-L and NOAA-M. Tsan Mo, May 1999.
- NESDIS 93 GOES Imager and Sounder Calibration, Scaling, and Image Quality. Donald W. Hillger, June 1999.
- NESDIS 94 MSU Antenna Pattern Data. Tsan Mo, Thomas J. Kleespies, and J. Philip Green, March 2000.
- NESDIS 95 Preliminary Findings from the Geostationary Interferometer Observing System Simulation Experiments (OSSE). Bob Aune, Paul Menzel, Jonathan Thom, Gail Bayler, Allen Huang, and Paolo Antonelli, June 2000.
- NESDIS 96 Hydrography of the Ross Sea Continental Shelf During the Roaverrs, NBP96-06, Cruise December 1996 - January 1997. Michael L. Van Woert, David Pryor, Eric Quiroz, Richard Slonaker, and William Stone, September 2000.
- NESDIS 97 Hydrography of the Ross Sea Continental Shelf During the Roaverrs, NBP97-09, Cruise December 1997 - January 1998. Michael L. Van Woert, Lou Gordon, Jackie Grebmeier, Randal Holmbeck, Thomas Henderson, and William F. Van Woert, September 2000.

NOAA Technical Report NESDIS 119

Calibration and Validation of NOAA-18 Instruments



Editors:
Fuzhong Weng and Tsan Mo
/NESDIS/ORA
52 NOAA 00 Auth Road
Camp Springs, MD 20746

Washington, DC
December 2005

U.S. DEPARTMENT OF COMMERCE

Carlos M. Gutierrez, Secretary

National Oceanic and Atmospheric Administration

Vice Admiral Conrad C. Lautenbacher, Jr., U.S. Navy (Ret.), Under Secretary

National Environmental Satellite, Data, and Information Service

Gregory W. Withee, Assistant Administrator

TABLE OF CONTENTS

Preface

Our Team

1. NOAA-18 HIRS ON-ORBIT VERIFICATION.....	5
<i>by Changyong Cao</i>	
2. NOAA-18 AMSU-A ON-ORBIT VERIFICATION.....	11
<i>by Tsan Mo</i>	
3. NOAA-18 MHS ORBIT VERIFICATION	20
<i>by Tsan Mo</i>	
4. NOAA-18 AVHRR ON-ORBIT VERIFICATION	29
<i>by Jerry Sullivan and Xiangqian Wu</i>	
5. NOAA-18 SBUV/2 On-Orbit Verification	35
<i>by Larry Flynn</i>	
6. NOAA-18 Instruments On-orbit Data: Geo-location, Navigation and Asymmetry	37
<i>By Thomas Kleespies</i>	
Appendix	48
<i>Presentations</i>	

PREFACE

To perform the NOAA-18 instrument on-orbit verification, NOAA/NESDIS/Office of Research and Applications (ORA) organized a calibration and validation (cal/val) team including the members from all ORA divisions, Joint Center for Satellite Data Assimilation (JCSDA), and other NWP centers. Our strong coordination and integrated research have led timely and accurate diagnosis of all possible factors affecting the instrument on-orbit performances. The anomalies associated with NOAA-18 HIRS/4 noise was first detected from ORA cal/val team and later confirmed from several independent observations. Our team provided many root cause analysis for the HIRS noise issues and have led further investigations by NOAA-18 instrument vendor, NOAA-18 program manager and others. Unlike the past cal/val activities which primarily involve the works from a few ORA calibration scientists, our NOAA-18 cal/val activities have been expanded to include following tasks:

- Monitor and quantify instrument noise through analyzing calibration target counts and channel space view measurements
- Assess instrument geolocation biases and co-registration and provide recommended solutions for satellite roll and pitch adjustments
- Characterize other systematic biases in radiance through rigorous forward modeling and inter-satellite calibrations
- Provide initial demonstration and assessments of NOAA-18 data for improving numerical weather prediction
- Validate product algorithms (e.g. ATOVS and MSPPS, TOAST, UV index, NDVI, SST, AOD) for transition into operation
- Communicate with NOAA-18 OV team, instrument vendors and users with timeliness diagnostics of instrument performances and provide root cause analyses

Most of these activities have directly supported the tests required in NOAA-N OV test plan. However, we also make sure our calibration results such as NEDT, bias correction algorithm and other quality control information timely delivered to NWP centers for their best preparation of uses of NOAA-18 data in operational data assimilation systems. The key findings from our cal/val results are

- Despite the significant noise drop since launch, some longwave channels of the NOAA-18/HIRS do not meet the NEDN specification. Meanwhile, the noise at its long wave channels continues fluctuating. HIRS channel 1 noise can not be quantified because of saturation of its space view count. To provide sustainable monitoring and analysis of HIRS noise, ORA has developed a website tool for HIRS noise trending analysis (<http://www.orbit.nesdis.noaa.gov/smcd/spb/multisensor/hirs/>). We are planning to expand this capability for other instruments. Overall AMSU-A calibration is good with quality control flags being properly set whenever there is anomaly in the data stream. On-orbit AMSU-A NEAT at all channels meets specification
- Overall MHS calibration is good with quality control flags being properly set whenever anomaly occurs. The NOAA-18 MHS NEAT for each channel is better than that of AMSU-B
- AMSU-A sounding channels continue displaying cross-track asymmetry in radiance. Several

antenna pattern correction algorithms were tested in order to reduce the asymmetry. It is found that for NOAA-18 AMSU-A, the antenna pattern correction coefficients measured from beam position 30 provide an optimal bias correction with a result of the smallest asymmetry.

- Initial post-launch calibration update for AVHRR solar channels was implemented. Results seem reasonable but expected to improve with time.
- The Met Office, UK have reported large positive impacts on NWP forecast scores from assimilating AMSU-A and MHS measurements.

The OV test results are summarized in Table 1 and details are give in individual articles. Appendix lists some of the presentations, which were presented at an ORA Cal/Val Work Group Meeting on August 9, 2005. If you have any technical questions, please contact Fuzhong.Weng@noaa.gov or

Dr. Fuzhong Weng, Chief
Sensor Physics Branch
Satellite Meteorology and Climatology Division
Center for Satellite Applications and Research
NOAA/NESDIS
5200 Auth Road, Room 712
Camp Springs, MD 20746
USA

Table 1. NOAA-18 On-orbit Verification Conducted by NOAA Scientists.

Task #	Task Name	Status	Key Results	Principal Investigators
AM1005/2005	Instrument trending	Completed	stable	Mo
AM1007/2007	Determination of optimal space view	Completed	A1 @ SV1, A2 @SV2	Mo
AM1008/2008	noise measurements-all channels	Completed	Meet the spec	Mo
AM1009	satellite to satellite comparison	Completed	some difference	Mo
AM1010/2010	BB PRT temperature accuracy	Completed	meet spec	Mo
AM1011	Earth-science bias characterization	Completed	A1 cross-track asymmetry	Weng, Kleespies
AM1012/2012	Channel co-registration	Completed	Along & cross track errors are quantified	Kleespies, Bennartz, Chalfant
MHS010	Lunar contamination in space view	on-going	Capture some signals	Mo
MHS011	Channel registration	Completed	Along & cross track errors are quantified	Chalfant, Kleespies
MHS013	MHS/AMSU-A 89 GHz comparison	Completed	Generally bias < 0.5K, nearly 1.0K in limb	Boukabara
MHS014	Earth-view bias characterizations	Completed	Small particular cross-track asymmetry	Kleespies
MHS016	MHS radiometric comparison with AMSU-B	Completed	noticeable difference at Ch17, 20	Reale, Ferraro, Kleespies
SBUA01	Range 3 Cathode/Anode	Completed	Consistent Change	SSAI
SBU012	Diffuser and Solar	Partially	Significant	SSAI
SBU007	Wavelength Scale	Completed	Small Shift	SSAI
SBUA05	OOBR estimation from position mode	Partially	Correction Needed	Flynn/SSAI
SBUA11	NOAA-16 Comparison	Partially	Differences noted	Kondragunta
AVH005	space clamp noise and stability	Completed	stable	Sullivan
AVH010	NEDT/Dynamic range - channel 3B,4,5	Completed	meet the spec	Sullivan
AVH011	instrument stability - channels 3B,4,5	Completed	stable	Sullivan
AVH014	operational calibration	Completed	ch1,2,3A	Wu/Sullivan
AVH018	Detection of land-sea boundary	Completed	nearly one pixel offset	Sullivan
AVH019	NOAA-18, 17, and 16 comparison	Completed	NDVI/SST/Aerosols	Tarpley/Ignatov
AVH022	striping evaluation	Completed	No striping	Wu/Sullivan
HIR011	NEDN - IR channels	Completed	Out of spec for most chs	Cao
HIR012	Instrument stability	Completed	noise fluctuated	Cao
HIR013	instrument trending	Completed	new website	Cao
HIR014	Detection of land-sea boundary	Completed	no geolocation errors	Chalfant/Cao
HIR015	Satellite-to-satellite comparison	on-going	Some biases	Reale

Our Team

Mitch Goldberg: ORA/SMCD Division Chief, - Management and Technical Oversight
Fuzhong Weng: ORA/SMCD/Sensor Physics Branch Chief and NOAA-18 cal/val team leader, instrument asymmetry and microwave products and algorithms, radiance bias assessments for NWP model applications
Changyong Cao: HIRS instrument calibration
Fred Wu: AVHRR VIS/NIR instrument calibration
Tsan Mo: AMSU/MHS instrument calibration
Jerry Sullivan: AVHRR thermal channel calibration/ NDVI validation
Tony Reale: HIRS/AMSU/MHS sounding channel/products validation
Mike Chalfant: HIRS/AMSU/MHS sounding channel/products validation /geolocation
Ralph Ferraro: AMSU/MHS window channels/MSPPS products validation
Larry Flynn: SBUV product validation
Tom Kleespies: AMSU on-orbit verification
Hank Drahos: Sounding product validation
Dan Tarpley: AVHRR product NDVI monitoring
John LeMarshall (JCSDA): Impacts assessments of NOAA-18 data for NWP applications
Stephen English (UK): tests of direct readout data and NWP impacts demonstration
Alex Ignatov: AVHRR SST and aerosol products
Ninghai Sun: Cal/val IT supports

1. NOAA-18 HIRS ON-ORBIT VERIFICATION

by Changyong Cao

1.1. NEDN Monitoring –IR channels

Plots of the NEDN of each IR channel during the OV period are used to monitor its stability over time. IDL software was developed for this test. An online instrument performance trending system is also developed for NOAA-18/HIRS and is updated daily. The website is at:

<http://www.orbit.nesdis.noaa.gov/smcd/spb/multisensor/hirs/>.

Channel	Specified NEdN	ITT Goal NEdN*	15° Baseplate NEdN for H303*
1	3.0	0.75	2.085
2	0.67	0.25	0.262
3	0.50	0.25	0.165
4	0.31	0.2	0.080
5	0.21	0.2	0.062
6	0.24	0.2	0.067
7	0.20	0.2	0.035
8	0.10	0.1	0.015
9	0.15	0.15	0.024
10	0.15	0.1	0.034
11	0.20	0.2	0.020
12	0.20	0.07	0.026
13	0.006	0.002	0.001
14	0.003	0.002	0.001
15	0.004	0.002	0.001
16	0.004	0.002	0.001
17	0.002	0.002	0.001
18	0.002	0.002	0.001
19	0.001	0.001	0.001

* For information only

The HIRS H305 instrument NEDNs for all shortwave IR channels met the specification. However, most longwave channels failed to meet the specification, specifically:

- 1). Shortly after launch, it was found that the noise was 4-5 times of the specification for most longwave channels. The noise dropped exponentially within a few months and several channels (such as ch 3, 8, 12) began to meet the specification by early September.
- 2). The noise increased significantly starting September 21, 2005, possibly triggered by a vibration originated from the solar array slew. As of October 3, 2005, all longwave channels do not meet the NEDN specification. Also, crosstrack striping are clearly visible on the images and the longwave channels cannot be used for product generation.
- 3). Shortly after launch, channel 1 spaceview counts drifted out of the dynamic range and therefore this channel cannot be calibrated.

(4). Weekly telecons have been held to investigate the HIRS/NOAA-18 noise problem. A technical interchange meeting was also held at ITT on September 29, 2005. Many possibilities have been ruled out but the root cause for the noise has yet to be determined.

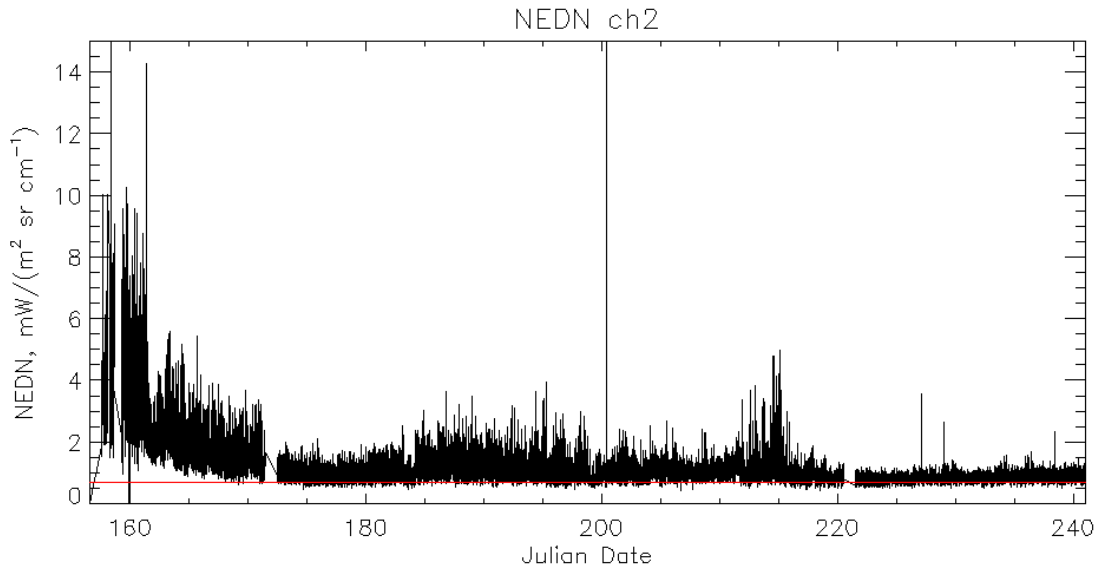


Figure 1. HIRS/NOAA-18 noise do not meet the instrument specification, despite the significant drop since launch. NEDN for each calibration cycle for channel 2 is shown here. Other longwave channels similar. Red line represents the instrument specification for the channel.

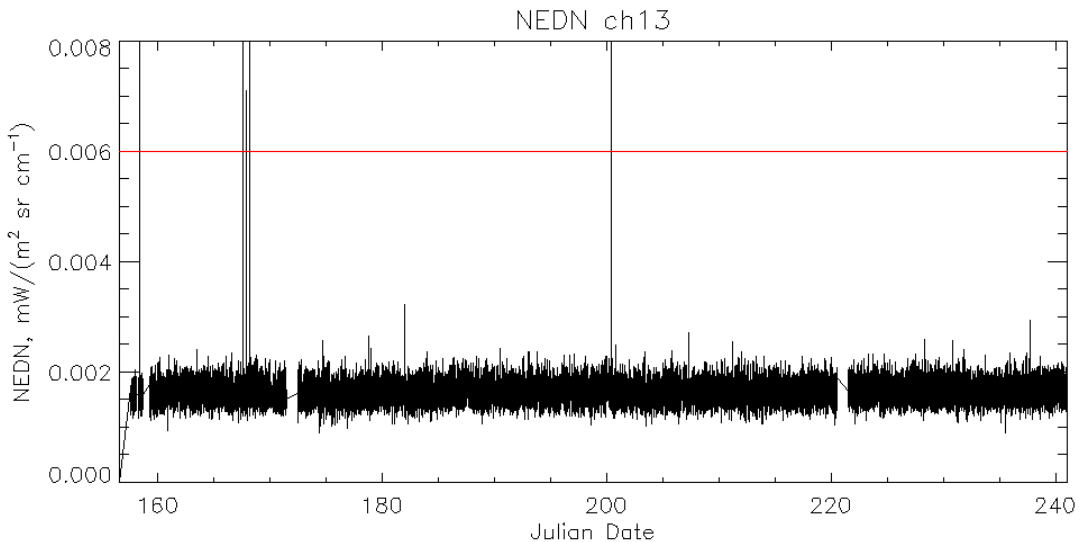


Figure 2. HIRS/NOAA-18 shortwave channel noise meet the instrument specification. Every calibration cycle is included in the figure here. The red line represents the NEDN specification for the channel. Channel 13 NEDN shown here, and other channels similar.

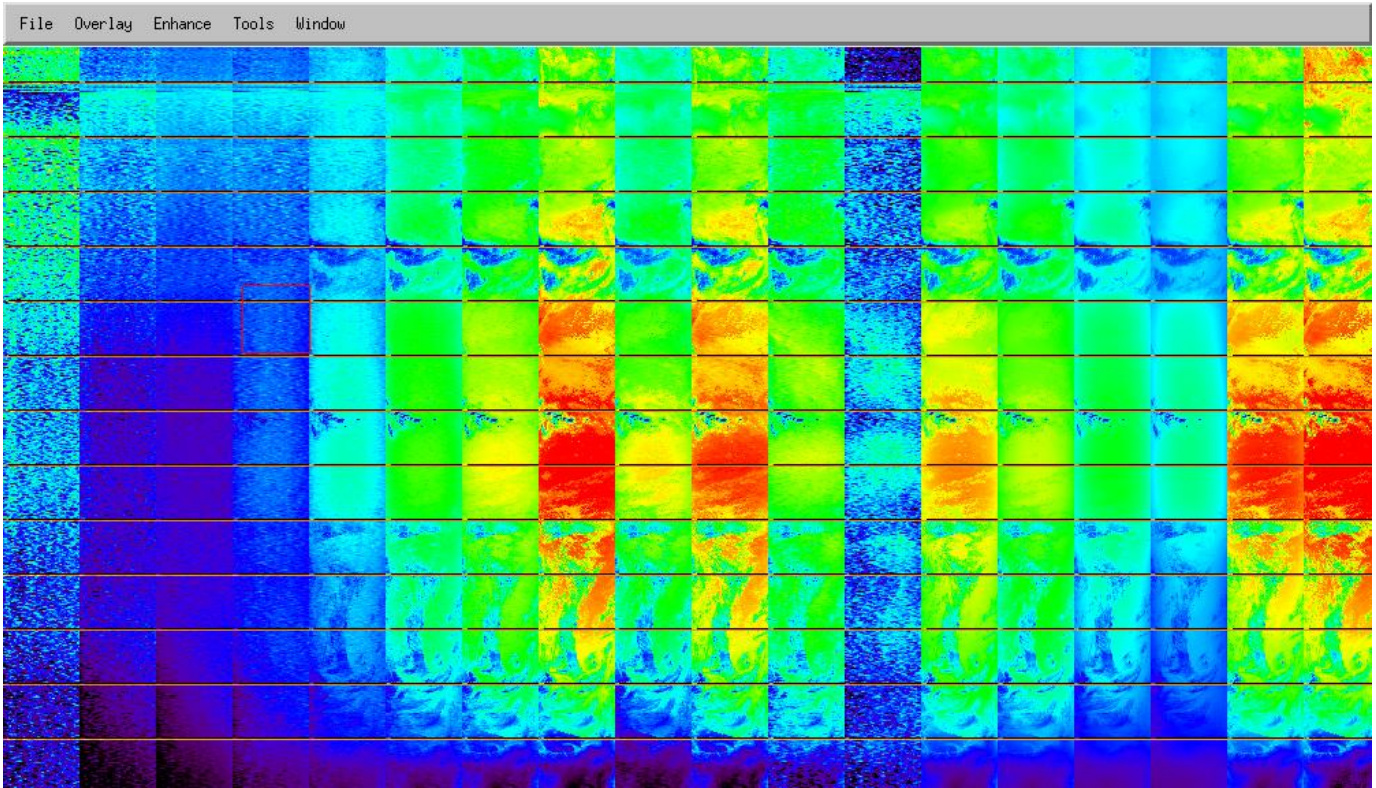


Figure 3. Example orbit of HIRS/NOAA-18 data. All channels are shown here. Long-wave channels do not meet the NEDN specification. Note the large noise in the cold channels sensing the upper atmosphere and water vapor (ch12). Sample orbit taken from June 7, 2005.

After several months of investigation, a general consensus was reached that the HIRS/NOAA-18 (Model H305) is extremely sensitive to both external and internal vibration-induced disturbances. It is possible that this high sensitivity is only specific to this model H305, but analysis also shows that there may be design issues with the HIRS/4 series with a 10 km resolution (which required several design changes to the previous model). ITT and the government team are working hard to find the “root cause” of the noise problem.

Currently the HIRS/NOAA-18 long-wave channels are very noisy and the data from several channels cannot be used in the operations. While it is possible that the noise may decrease when it stabilizes as it occurred previously, there are considerable risks in relying on data from this instrument for operational use. It is recommended that the impact on operations should be assessed and possibly alternative solutions should be considered. It is noted that if the root cause is traced to the optical design, it may also introduce uncertainties for other HIRS/4 models on future spacecrafts.

1.2. Instrument Stability

Instrument stability is monitored as calibration curve (slope and intercept) behavior for channels 1-19. Slopes and intercepts for both daily averages and sample orbits were plotted to examine the stability during the OV period. IDL software was developed for this test. In addition, an online trending system is developed to monitor the changes. Samples of level 1b data from day 160 to day 240 were used.

Despite the large noise in the long-wave channels, the slope and intercepts are relatively stable for both the long-wave and shortwave channels of HIRS/NOAA-18. A small downward trend is observed in the shortwave channels slopes, probably related to instrument degradation over time.

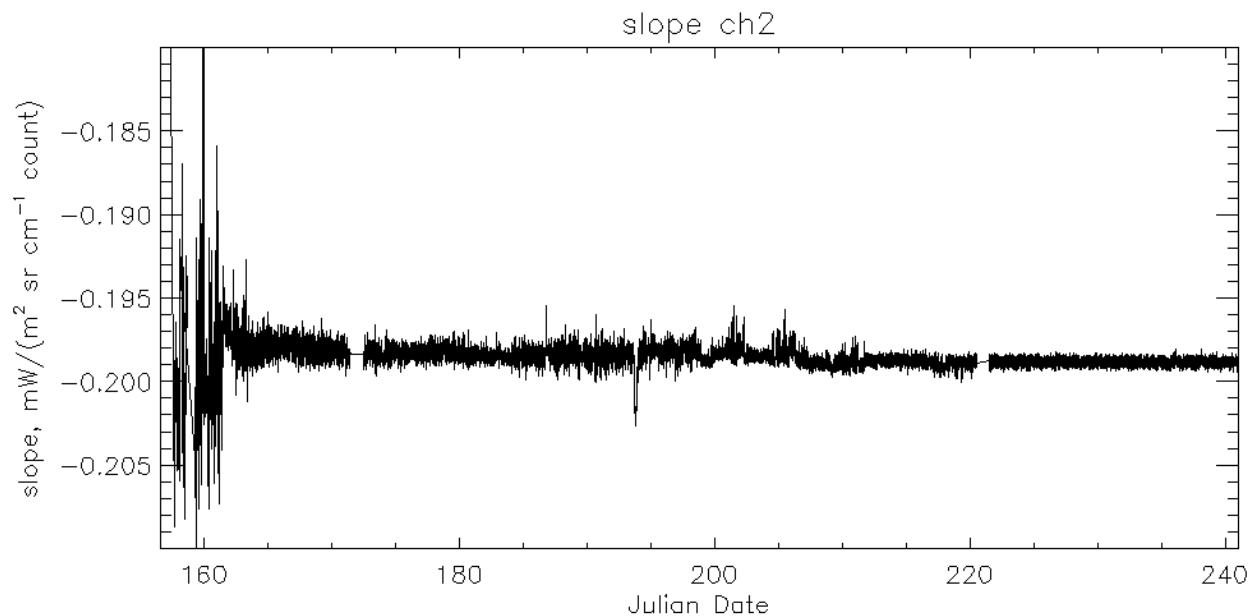


Figure 4. Despite the large noise, the slopes for the long-wave channels are relatively stable. The stability improved as the noise decreased. Channel 2 slope is shown here, and other channels are similar.

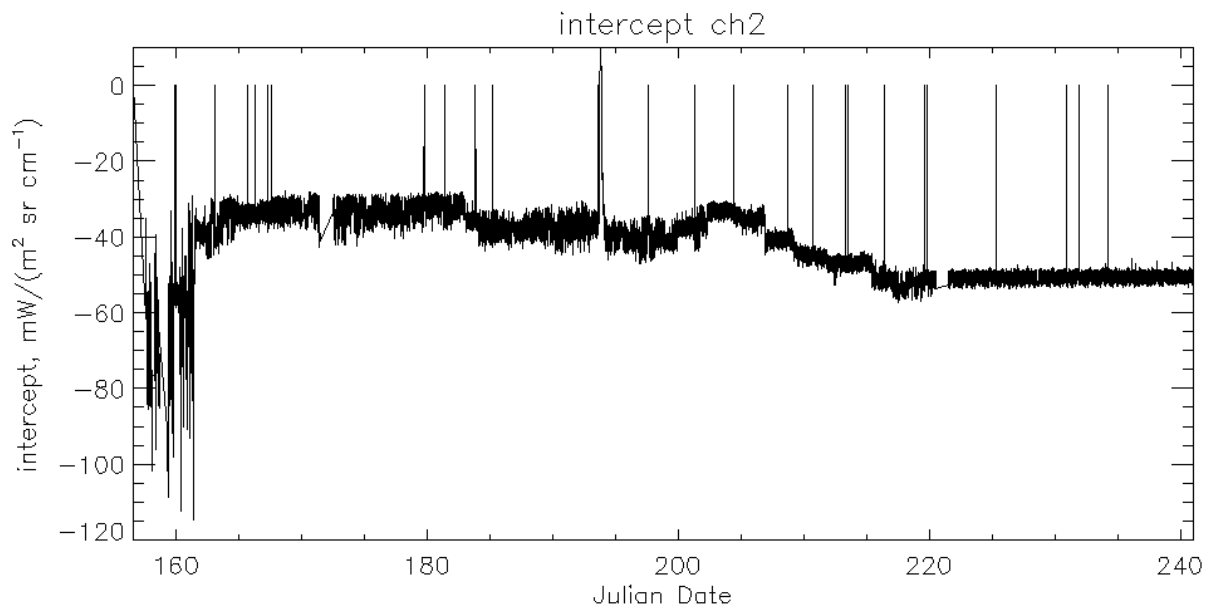


Figure 5. The intercept represents the change in the self-emission of the instrument. During the OV period, the intercept is relatively stable. The stability improved over time as the noise decreased. Intercept for channel 2 for all calibration cycles are shown here. Other channels are similar.

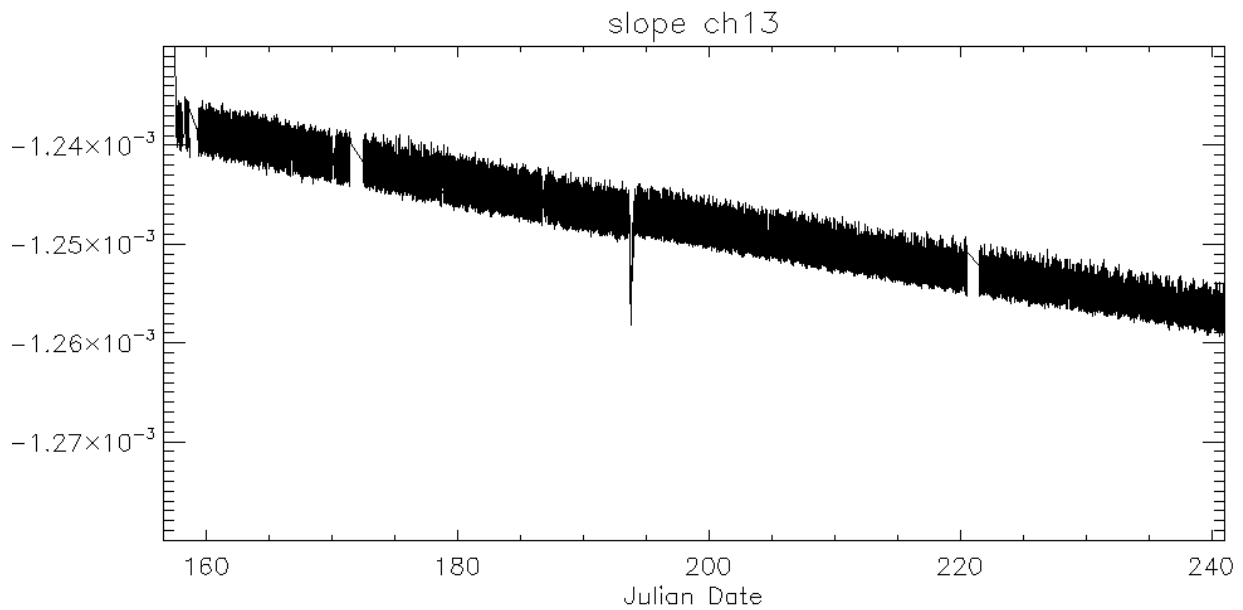


Figure 6. The slopes for the short wave channels are stable. The downward trend is probably related to degradation over time, which has been seen for previous instruments.

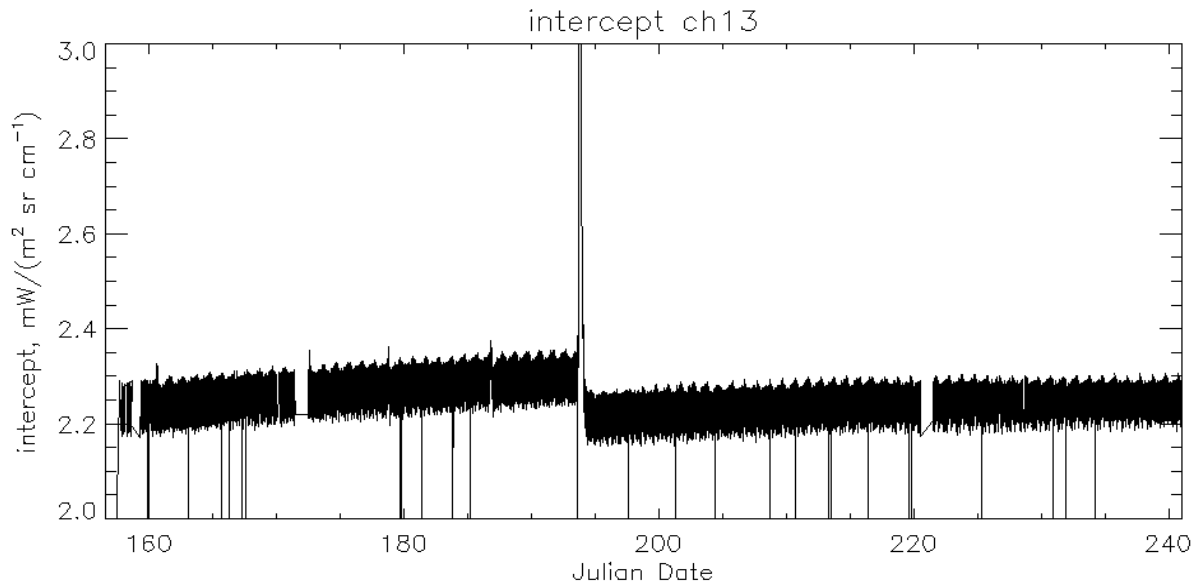


Figure 7. The intercept for the shortwave channels are stable. The spike around day 194 is caused by the test of filter wheel in high power mode for noise diagnosis. Intercept for channel 13 for all calibration cycles are shown here. Other channels are similar.

1.3. Major Navigation Errors

High resolution digital map is overlaid on HIRS window channel images to check for major navigation errors (> 1 FOV). The HIRS/NOAA-18 nadir positions were independently predicted with SGP4 orbital perturbation model using the same timing information embedded in the level 1b data. The predicted latitude/longitude were compared with those of the nadir pixels in the level 1b data. The results show that the distance between the level 1b and the predicted locations vary between 0 -3 KM over an orbit. In addition, the HIRS images are overlaid with digital maps to check geolocation accuracy. The results show that there are no major displacements in the HIRS navigation.

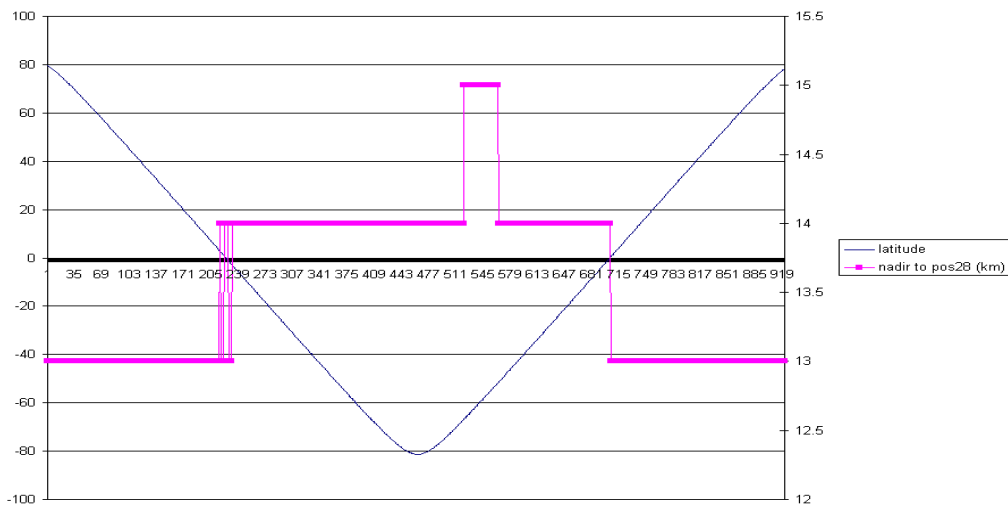


Figure 8. Distances between independently predicted and level 1b nadir positions vary between 0 -3 KM, suggesting that the geolocation error is small.

2. NOAA-18 AMSU-A ON-ORBIT VERIFICATION *by Tsan Mo*

The NOAA-18 AMSU-A On-orbit Verification was performed at the NOAA Office of Research and Applications (ORA). A systematic post-launch calibration and validation (Cal/Val) of the AMSU-A instrument performances were conducted with on-orbit data. The long-term trends of the radiometric counts from the cold space and warm targets, channel gains, NE Δ T, and the housekeeping sensors and are monitored for checking the instrument performances. Some sample results are presented in the following.

In addition, the angular distributions of the observed brightness temperatures over the Libyan Desert are also employed for evaluation of the instrument performance. The results from both NOAA-16 and NOAA-18 measurements are presented for comparison. The AMSU-A is the first satellite borne instrument that has provided good measurements of angular distributions of brightness temperatures over global scenes. Observed brightness temperatures over selected areas (e.g., the Libyan Desert) have been used for evaluation of the instrument performance¹. The establishment of a land calibration target is an important addition to the few tools available to date for calibration and validation of space-borne microwave instruments.

Figure 1 shows the long term trending of radiometric cold counts starting from May 30 to October 1, 2005. Each data point represents an averaged value over an orbit of data. There are some elevated values at channel 15 from day 210 to 260. Similar elevated values are also observed in the warm counts (see Fig. 2). The cause of these elevated values in the calibrations is unknown at the present time and its impact on the measured brightness temperatures remains to be determined. Figure 2 presents the long term trending of radiometric warm counts. The trending of channel gains is shown in Figure 3 whereas that of NE Δ T is displayed in Figure 4. The trending of antenna motor temperature and current for both AMSU-A1 and AMSU-A2 is given in Figure 5 which also shows the temperature and current of the AMSU-A2 compensator motor. The antenna pointing accuracy was selectively checked at the beam positions #1, 15, 30, cold and warm calibration positions, respectively. The results are shown in Figure 6. The nominal readings of position counts are also listed in plots. The AMSU-A specification allows ± 10 counts of the position readings from the nominal values. The Cold Calibration position reading does not meet the specification. According to Northrop Grumman, the nominal value for this position should be 741 instead of 714 (as a typo in the AMSU-A Calibration Log Book). The angular distributions of NOAA-16 and NOAA-18 AMSU-A brightness temperatures observed over Libyan Desert at the 4 window channels are shown in Figure 7. The AMSU-A asymmetries were corrected by the antenna pattern correction. In Figure 7, the angular distributions of observed brightness temperatures from the two satellites are compared. The measured brightness temperatures are approximately the same. The NE Δ T values of individual channels for both pre-launch and on-orbit were calculated and the results are shown in Figure 8.

Overall, the NOAA-18 AMSU-A calibration is good with quality control flags set properly whenever there is any anomaly in the data stream. The NE Δ T values calculated from the on-orbit data meet the specification. The Cal/Val of The NOAA-18 AMSU-A is considered successful.

¹ Tsan Mo, "A study of the NOAA 16 AMSU-A brightness temperatures observed over Libyan Desert," J. Geophys. Res. 107, D14, 10.1029/2001JD001158, 2002.

NOAA-18 AMSU-A CAL/VAL: Orbital Mean Space Counts

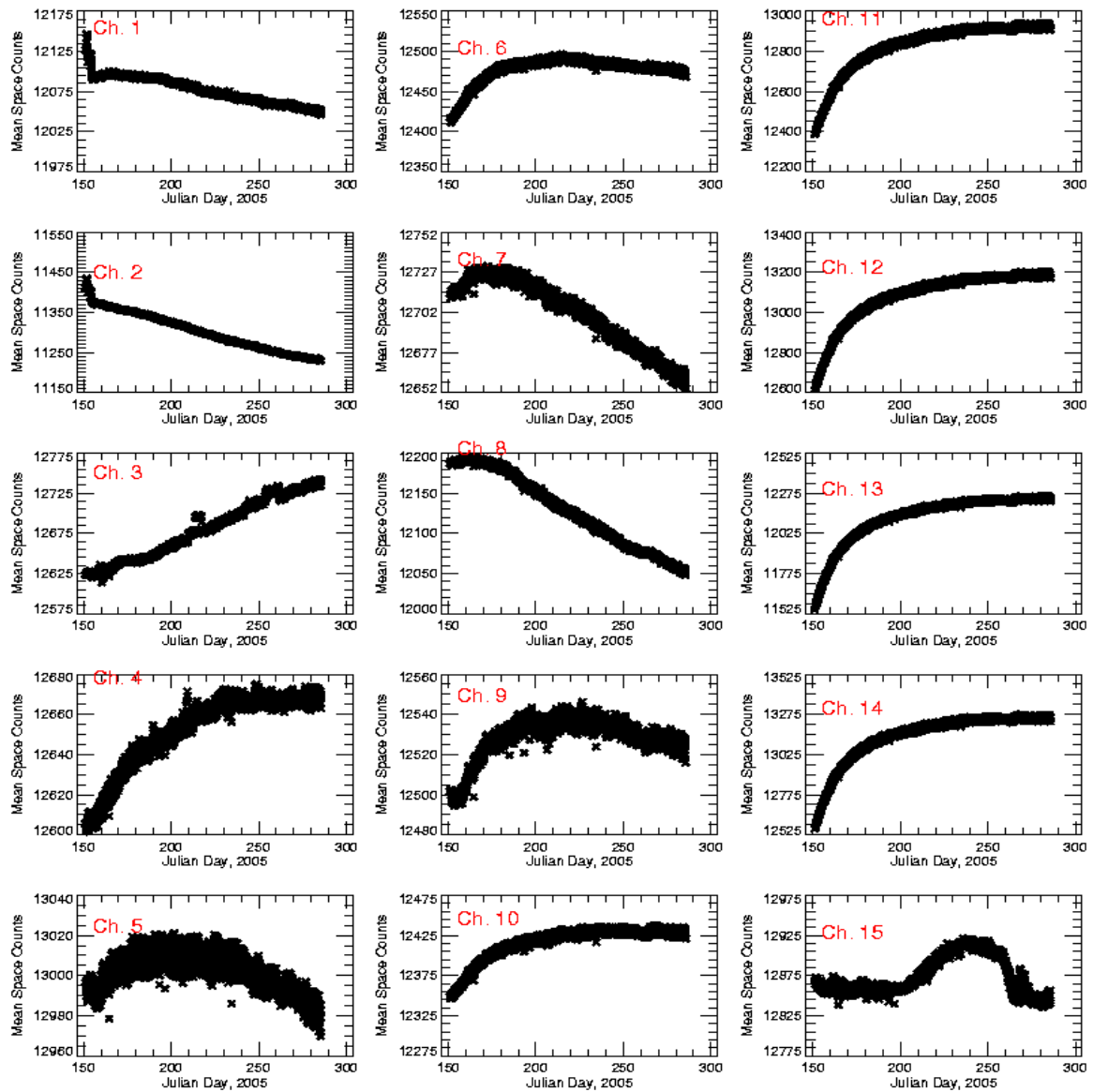


Figure 1. NOAA-18 AMSU-A: Long term trending of radiometric cold counts. Note the elevated values at channel 15 from day 210 to 260.

NOAA-18 AMSU-A CAL/VAL: Orbital Mean Warm Counts

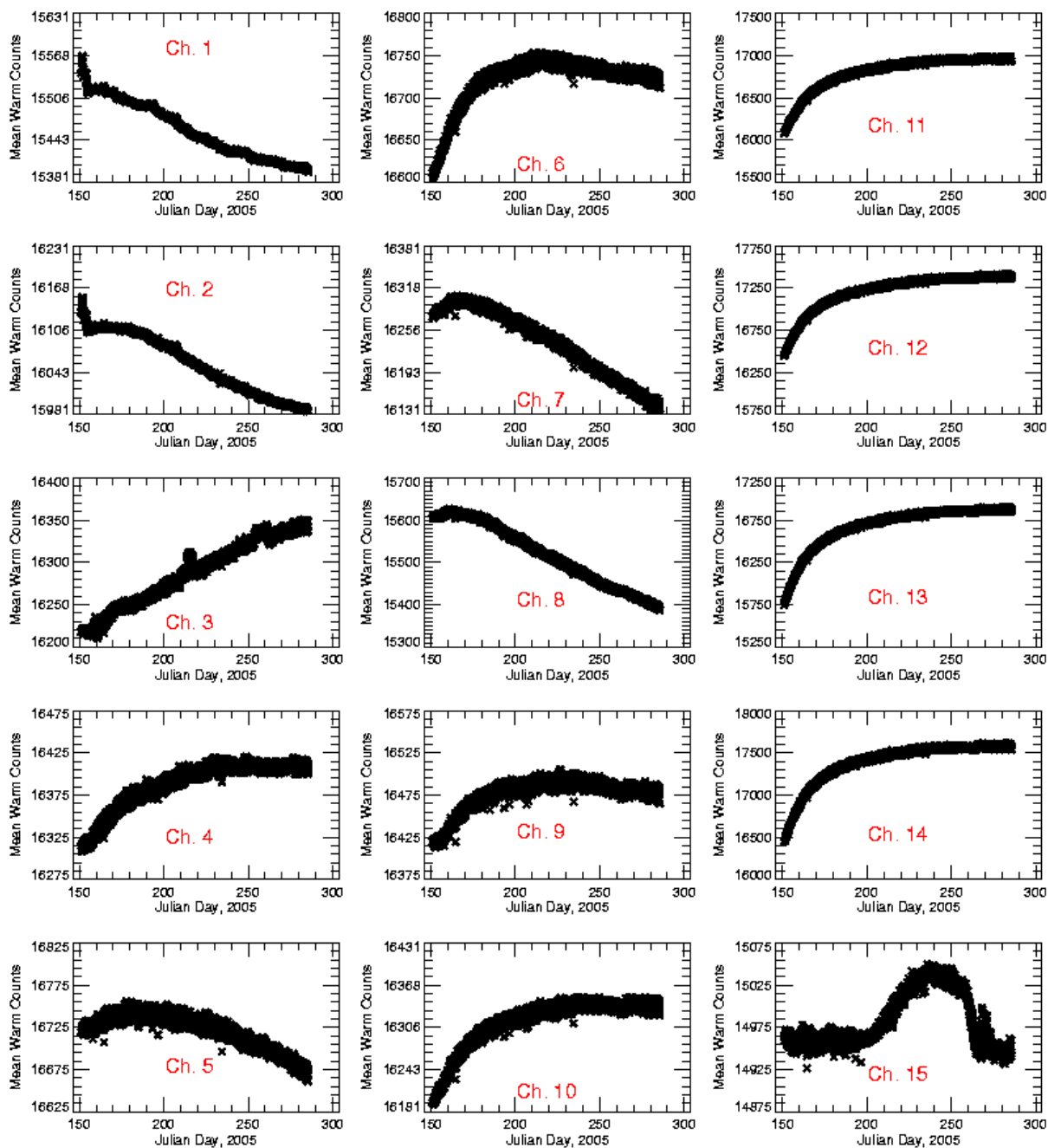


Figure 2. NOAA-18 AMSU-A: Long term trending of radiometric warm counts. Note the elevated values at channel 15 from day 210 to 260.

NOAA-18 AMSU-A CAL/VAL: Orbital Mean Gain

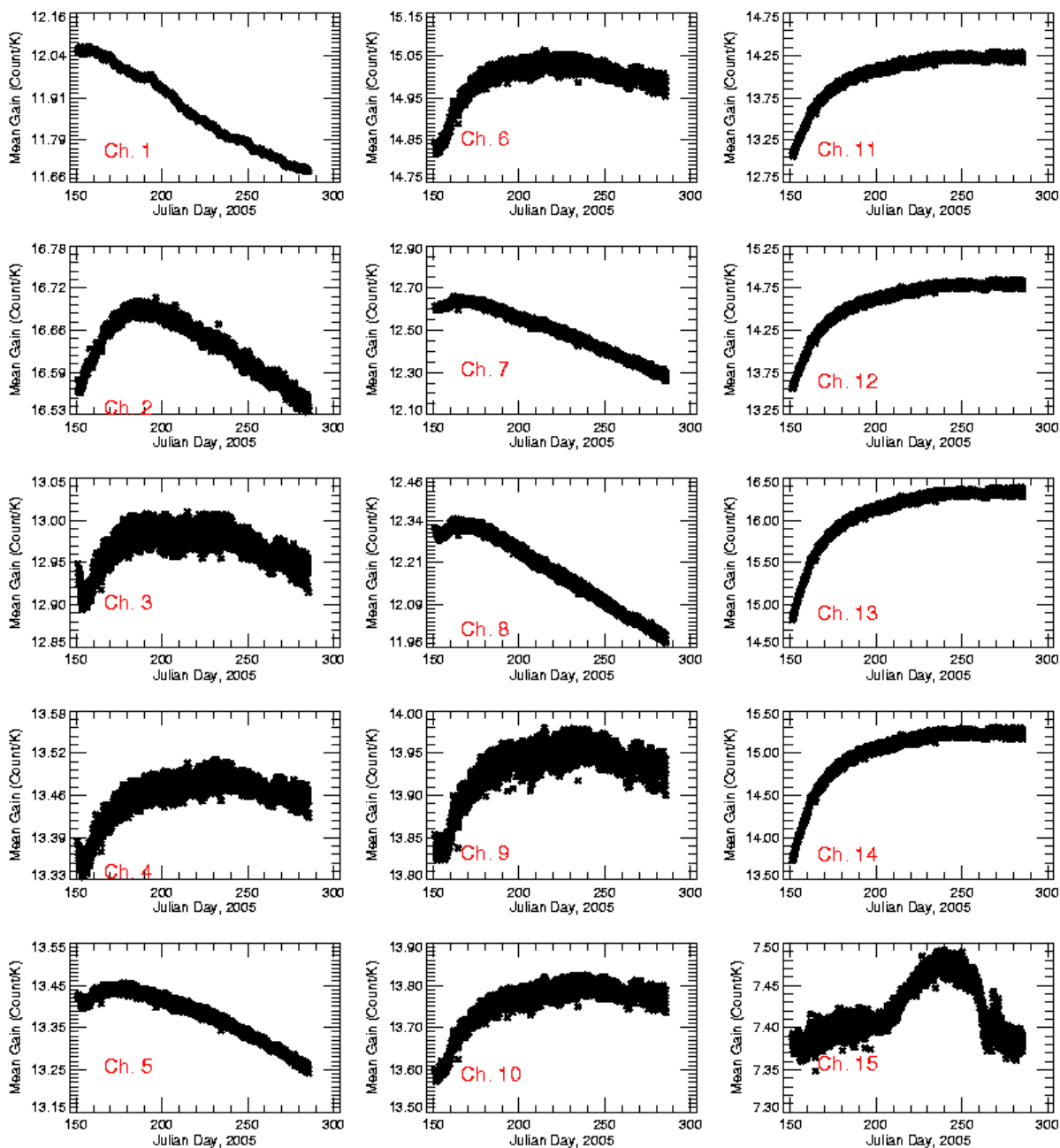


Figure 3. NOAA-18 AMSU-A: Long term trending of channel gain. Note the elevated values at channel 15 from day 210 to 260.

NOAA-18 AMSU-A CAL/VAL: NEAT

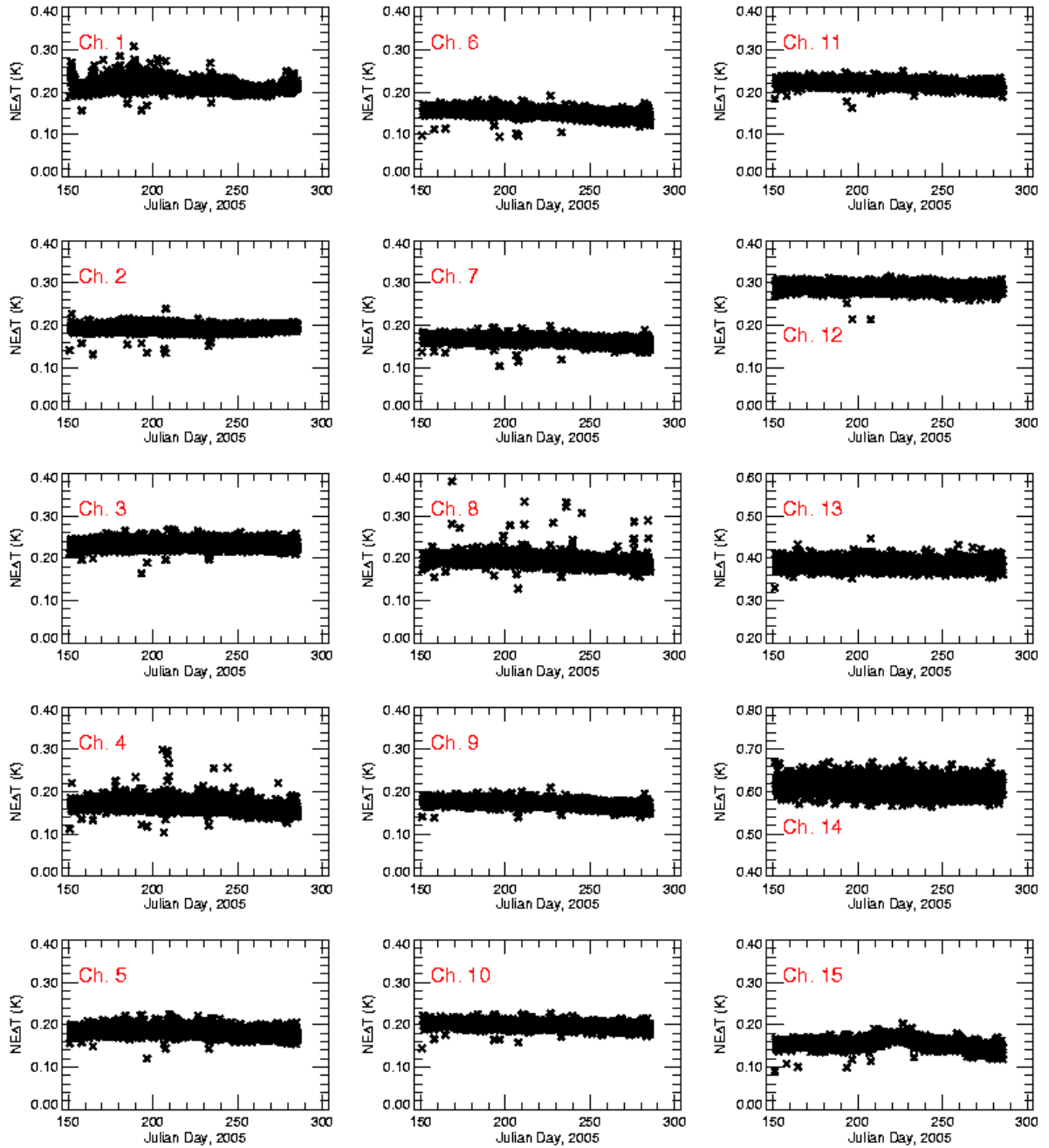


Figure 4. NOAA-18 AMSU-A: Long term trending of NEAT.

NOAA-18 AMSU-A CAL/VAL: Analog Telemetry

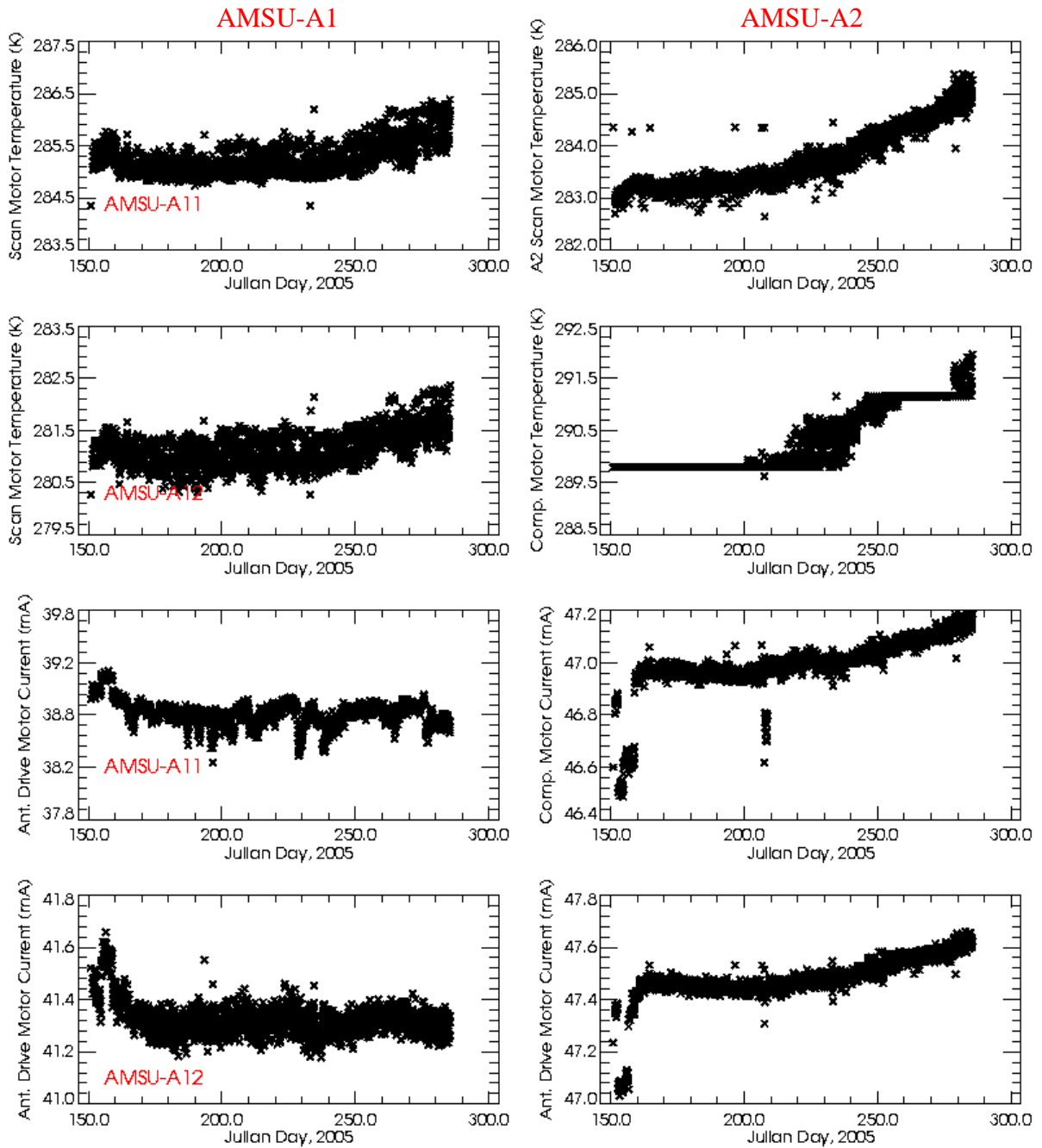


Figure 5. NOAA-18 AMSU-A: Long term trending of antenna motor temperatures and currents.

Start: NSS.AMAX.NN.D05174.S0750.E0945.B0047778.GC
 End: NSS.AMAX.NN.D05174.S0750.E0945.B0047778.GC

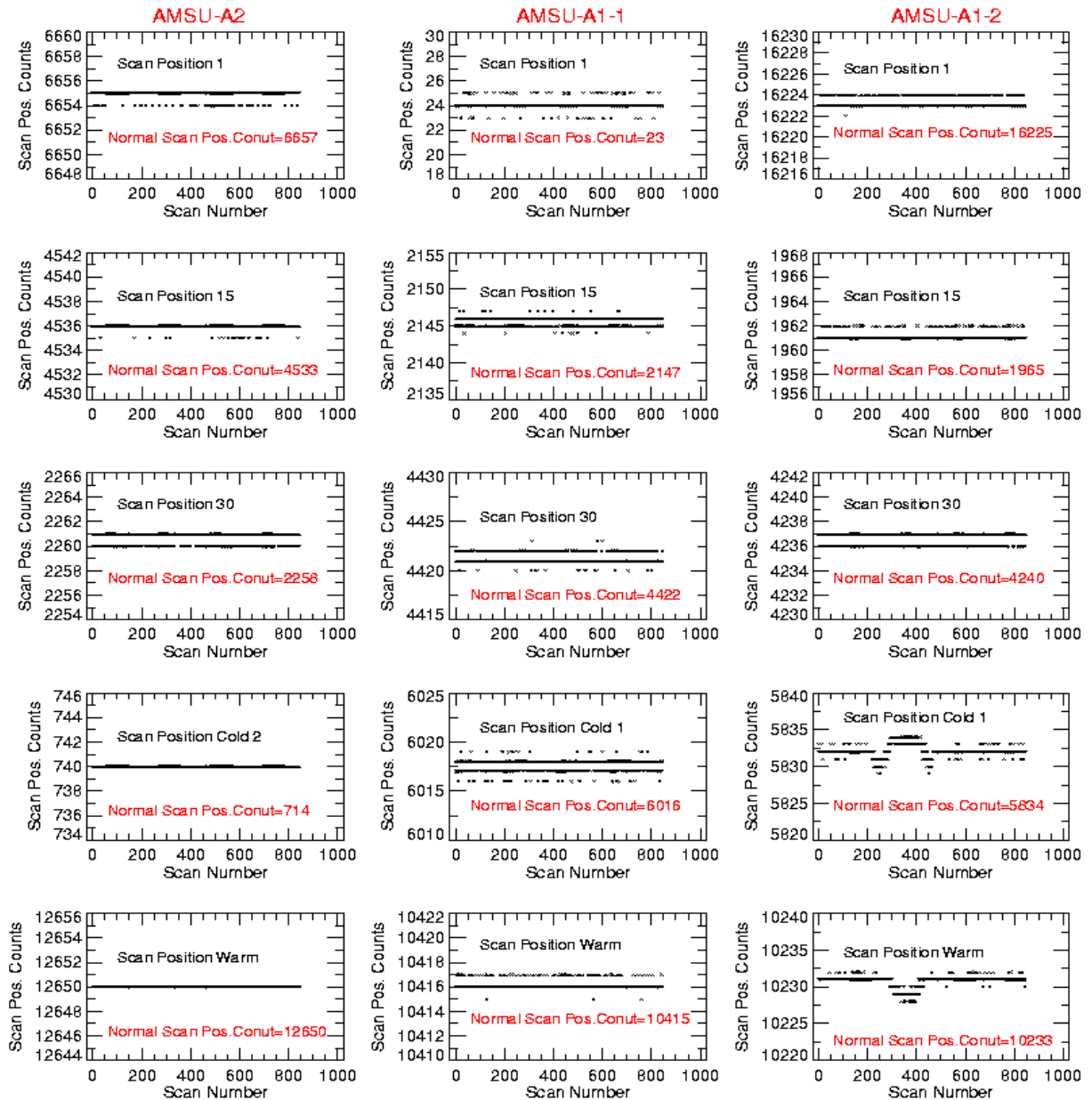


Figure 6. NOAA-18 AMSU-A: Validation of antenna pointing accuracy. The nominal position reading in count is listed at individual beam positions. The AMSU-A specification requires ± 10 counts (0.2 degrees) in the beam position readings. The Cold Calibration position #2 reading does not meet the specification. According to Northrop Grumman, the nominal value for this position should be 741 instead of 714 (as a typo in the AMSU-A Calibration Log Book).

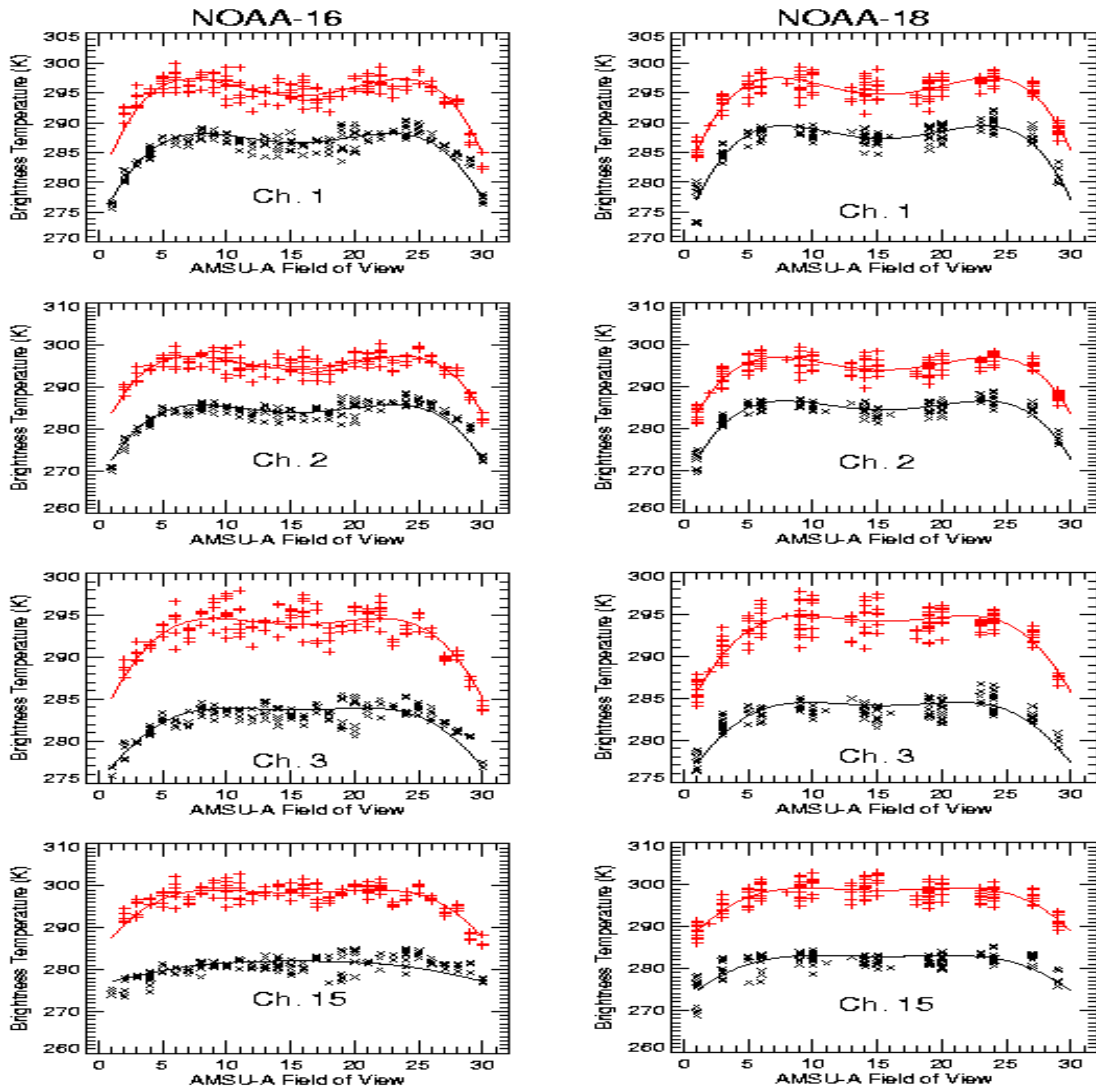


Figure 7. Comparison of NOAA-16 and NOAA_18 AMSU-A Brightnesstemperatures observed over the Libyan Desert in July 2005. The pluses denote the ascending (2 PM) data and the crosses are the descending (2 AM) data. The solid curves are the best-fit results with a radiative transfer model.

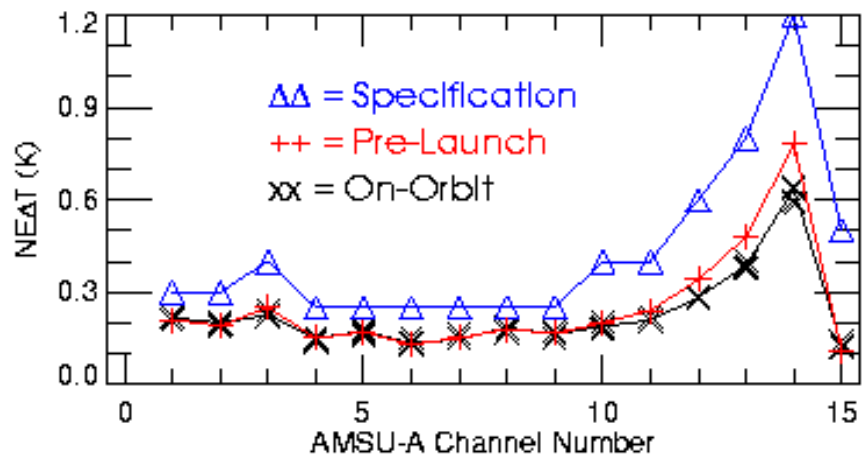


Figure 8. NOAA-18 AMSU-A NE Δ T: Comparison the pre-launch NE Δ T values with respect to those obtained with on-orbit data.

2.1 Determination of Optimal AMSU-A Space Views (SV)

Determination of optimal AMSU-A Space Views was performed following the procedure established in NOAA-16 AMSU-A OV. The linearly fitted parameters and the adjusted daily averaged counts are listed in Table 1. Optimal space counts are shown in red. The AMSU-A1 SV1 and AMSU-A2 SV2 are shown as the optimal space views. These are the same as in case of NOAA-16 AMSU-A. SV4 data, which were taken at unstable condition, are not used.

Table 1. Determination of of Optimal AMSU-A Space Views. Optimal space counts are in red.

Channel	Intercept (count)	Slope (count/day)	Adjusted Daily Averaged Counts			RMS (count)
			A1 at SV3 A2 at SV3	A1 at SV2 A2 at SV1	A1 at SV1 A2 at SV2	
1	12022.90	0.4439	12092.21	12093.97	12090.42	1.32
2	11466.83	-0.6013	11372.38	11371.78	11374.82	0.88
3	12250.27	2.3829	12626.65	12623.26	12617.00	2.06
4	12393.10	1.3689	12609.36	12607.54	12603.82	2.23
5	13011.71	-0.1275	12992.20	12991.09	12992.72	3.33
6	11938.70	3.1328	12432.46	12431.40	12419.78	1.67
7	12563.17	0.9799	12717.90	12716.80	12713.93	1.77
8	12005.29	1.1724	12189.54	12190.70	12184.80	1.67
9	12315.68	1.1774	12501.16	12500.93	12496.40	1.60
10	11908.23	2.8906	12363.44	12363.48	12351.73	1.81
11	9524.21	19.0746	12527.40	12528.68	12450.17	4.43
12	9542.91	20.4934	12769.23	12771.28	12686.27	4.21
13	7782.48	25.2434	11756.25	11759.67	11654.05	4.14
14	8757.59	25.4258	12760.35	12763.18	12657.42	5.65
15	12903.66	-0.2790	12860.21	12859.29	12861.34	3.53

3. NOAA-18 MHS ORBIT VERIFICATION *by Tsan Mo*

The NOAA-18 MHS On-orbit Verification was performed at the NOAA Office of Research and Applications (ORA). A systematic post-launch calibration and validation (Cal/Val) of the MHS instrument performances were conducted with on-orbit data. Scan-by-scan examination of the early orbits of data were conducted to check the operational software and the instrument performance. The long-term trends of the radiometric counts from the cold space and warm targets, channel gains, NE Δ T, and the housekeeping sensors and are monitored for checking the instrument performances. Some sample results are presented in the following.

Overall, the NOAA-18 MHS calibration is good with quality control flags set properly whenever there is any anomaly in the data stream. The NE Δ T values calculated from the on-orbit data meet the specification. The NE Δ T values are about a factor 2 smaller than the corresponding ones of AMSU-B. The Cal/Val of The NOAA-18 MHS is considered successful.

Figure 1 shows some of NOAA-18 MHS sample data of scan-by-scan radiometric space and warm calibration counts. Sample data of scan-by-scan channel gains and blackbody radiometric temperatures are shown in Figure 2. Comparison of the NE Δ T values obtained from the pre-launch calibration data and the on-orbit data, respectively, are presented in Figure 3.

Figure 4 shows the NOAA-18 the OV of the MHS PRTs by calculating the difference of the minimum and maximum PRT temperatures from individual scans. The procedure is as follows,

- (1). Compute the temperature difference, ΔT (=max. – min.) for each scan
- (2). Plot the frequency distribution of the ΔT values
- (3). Identify individual PRTs that introduce ΔT larger than 0.2K which is the MHS specification.

Lunar contamination in the space counts was observed during the OV period and this is shown in Figure 5. Only the first sample of the space counts is contaminated.

Long-term trending of the radiometric space and blackbody calibration counts is presented in Figure 6. The discontinuities at channels 18 and 19 are due to change of the offsets of the A/D converters. Long-term trending of the channel gains and NE Δ T is shown in Figure 7. Figure 8 shows the NOAA-18 MHS long-term trending of the blackbody temperature and two instrument temperatures.

Start: NSS.MHSX.NN.D05160.S0115.E0310.B0027677.WI
End: NSS.MHSX.NN.D05160.S0642.E0829.B0027980.WI

First Sample=+++ , Second=*** , Third=xxx , Fourth=...

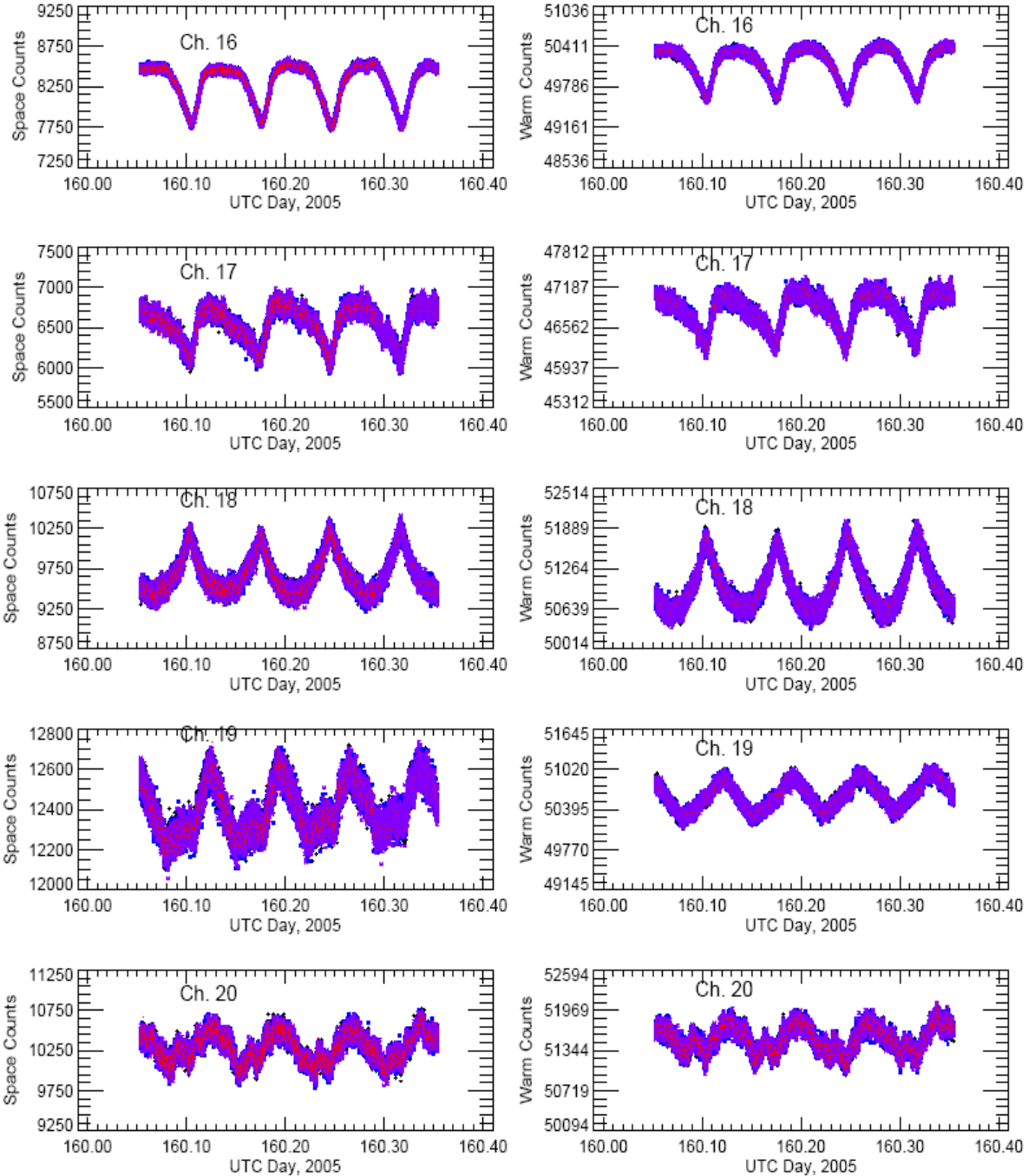


Figure 1. NOAA-18 MHS: Sample data of scan-by-scan radiometric space and warm calibration counts.

Start: NSS.MHSX.NN.D05160.S0115.E0310.B0027677.WI
End: NSS.MHSX.NN.D05160.S0642.E0829.B0027980.WI

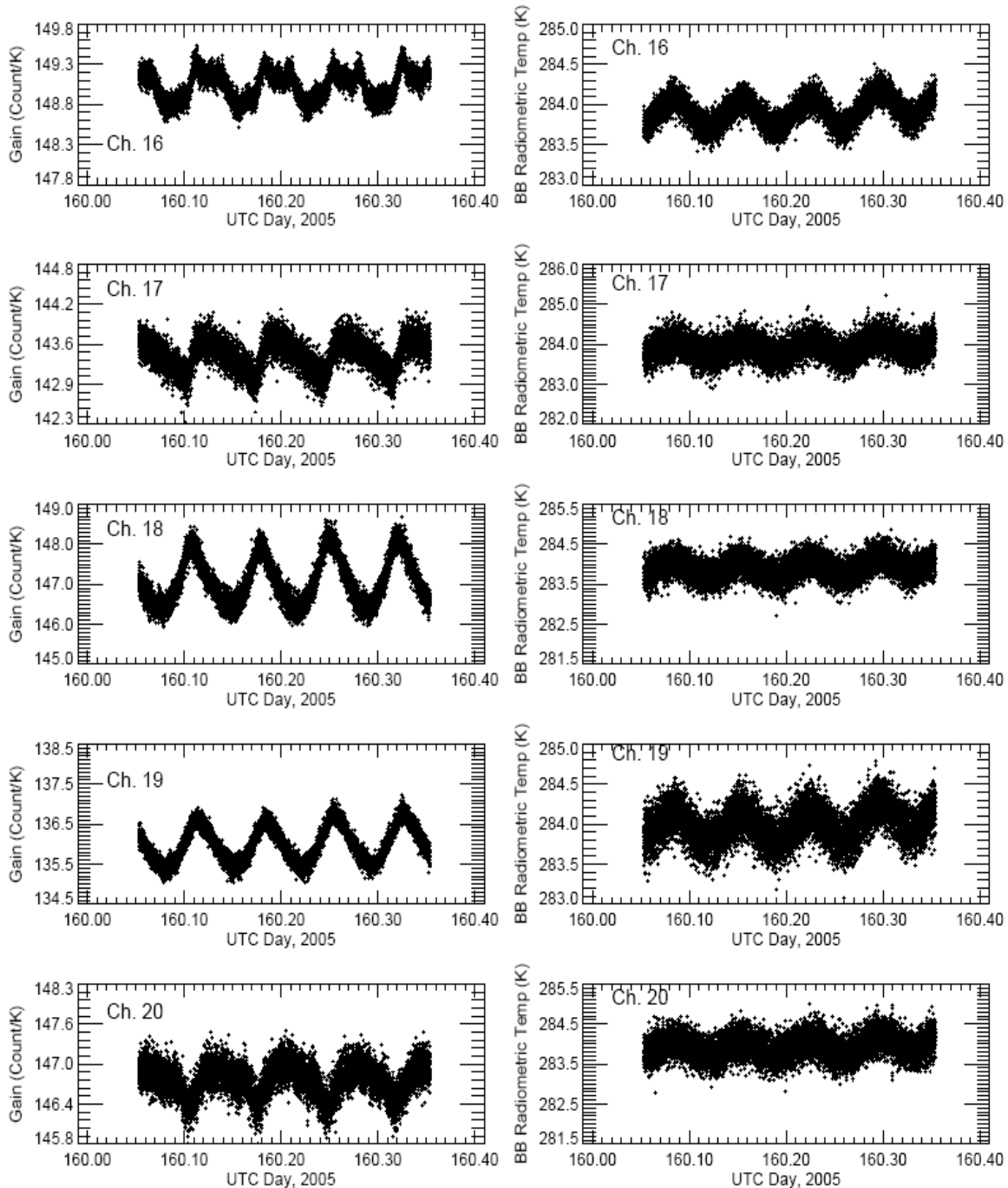


Figure 2. NOAA-18 MHS: Sample data of scan-by-scan channel gains and blackbody radiometric temperatures.

Specification: 1 K

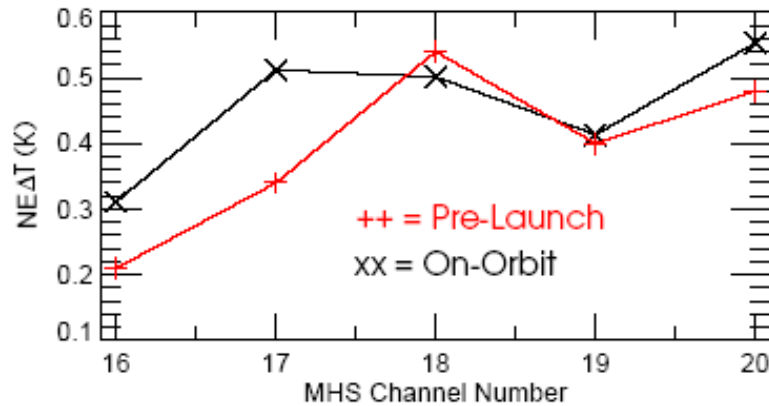
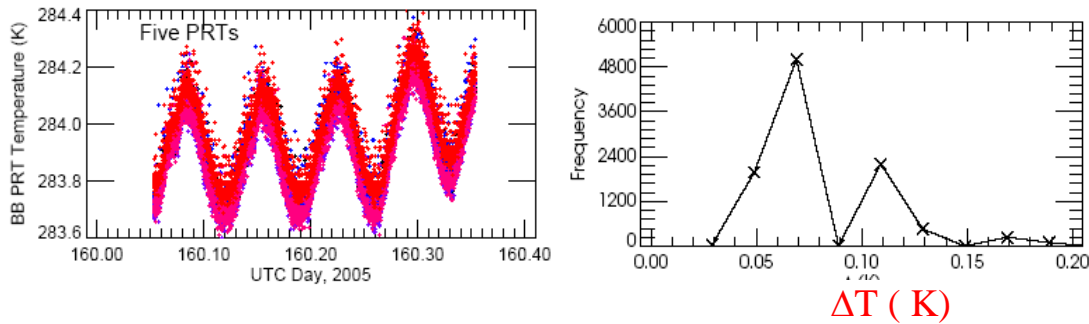


Figure 3. NOAA-18 MHS: Comparison of the NEAT values obtained from the pre-launch calibration data and the on-orbit data, respectively.

$$\Delta T = \text{Max. } T - \text{Min. } T$$



$$\text{Spec: } \Delta T < 0.2 \text{ K}$$

Figure 4. NOAA-18 MHS: On-orbit Verification of PRTs. On the left-hand side, the blackbody temperatures measured by five PRTs from each scan are plotted. The difference (ΔT) between the maximum and minimum PRT temperatures from individual scans were calculated. The frequency distribution is shown on the right-hand side.

Start: NSS.MHSX.NN.D05167.S1658.E1843.B0038385.WI
End: NSS.MHSX.NN.D05168.S0515.E0708.B0039192.WI

First Sample=+++, Second=***, Third=xxx, Fourth=...

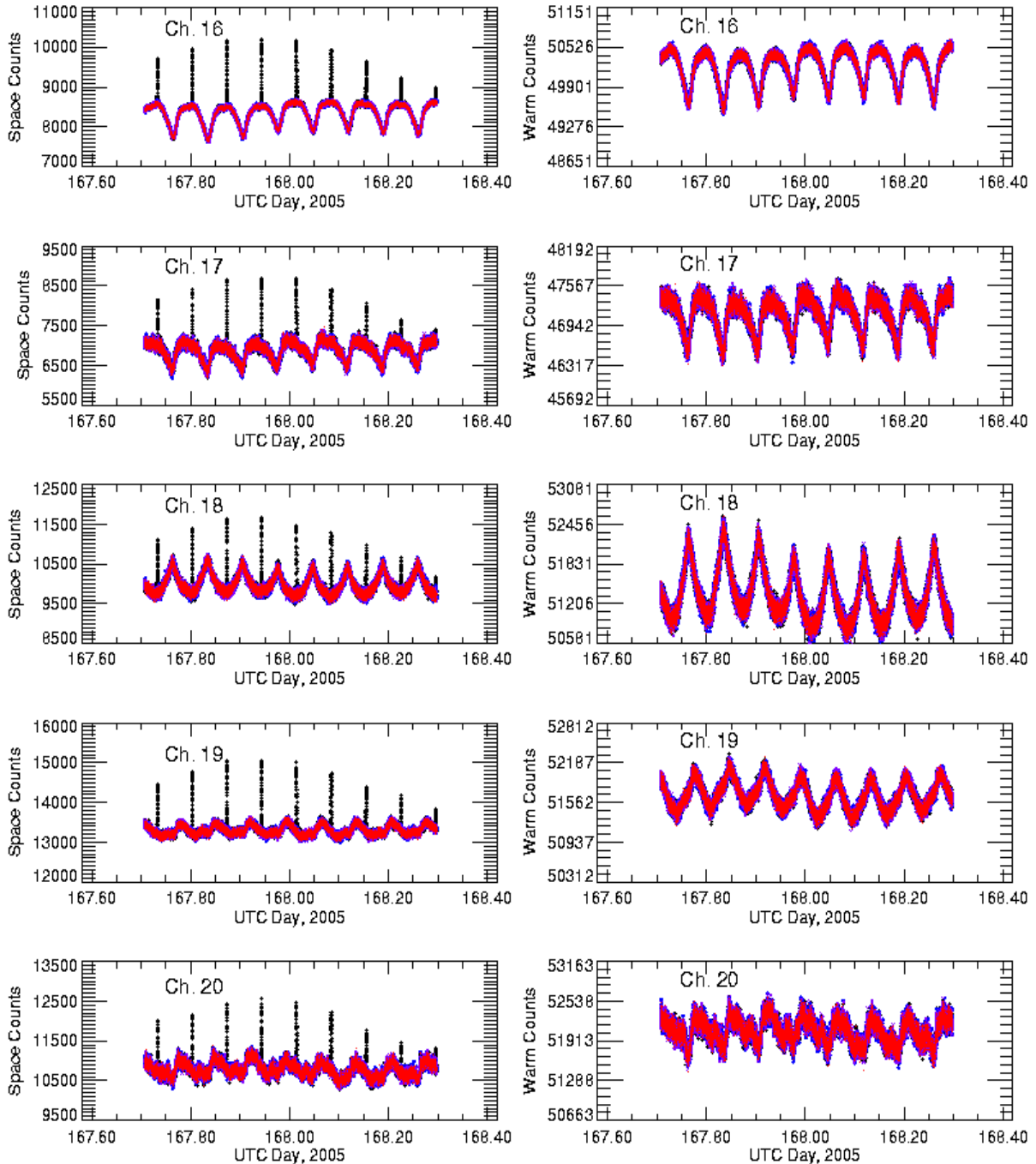


Figure 5. NOAA-18 MHS: Lunar contamination appears in the space counts. Only the first sample of the space count is contaminated.

NOAA-18 MHS CAL/VAL: Averaged calibration Counts

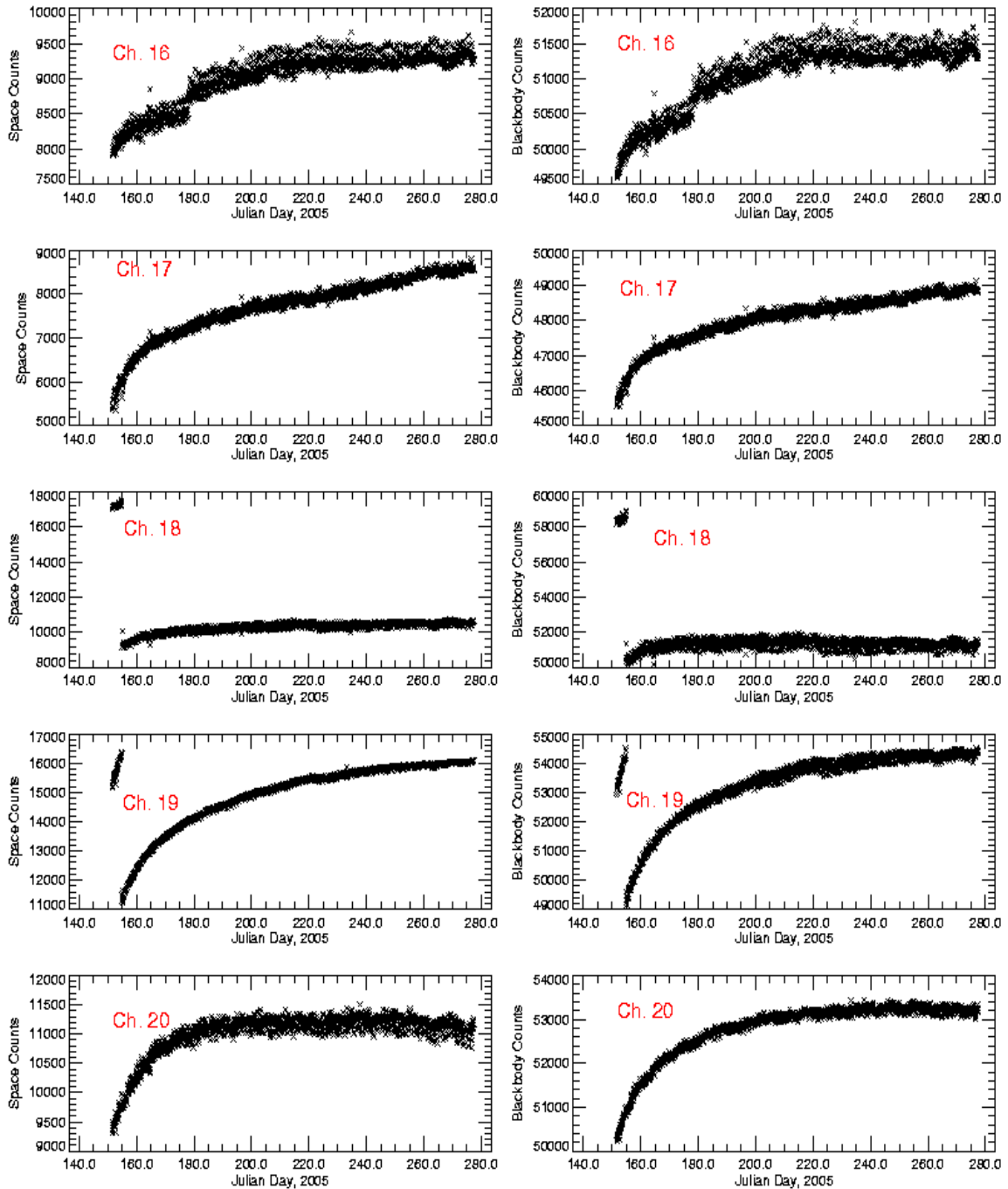


Figure 6. NOAA-18 MHS: Long-term trending of the radiometric space and blackbody calibration counts. The discontinuities at channels 18 and 19 are due to change of the offsets of the A/D converters.

NOAA-18 MHS CAL/VAL: Gain and NEAT

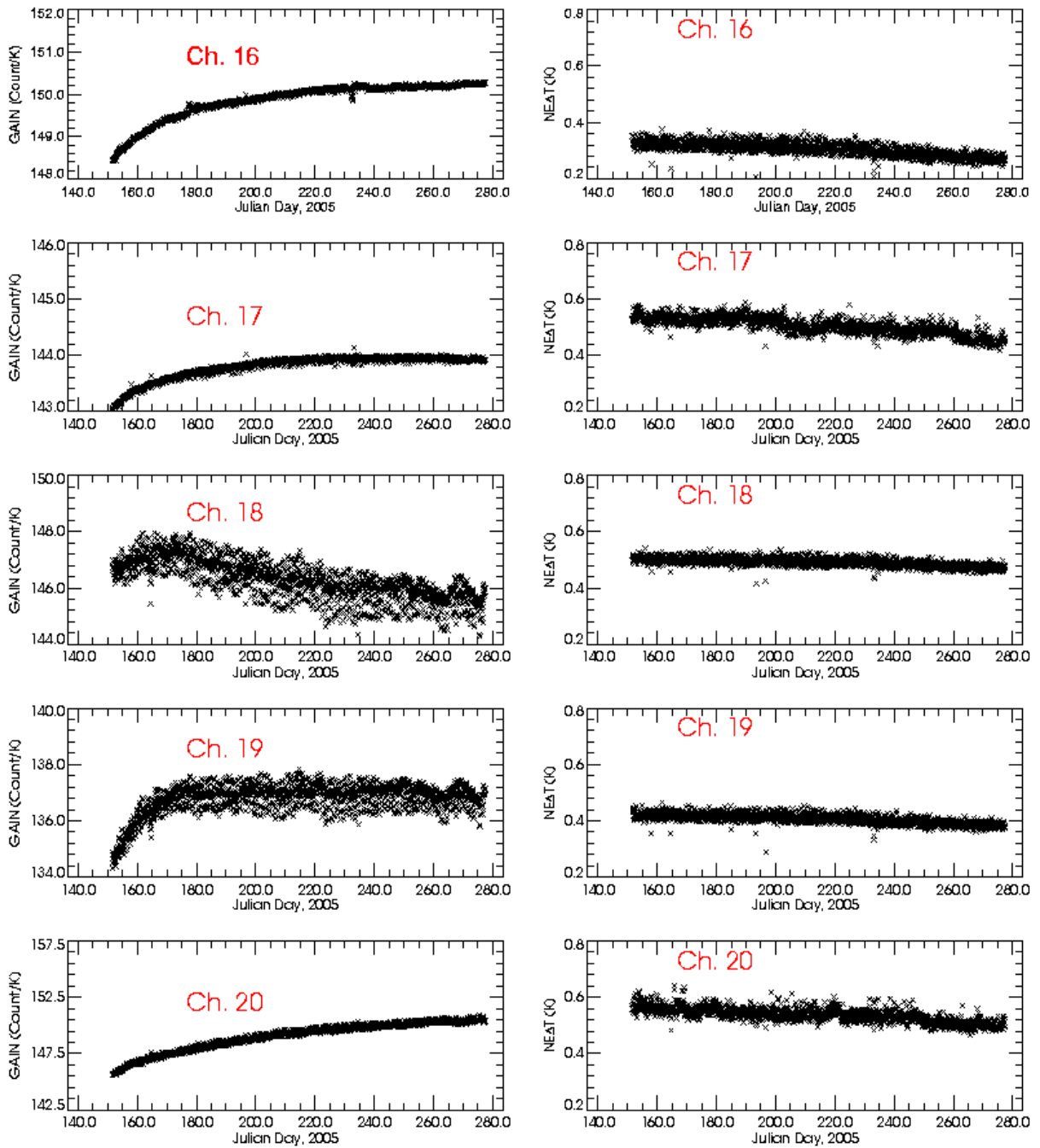


Figure 7. NOAA-18 MHS: Long-term trending of the channel gains and NEAT.

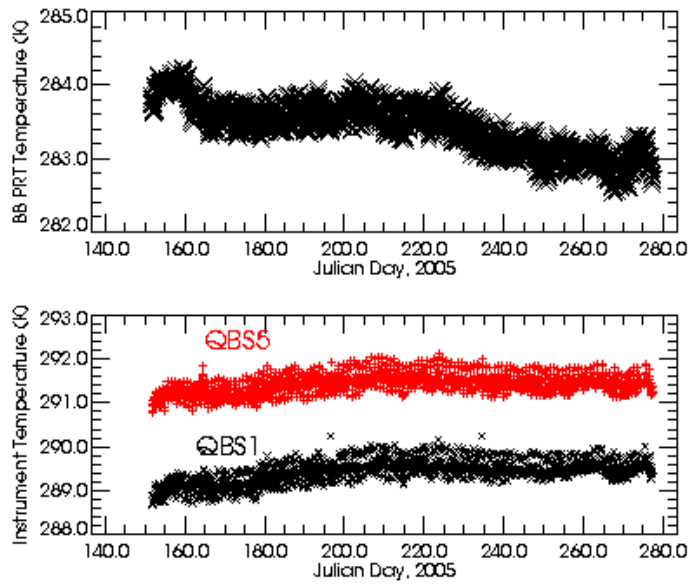


Figure 8. NOAA-18 MHS: Long-term trending of the blackbody temperature and two instrument temperatures.

4. NOAA-18 AVHRR ON-ORBIT VERIFICATION *by Jerry Sullivan and Xiangqian Wu*

The following tests were performed at ORA. A brief description and the test results for individual tests are given as follows,

4.1. NOAA-18 and NOAA-17 Comparison.

To verify that NOAA-18 AVHRR Channel 1, 2, and 3A radiances comparable to those from the NOAA-17, two Simultaneous Nadir Overpass events (when NOAA-18 and NOAA-17 viewed the same nadir point within a minute) are examined. It is that the difference between NOAA-18 and NOAA-17 AVHRR is 0.2%-0.4% for Channel 1 and 0.9%-1.2% for Channel 2. Channel 3A has been deactivated.

4.2. Change in Response of the Visible Channels.

To quantify the response change of visible channels 1, 2, and 3A on the “day after launch” multiple nadir observations of Libyan Desert by NOAA-18 AVHRR Channel 1 and 2 were obtained during the OV period. These, together with the bidirectional reflectance distribution functions derived in the past, enabled the calibration update immediately after launch. It was found that the pre-launch calibration overestimates the Channel 1 reflectance and underestimates the Channel 2 & 3A reflectances. In general, NOAA-18 AVHRR is similar to other AVHRR/3 starting with NOAA-15. (see Fig.1)

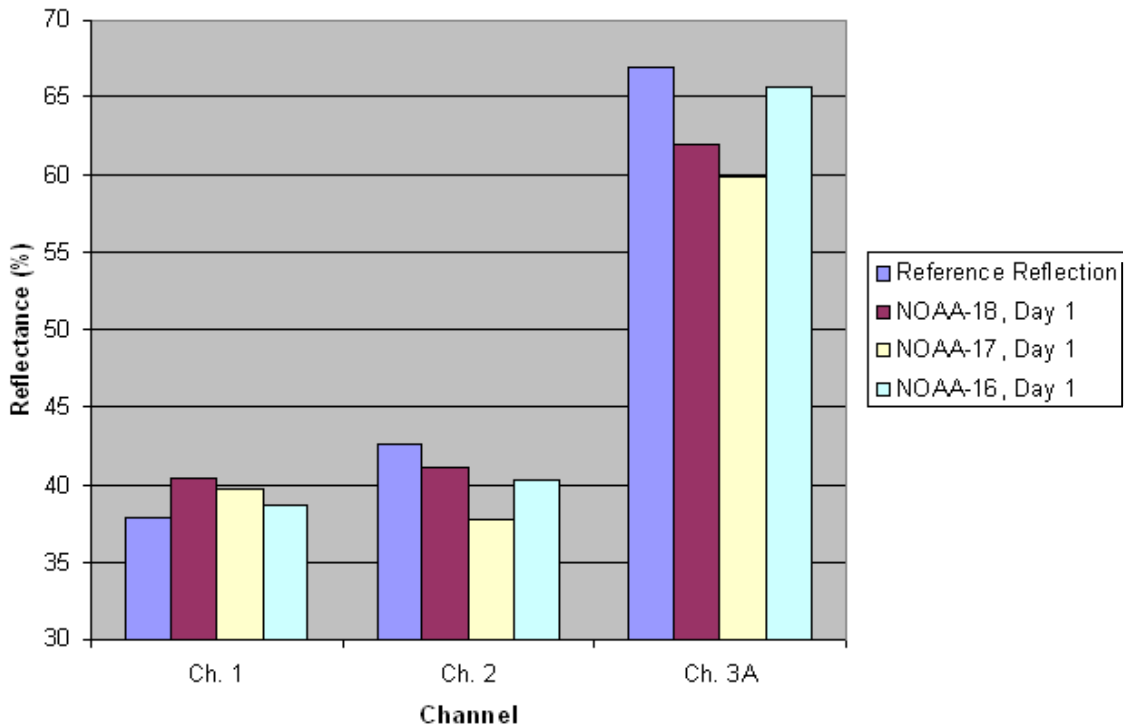


Figure 1. Initial assessment of NOAA-18 AVHRR VIS NIR calibration

4.3. Space Clamp Noise and Stability

To ensure that the space counts are clamped by the electronic circuitry to a constant value, a running 120-scan line block (1 minute) of GAC data was used to compute the space count average and standard deviation from the average for an entire orbit to monitor stability as a function of time in orbit. The process is repeated for 14 orbits (1 day) to monitor stability as a function of day. Plot the data in time series form for ease in checking (June 6, 2005 - 14 orbits GAC)

For all three AVHRR thermal channels, the short-term space count averages (120 scan lines) differ by only 0.1 to 0.2 counts from the long-term daily average, which has a value of approximately 990 counts.

4.4. Striping Check - Channels 3B, 4, and 5

To verify that there is no “horizontal striping” in the thermal channel data, the PRT data with consecutive scan line groups in an orbit where the RMS difference of the Internal Calibration Target (ICT) temperature from the average being less than 0.03K is employed. (Groups of 120 scan lines usually occur). For these 120-scan line GAC data blocks, compare the ICT count line-to-line variance value to the ICT count within-line variance. Many orbits were randomly selected during June-August, 2005.

Horizontal striping occurs when calibration count noise is not distributed randomly within a group of scan lines but rather tends to act as a positive count bias across some scan lines and as negative bias across others, producing “horizontally-striped” count noise characteristics. The presence of horizontal striping is tested for by a statistical index, defined as the ratio of the within-line count variance divided by the line-to-line count variance. For a sample of 10 ICT counts per scan line and a large enough number of scan lines (120 suffices), the theoretical ratio should be 9 for a truly random distribution of count noise. We have found empirically that a ratio of 3-4 or greater indicates that striping will not be a problem for NESDIS products. In general, ratio values show that NOAA-18 thermal channels 3B, 4, and 5 have no striping problems. A small percentage of the channel 5 120-scanline blocks have ratios near the lower limit. Randomly selected orbits throughout the OV period reproduce the same conclusion.

Within-line variance = Compute the count average for a single scan line, then the variance around this average. Repeat the process for all 120 scan lines, add the 120 individual variances together, and divide by 120.

Line-to-line variance = Compute the grand count average using counts from all 120 scan lines. For each scan line, subtract the grand average from the individual scan line count average, square the result, add the squared differences from 120 scan lines, and divide by 120.

4.5. Stability of Thermal Channels 3B, 4, and 5 When Viewing the Internal Calibration Target (ICT)

To monitor the stability of thermal channels 3B, 4, and 5 when they view the ICT during an “isothermal” part of the orbit, the PRT data, locate consecutive scan line groups in an orbit where the RMS difference of the ICT temperature from the average being less than 0.03 K were used. (Groups of 120 scan lines usually occur). Using data from these “isothermal” scan line groups, compute the average and standard deviation of the ICT count data for GAC datasets throughout a day on June 6, 2005 For 120-scan line GAC blocks and stable internal blackbody (ICT) temperatures, the NOAA-

18 thermal channel response generally alternates between a given count value and the count value closest to it; for example, the output is either 538 or 537 counts. The RMS variation around the 1-minute average is typically around 0.5 counts for N-18 channels 3B, 4, and 5.

4.6. Examination of the “Stray Light” Problem at Channels 3B, 4, and 5

To monitor the intensity and duration of the stray light problem is required as the AVHRR has a large scan swath of 55 degrees on either side of nadir, certain sun / instrument geometries allow unwanted radiation to leak into the AVHRR. Plot the Internal Calibration Target (ICT) blackbody temperature and the AVHRR (delta) count output when viewing this blackbody, as a function of time or scan line. During an orbit the ICT temperature changes by ~ 2K. Over this small temperature range, the ICT temperature time series and the AVHRR count output time series when viewing the ICT should overlap, when properly scaled. Anomalies indicate portions of the orbit where unwanted radiation is encountered for the GAC orbit on August 25, 2005

Figure 2 shows the ICT temperature / AVHRR count output time series as a function of scan line, for a GAC orbit from August 25, 2005. Darkened circles near the bottom of the figure indicate when the satellite is in darkness; yellow circles indicate that the satellite is in sunlight. After the satellite moves from darkness into light near scan line 6,800, there is a small anomaly (bump) in the AVHRR channel 3B count output. When converted to brightness temperatures, this count anomaly leads to an unrepresentative temperature error of about 0.15K. Channel 4 and 5 temperature errors are smaller. These fairly small errors are typical for AVHRRs on satellites that have an afternoon orbit, such as the NOAA-18. Randomly selected orbits throughout the OV period always reproduce this conclusion.

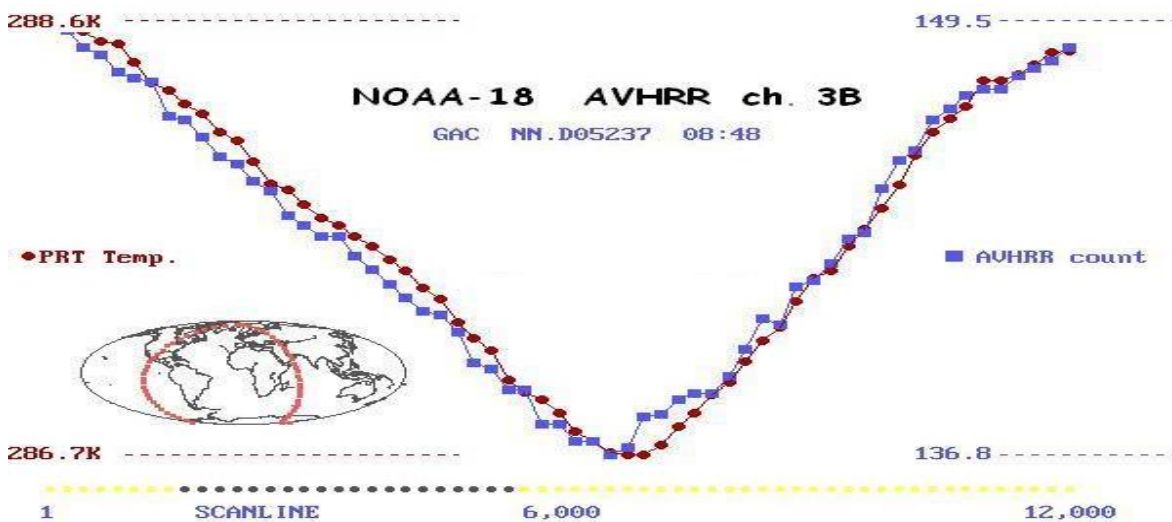


Figure 2. Near scanline 6,800, the AVHRR count output curve (blue) jumps slightly from the PRT temperature curve (red). This amounts to a 0.15 K anomaly, which is most likely due to stray light.

4.7. NOAA-18 and NOAA-17 Comparisons for the Thermal Channels.

To verify that NOAA-18 AVHRR radiances/temperatures and the NOAA-17 AVHRR values comparable, the SNO method was used. A few times each month at latitudes close to either Pole, the Earth tracks from any two polar orbiting satellites match closely in the sense that each AVHRR views the same nadir pixel (separation distance ~ 1 km) less than one minute apart in time. Scene variables

and viewing angles change very little in 30-60 seconds. Obtain NOAA-17 GAC data sets that match NOAA-18 GAC data sets closely in space and time. Compare radiance/temperature values for thermal channels 3B, 4, and 5.

On June 19, 2005 at 15:05:42, the nadir sub-point of the NOAA-18 satellite was in the middle of Greenland at (43.78W, 71.25N). 52 seconds later, the nadir sub-point of the NOAA-17 satellite was at nearly the same location (43.78W, 71.24N). During 52 seconds the sun moves little so the viewing geometry for both AVHRRs is very similar. Also, land/sea temperatures and cloud properties change very little. This provides an excellent opportunity to compare the responses of the NOAA-18 and the NOAA-17 AVHRR thermal channels. Furthermore, the interior of Greenland is a fairly homogeneous surface and summer temperatures change relatively slowly during the day. Figure 3 shows “modified” channel 4 count values from the two AVHRRs. (Modified means I subtracted 598 counts from N-18 and 595 from N-17, to make easily-readable single integer values.) The spatial patterns match very well. When counts are converted to radiance and radiance converted to equivalent brightness temperature, the 150-pixel area-averaged temperatures for channel 4 from the two AVHRRs are within 0.05K of each other. This was the best case, most likely because of the homogeneous surface in Greenland. Other matchups showed area-averaged temperature differences in the 0.2K to 0.4K range. Channel 5 showed similar results.

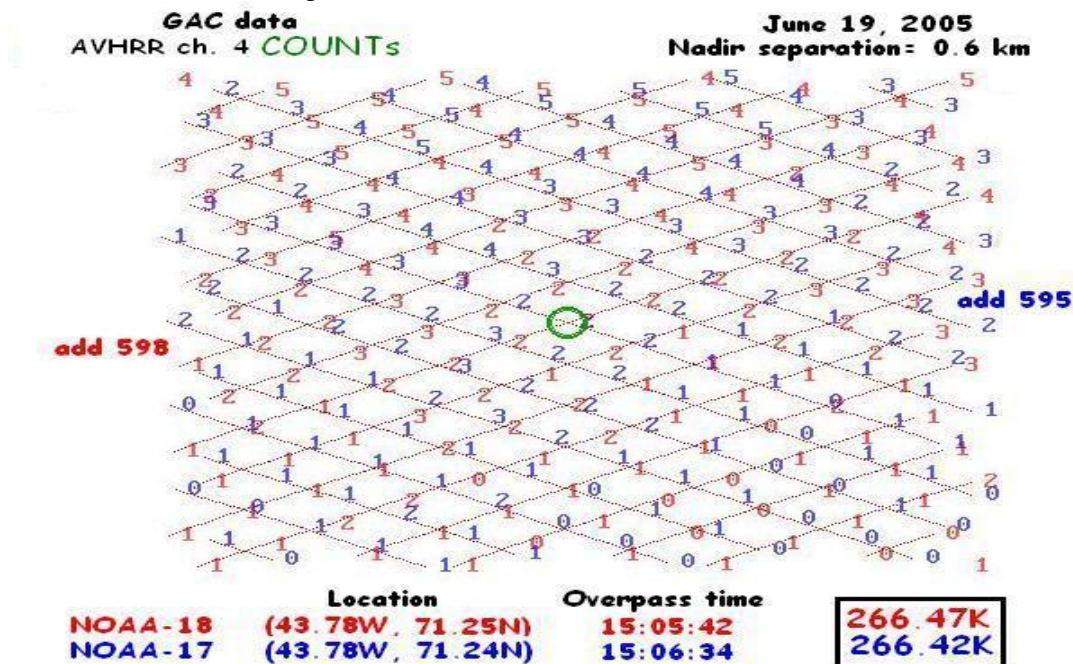


Figure 3. AVHRR Channel 4 counts for NOAA-18 (red) and NOAA-17 (blue). The green centers of scenes were 1 km and 1 minute apart. Count patterns correlate well and the 150-pixels temperature averages (box on lower right) were only 0.05 K apart.

4.8. Navigation (geo-location) using visible channel imagery

To quantitatively determine the geo-location accuracy the AVHRR 1b LAC, the Normalized Difference Vegetation Index (NDVI), defined by

$$NDVI = (A2 - A1) / (A2 + A1),$$

where A1 = channel 1 albedo and A2 = channel 2 albedo is an excellent land/sea indicator. The

contrast in the index between land and sea is large, even when channel albedos are only approximately calibrated. Values of the index > 0 indicate land and values < 0 indicate water. For each LAC pixel, the index is given the appropriate color and plotted on the computer screen in the Plate Carree projection ((long,lat) \rightarrow (x,y)), using longitudes and latitudes from the AVHRR 1b file. In addition, a geographical boundary from the World Vector Shoreline (WVS) file is overlaid on the image as a reference. The positions of the water screen pixels that “leak” onto land (and vice-versa) are converted to actual distance in kilometers, to assess the accuracy.

LAC orbits were selected during the OV period. Figure 4 shows the results of the test, applied to one day from the OV period. The same result occurred on every orbit I tested during the summer 2005 period. The NDVI is imaged for the area in and around Lake Michigan, USA. This area was chosen because of its quasi-rectangular shape, useful for determining both along-track and cross-track navigation errors. Data was collected on days where the nadir ground path (shown in red in Fig. 4) passed through Lake Michigan. LAC nadir pixels are nearly 1 km x 1 km in area. Pixels that the NDVI designates as land are colored green and those designated as water are colored black. The pixels were plotted on the screen in a straight longitude-latitude projection, called Plate Carree, and at a resolution where 1 screen pixel = 1 km. The longitudes and latitudes for the pixels were obtained from the NESDIS 1b file. Overlaid on top of the NDVI image is the outline of the Lake Michigan shoreline, obtained by plotting longitudes and latitudes from the WVS database, plotted in the same projection as the NDVI image. The accuracy of the WVS database is reported as 0.5 km. Basically, if the eye sees any “leak” of water to land or vice-versa, the navigation error is 1 km or greater. Semi-quantitative computer tests, where the image was shifted pixel by pixel in both the vertical and horizontal direction, confirmed that the NESDIS LAC 1b navigation was off by approximately 2-3 pixels along-track and 1-2 pixels cross-track. Performing the same test using the coast of Florida, USA gave the same results.

It seems that the geo-location should be more accurate; as the NOAA-17 AVHRR LAC data had a geo-location error closer to 1 km. More tests will be taken to confirm these results.

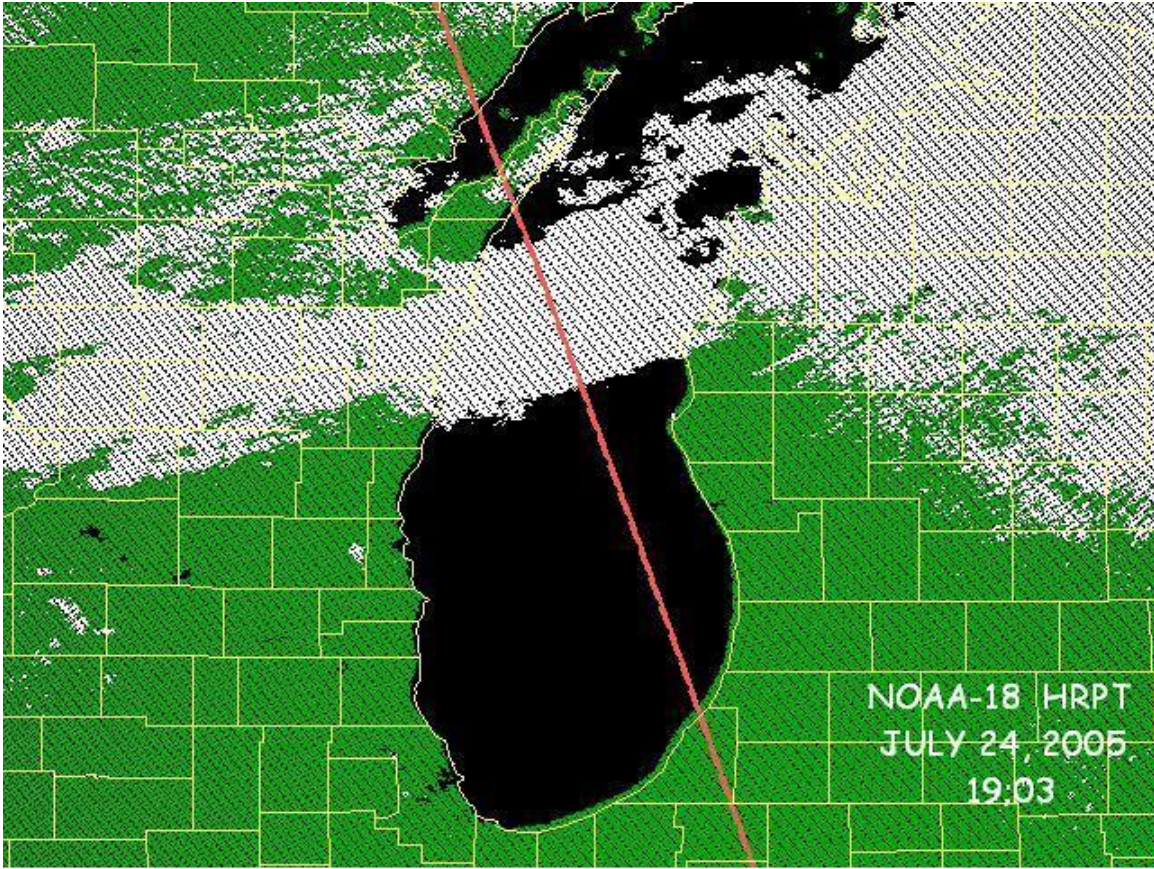


Figure 4. NOAA-18 navigation, comparing land/sea tags indicated by a standard vegetation index (NDVI) and NESDIS 1b (long, lat) coordinates with the World Vector Shoreline coordinate in yellow.

5. NOAA-18 SBUV/2 ON-ORBIT VERIFICATION *by Larry Flynn*

The following tests were performed at ORA. A brief description and the test results for individual tests are given as follows,

- Range 3 Cathode: Collect data in Range 3 cathode mode to evaluate instrument performance. It was found that the Range 3 data noise was consistent with the NOAA-16 SBUV/2 instrument. Interrange ratios were consistent with pre-flight alterations.
- CCR/Monochromator Comparison: Collect data using wavelength at 380 nm to simulate cloud cover radiometer (CCR) bandpass at 380 nm with monochromator wavelength. This test was altered to use a single wavelength as the three-wavelength test with NOAA-17 showed good correlation of all three channels. Obtain a baseline for comparison of the PMT and the photometer. The test was completed successfully. Baseline was established.
- Out-of-Band Response Estimation: Collect data in normal Earth-view using position mode at standard profiling wavelengths to evaluate stray light. Part of this test was completed successfully in OV. Measurements at two additional wavelengths were taken after OV. Comparisons of monochromator variations to photometer variations provided estimates of OOB. R.
- Range 3 Noise Periodicity: Check for 8-second periodicity noise seen on NOAA-16 SBUV/2. Used data from SBUA01 and SBU012. No evidence of this problem. A variation in pitch was found in the solar measurements and report to the pitch anomaly team.
- Range 1 Noise Levels: Check for noisy Range 1 measurements seen on NOAA-16 SBUV/2. Used dark-side measurements in SBU004. Noise for Range 1 is not at elevated levels.
- Mg II in Earth View: Estimate additive stray light in OOB from measurements across a solar feature at 280 nm in Earth-view. Test was performed in OV. Data are awaiting analysis.
- Comparisons to NOAA-16 SBUV/2: Establish a baseline for differences between the two instruments measurements and ozone retrievals. Comparisons continue as NOAA-18 SBUV/2 calibration and characterization adjustments are implemented. The goals are less than 1% bias between total ozone and reflectivity products and less than 5% bias between ozone profile products.

Additional Trending recommendations (during OV and beyond)

- Instrument Throughput : Monitor changes in instrument throughput as dichroics outgas water vapor. There is inadequate frequency of solar diffuser measurements to characterize changes. (Note: SBU013 was not performed.)
- Mg II Index: Begin producing Mg II Index as soon as possible. There is inadequate frequency of solar diffuser measurements to make index.
- Range 3 Anode/Cathode Evolution: Track performance of photometer in cathode versus anode mode. Measurements started with SBUA01 and are repeated weekly in the operational schedule.

- Monochromator/Photometer Evolution: Track performance of photometer versus monochromator. Measurements started with SBUA04 and will be repeated after six months.

There is additional trending and characterization analysis performed on the inter-range ratios, diffuser reflectivity, wavelength scale, instrument throughput, and measurement noise. A new nonlinearity adjustment was derived from data collected during the OV, and wavelength dependent corrections for the OOB were developed.

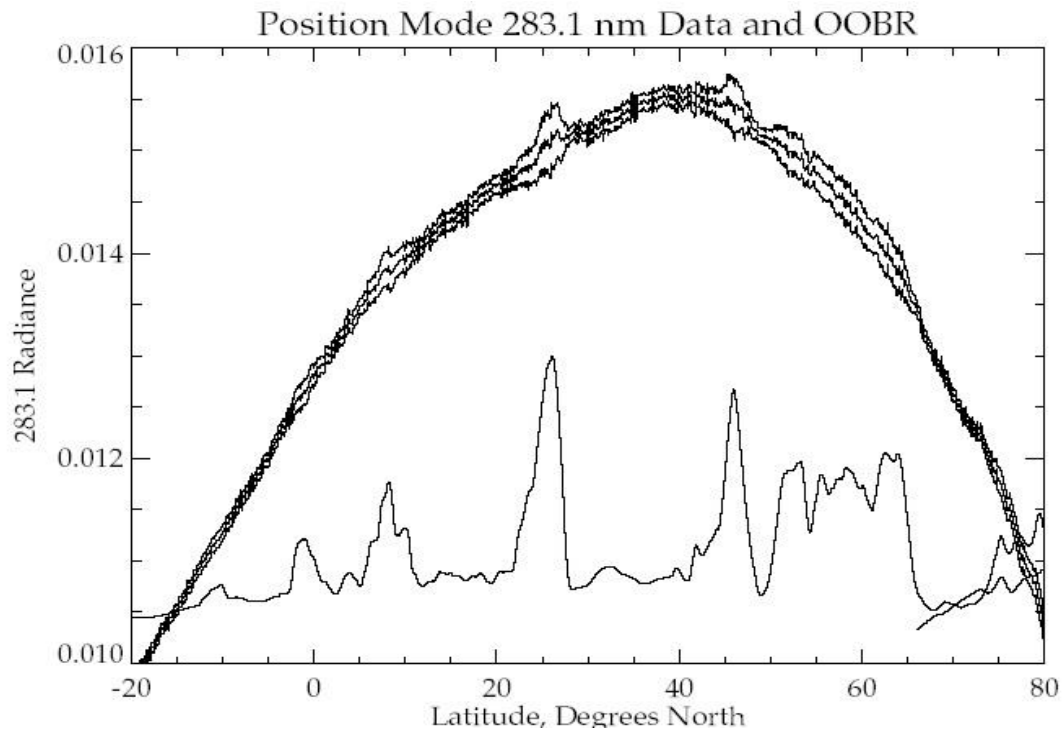


Figure 1. Shows position mode data for 283.1 nm compared to scaled, coincident cloud cover radiometer measurements. The topmost of the three dark curves is the original data and the middle of the three is after OOB corrections. (See SBUA05.)

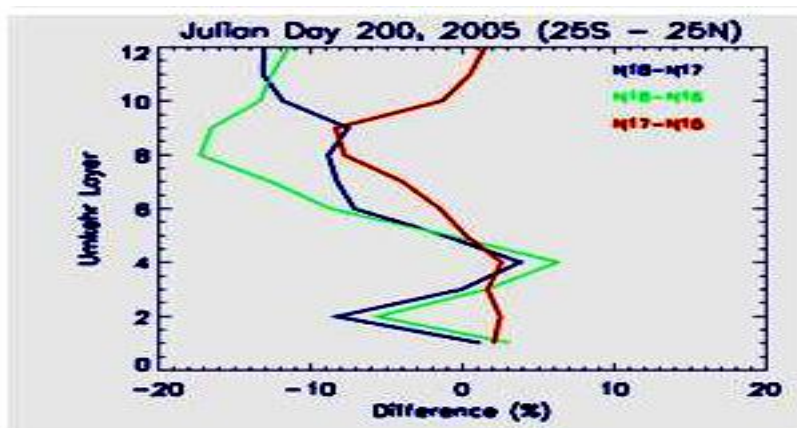


Figure 2. Profile comparisons between NOAA-18 SBUV/2 and NOAA-16 SBUV/2 (Green), NOAA-18 SBUV/2 and NOAA-17 SBUV/2 (Blue), and NOAA-17 SBUV/2 and NOAA-17 SBUV/2 (red).

6. NOAA-18 INSTRUMENTS: GEO-LOCATION, NAVIGATION, AND ASYMMETRY

by Thomas Kleespies

Results from the following tests are summarized as follows:

6.1 Determination of Absolute Navigational Accuracy of AMSU-A

AMSU-A11 has about 5 km positive along track and 6 km positive cross track geo-location error and AMSU-A12 has about 3 km positive along track and no meaningful cross track geo-location error. AMSU-A2 has about 9 km negative along track and 4 km negative cross track geo-location error.

The absolute navigation accuracy are derived by convoluting a high-resolution (550m) land-sea mask to the spatial resolution of the instrument. By varying the spatial position of the footprints and using knowledge of the sea surface temperature and homogeneous land temperatures near the coastline, the navigation accuracy can be determined and possible offsets can be identified via cross-correlation analysis.

Fifteen passes over northern Europe and Indonesia on four consecutive days (2005/247-250) were used for this test. The results for AMSU-A1 Channel 3 (.3 GHz) are given in Table 1, which shows the accuracy of AMSU-A1 50 GHz navigation for 15 different overpasses over northern Europe and Indonesia. 'Start time' and 'day' identify the orbits according to NESDIS Level 1b file naming conventions. 'Correlation' gives the maximum correlation between land/sea-mask and observed antenna temperatures. The values for dx and dy are the corresponding navigation shifts in cross-track and along-track track direction. They are given in units of MHS instrument FOVS for the cross-track direction (i. e. a value of +1 means that the navigation has to be shifted by one MHS FOV in positive scan direction) and in units of MHS scan lines for the along track direction (i. e. a number of +1 means that the navigation has to be shifted by one MHS scan line in positive flight direction). The resulting average geo-referencing errors and standard deviations of the errors are also given in km for nadir observations in the last two rows.

Table 1. Accuracy of AMSU-A1 Channel 3 (50.3 GHz) navigation for 15 different over passes over northern Europe and Indonesia.

Day	Start	Correlation	DX	DY	Desc/Asc	Area
D05247	S0145	0.91	0.00	-0.40	D	Baltic
D05247	S0334	0.86	0.00	0.40	A	Indo
D05247	S0523	0.77	0.00	-0.20	A	Indo
D05247	S1023	0.92	0.00	-0.20	A	Baltic
D05247	S1535	0.85	0.00	-0.80	D	Indo
D05247	S1652	0.84	0.20	-0.40	D	Indo
D05248	S0134	0.91	0.00	-0.40	D	Baltic
D05248	S0324	0.83	0.00	0.20	A	Indo
D05248	S0513	0.78	0.40	-0.20	A	Indo
D05248	S1013	0.92	-0.20	-0.20	A	Baltic
D05248	S1642	0.81	0.20	-0.40	D	Indo
D05249	S0119	0.92	0.00	0.00	D	Baltic
D05249	S0457	0.77	0.00	0.40	A	Indo
D05249	S1003	0.92	0.00	0.00	A	Baltic
D05250	S0120	0.94	0.00	-0.40	D	Baltic
	Mean	Sdev	Mean[km]	Sdev[km]		
DX :	0.04	0.14	0.72	2.43		
DY :	-0.17	0.33	-3.12	5.91		

Table 2 gives the same results as those in Table 1 but for AMSU-A1 89 GHz. Note, there is slightly

fewer orbits at 89 GHz than at the lower frequencies, since the occurrence opaque clouds sometimes does not permit a meaningful cross-correlation analysis. The geo-location of the AMSU-A1 should be examined.

Table 2. Same as Table 1 but for AMSU-A11 Channel 15 (89 GHz).

D05247	S0145	0.83	-0.40	-0.80	D	Baltic
D05247	S0334	0.69	0.00	0.40	A	Indo
D05247	S1023	0.90	-0.40	-0.60	A	Baltic
D05247	S1652	0.75	-0.20	-0.80	D	Indo
D05248	S0134	0.86	-0.40	-0.60	D	Baltic
D05248	S0324	0.68	-0.20	0.60	A	Indo
D05248	S0513	0.65	0.00	-0.40	A	Indo
D05248	S1013	0.89	-0.60	-0.40	A	Baltic
D05248	S1642	0.70	0.00	-1.20	D	Indo
D05249	S0119	0.85	-0.60	-0.20	D	Baltic
D05249	S0457	0.70	-0.20	0.40	A	Indo
D05249	S1003	0.92	-0.60	-0.40	A	Baltic
D05250	S0120	0.88	-0.40	-0.60	D	Baltic
	Mean	Sdev	Mean[km]	Sdev[km]		
DX:	-0.31	0.23	-5.54	4.06		
DY:	-0.35	0.53	-6.37	9.54		

Table 3 gives the same results as those in Table 1 but for AMSU-A1 channel 1 at 23.8 GHz.

Table 3. Same as Table 1, except for ASMSU-A2 Channel 1 at 23.8 GHz.

Day	Start	Correlation	DX	DY	Desc/Asc	Area
D05247	S0145	0.95	0.20	0.60	D	Baltic
D05247	S0523	0.76	0.40	0.60	A	Indo
D05247	S1023	0.97	0.20	0.60	A	Baltic
D05247	S1535	0.80	0.00	0.20	D	Indo
D05247	S1652	0.84	0.20	0.20	D	Indo
D05248	S0134	0.95	0.20	0.60	D	Baltic
D05248	S0513	0.79	0.40	0.60	A	Indo
D05248	S1013	0.96	0.00	0.60	A	Baltic
D05248	S1642	0.81	0.20	0.20	D	Indo
D05249	S0119	0.95	0.20	0.60	D	Baltic
D05249	S0457	0.80	0.20	0.80	A	Indo
D05249	S1003	0.97	0.20	0.80	A	Baltic
D05250	S0120	0.96	0.20	0.40	D	Baltic
	Mean	Sdev	Mean[km]	Sdev[km]		
DX:	0.20	0.11	3.60	1.92		
DY:	0.52	0.21	9.40	3.76		

6.2 Determination of Pointing or Navigation Errors

AMSU-A11 appears to be geo-located slightly positive along track and slight positive cross track and AMSU-A12 seems to be geo-located correctly. AMSU-A2 appears to be geo-located negatively both along track and cross track.

Global 1B antenna temperatures were binned and averaged in 0.5 deg latitude-longitude boxes separately for ascending and descending nodes. These values were differenced. Any systematic pointing or navigation errors appear as red and blue shadows on opposite sides of continental coastlines.

Global 1B data for days 2005 152-172 were used in this study. The results show that AMSU-A11 appears to be geo-located slightly positive both along track and cross track . Figure 1 shows the test results for the AMSU-A11 Channel 15 Ascending/Descending antenna temperature comparison for days 201-245. AMSU-A12 appears to be geo-located correctly (Fig. 2). Figure 3 shows the results for AMSU-A2 channel 1. There are hints of colored shadows along coastlines.

Zoom in on Europe

AMSU-A11 appears to be geolocated slightly positive both along track and crosstrack

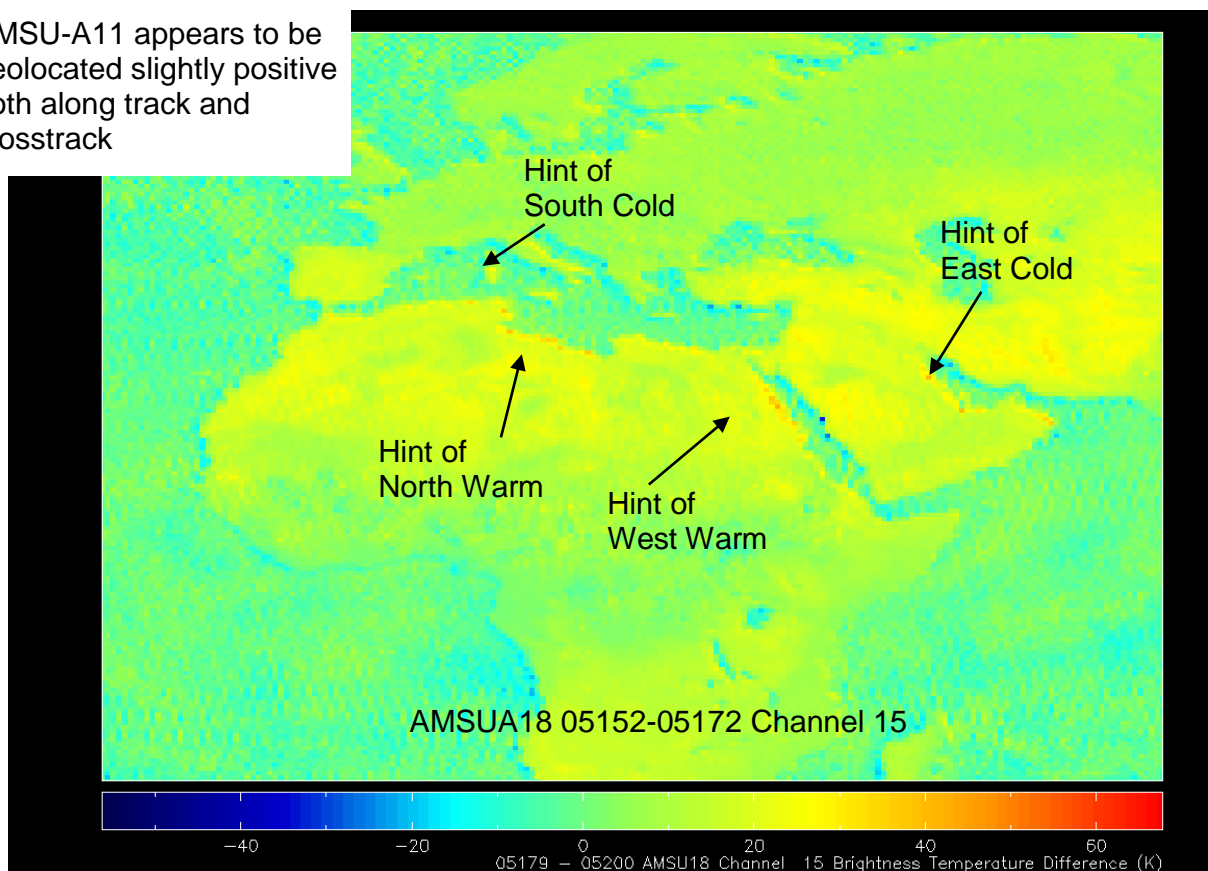


Figure 1: Results from Test of A12 Channel 3 Ascending/Descending antenna temperature comparison for days 201-245. There are hints of colored shadows along coastlines..

Zoom in on Europe

AMSU-A12 appears to be correctly geolocated

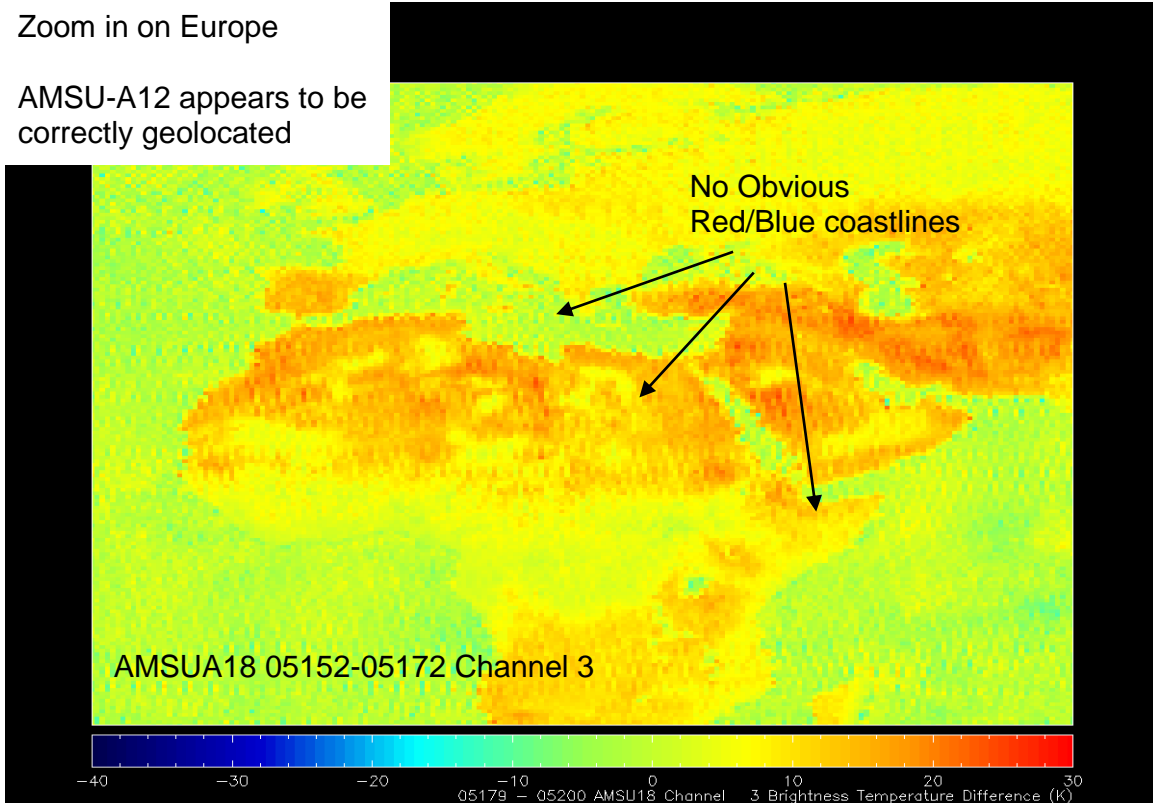


Figure 2: Results from Test of A12 Channel 3 Ascending/Descending antenna temperature comparison for days 201-245. There are no obvious red/blue shadows.

Zoom in on Europe

AMSU-A2 appears to be geolocated negatively in both along track and crosstrack direction.

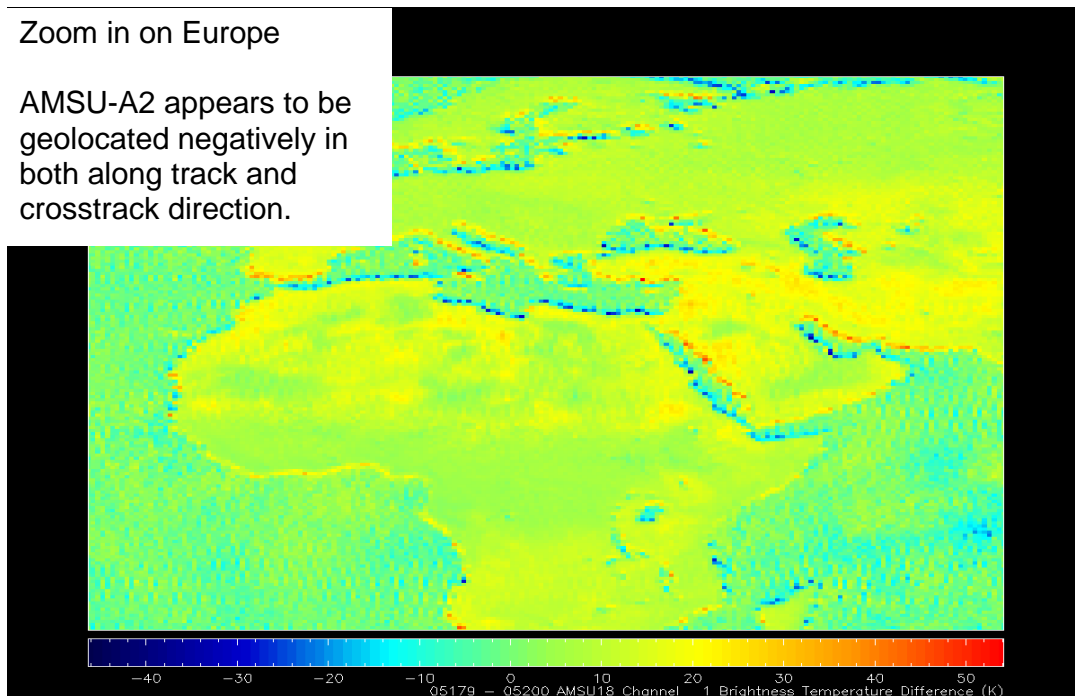


Figure 3: Results from Test of A2 Channel 1 Ascending/Descending antenna temperature comparison for days 201-245. There are hints of colored shadows along coastlines..

6.3 Determination of Cross scan Bias in the Data

Global 1B antenna temperatures were binned and averaged for each scan position. A scan bias will be evident if one side is warmer or colder than the other. Data are differenced symmetrically about nadir, high numbered field of views (FOVs) minus low numbered FOVs. Level 1B antenna temperatures from twenty-one days (2005 152-173), 40N-40S, ocean only (cloud and precipitation screened) were used in this study. Figure 3 shows the results. AMSU-A2 left side appears warmer than right side. AMSU-A1 right side appears warmer than left side by ~ 1 K, but varies by channel (Figure 4). Window channels display ascending/descending disparity. Sounding channels ascending/descending behavior consistently. Differences between the observed and simulated radiance statistics from the Global Data Analysis System at NCEP/EMC reveal the same sign and magnitude of the scan bias. Thus this is instrument related, not an artifact of the diurnal cycle. As long as this bias is stable, the analysis model can remove the bias and assimilate the data. It should be noted that most of these asymmetries can be corrected or reduced considerably if an appropriate antenna pattern correction is applied (see Weng et al., in Appendix).

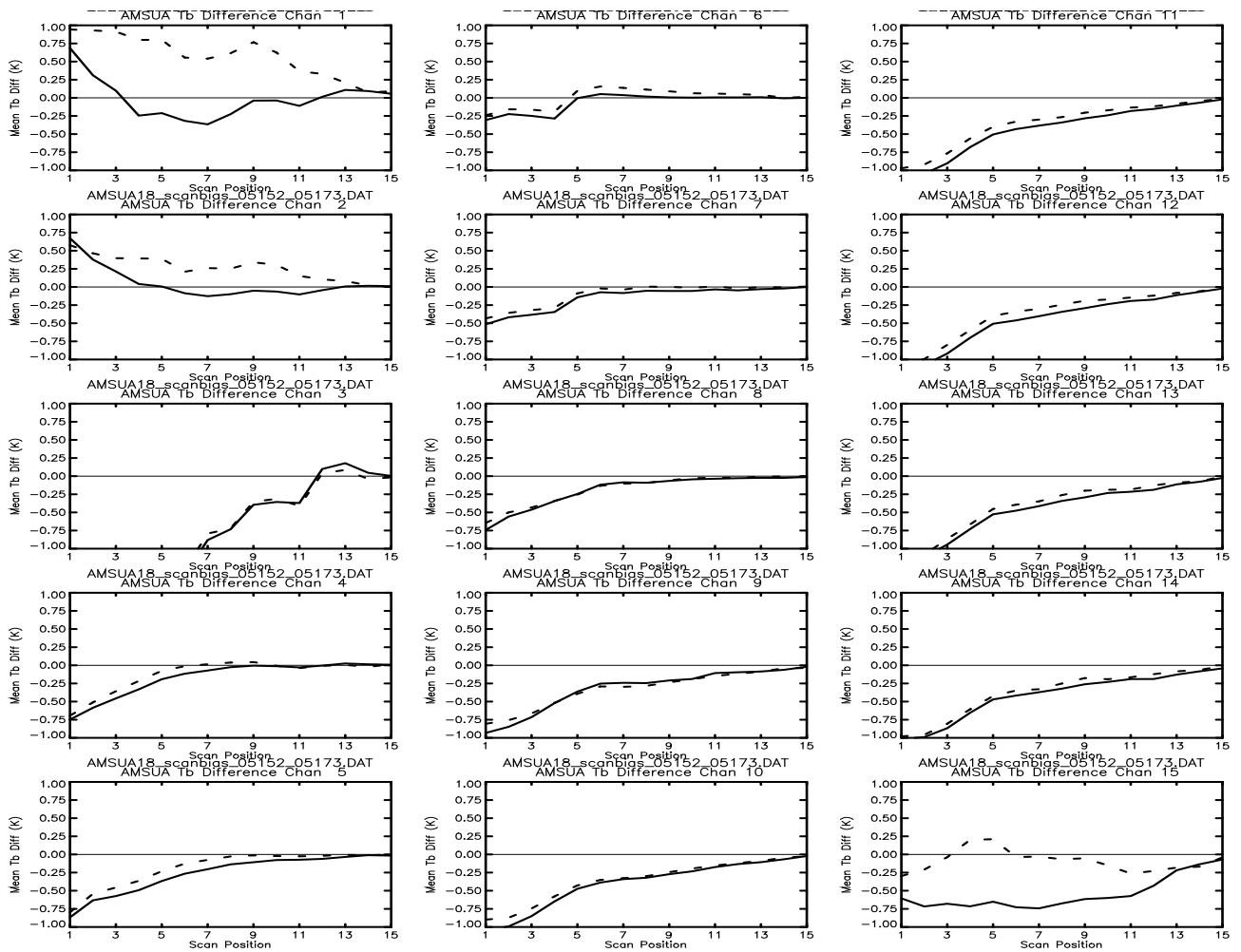


Figure 4: Pairwise Left-Right Side Antenna temperature Difference. Solid is ascending, dashed is descending.

6.4 Ascending/descending antenna temperature comparison

To determine pointing or navigation errors, global 1B antenna temperatures are binned and averaged in 0.5 deg latitude-longitude boxes separately for ascending and descending data. These values are then differenced. Any systematic pointing or navigation errors are revealed by red and blue shadows on opposite sides of continental coastlines.

Global 1B data for days of 152-172, 2005 are used in this study. The result shows that AMSU-A2 appears to be geo-located negatively in both along track and cross track directions (Figure 5). The AMSU-A2 navigation and pointing function in the operational software should be examined.

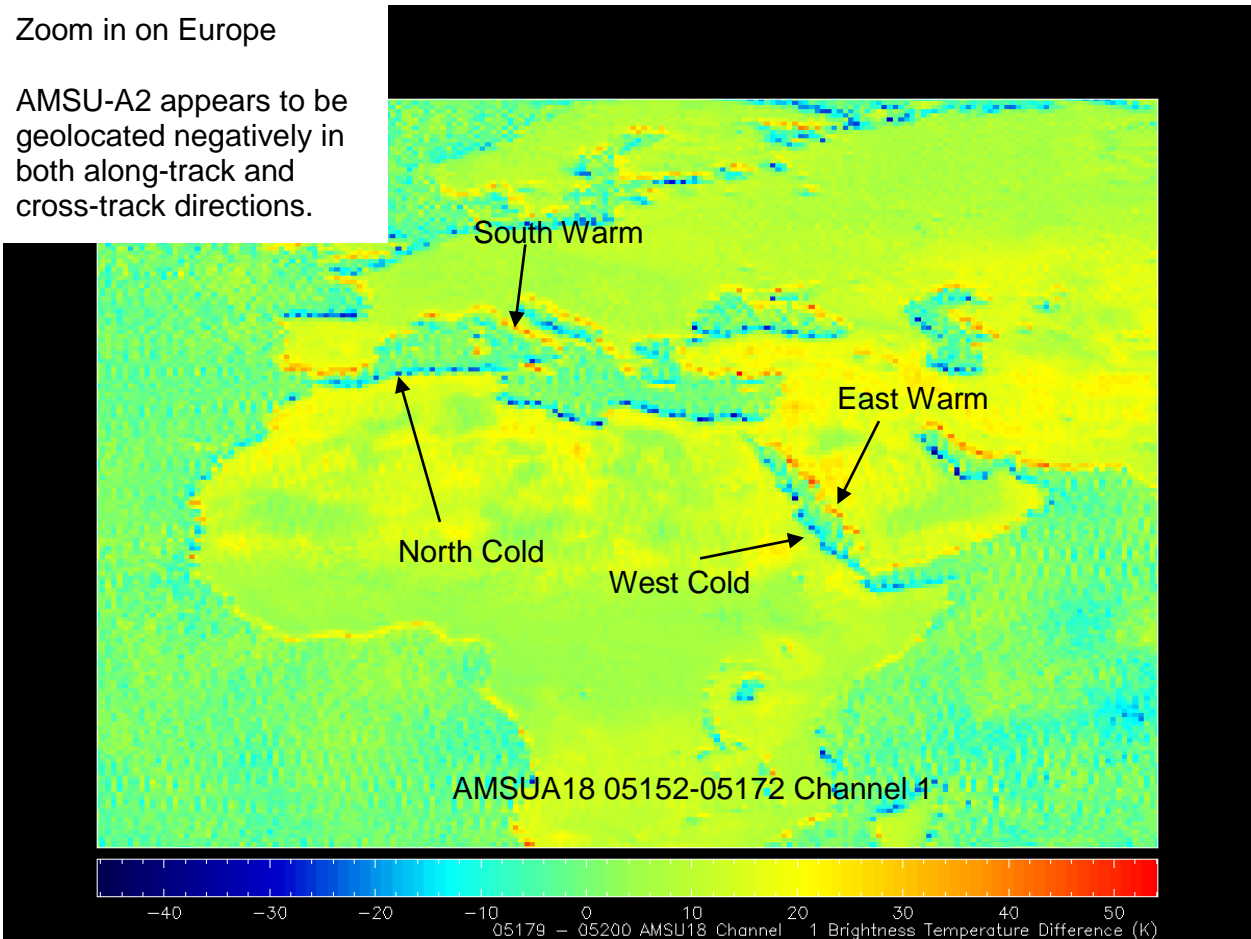


Figure 5. Results from Test of AMSU-A2 Channel 1 Ascending/Descending antenna temperature comparison

6.5 Relative pointing accuracy of MHS to AMSU-A.

To verify the consistency of readings from the AMSU-A Channel 15 with those from MHS Channel 16 (both 89 GHz window channels), MHS 89 GHz data are convoluted to AMSU-A field of view using Backus-Gilbert (Bennartz, 2000). The averaged antenna temperatures for the MHS are then plotted against the AMSU-A. The mean and standard difference is computed as a function of scan angle. A difference of greater than 1K indicates a problem in co-registration.

The weights of the Backus-Gilbert convolution will then be adjusted in order to minimize any antenna temperature difference in order to determine any offset between the two instruments.

Two orbits of data from each instrument over northern Europe and Indonesia on two consecutive days (247-250 in 2005), were used in this study.

The MHS and the AMSU-A1 appear to be mis-registered by about a half MHS field-of-view in both the along-track and cross-track directions. This corresponds to about 8 km (see Fig. 6). The geo-location and relative alignment of these two instruments should be further examined.

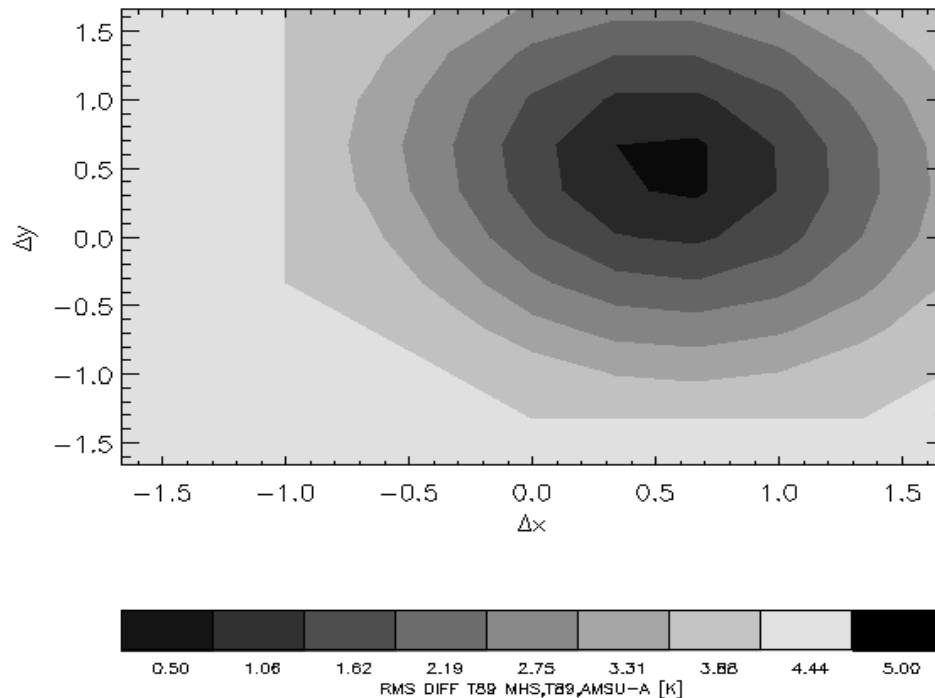


Figure 6. RMS-deviation (bias-corrected) between AMSU-A 89 GHz and Backus-Gilbert convoluted MHS 89 GHz antenna temperatures. The x-axis gives the cross-track shift in units of instrument MHS FOVS for the cross-track direction (i. e. a value of +1 means that the relative navigation of MHS to AMSU-A has to be shifted by one FOV in positive scan direction). The y-axis gives the along-track shift values of scan (i. e. a number of +1 means that the navigation has to be shifted by one scan line in positive flight direction).

6.6 Ascending/descending MHS antenna temperature comparison.

To determine pointing or navigation errors, global 1B antenna temperatures are binned and averaged in 0.5 deg latitude-longitude boxes separately for ascending and descending data. These values are then differenced. Any systematic pointing or navigation errors are revealed as red and blue shadows on opposite sides of continental coastlines.

Global 1B data for days 152-172 and 247-275 in 2005 are used in this study. Figure 7 shows a zoom in of Europe and the middle east with their complex coastlines. There is obviously a along track error and possibly a cross track error. Analysis revealed that the stepping angle in the ingestor was set to 1.1 degrees instead of the correct 10/9 degrees. Further analysis found that there was an undocumented 8/3 second buffer in the MHS Interface Unit (MIU). When both of these items were addressed in the ingestor, the navigation appears correct, as shown in Figure 8.

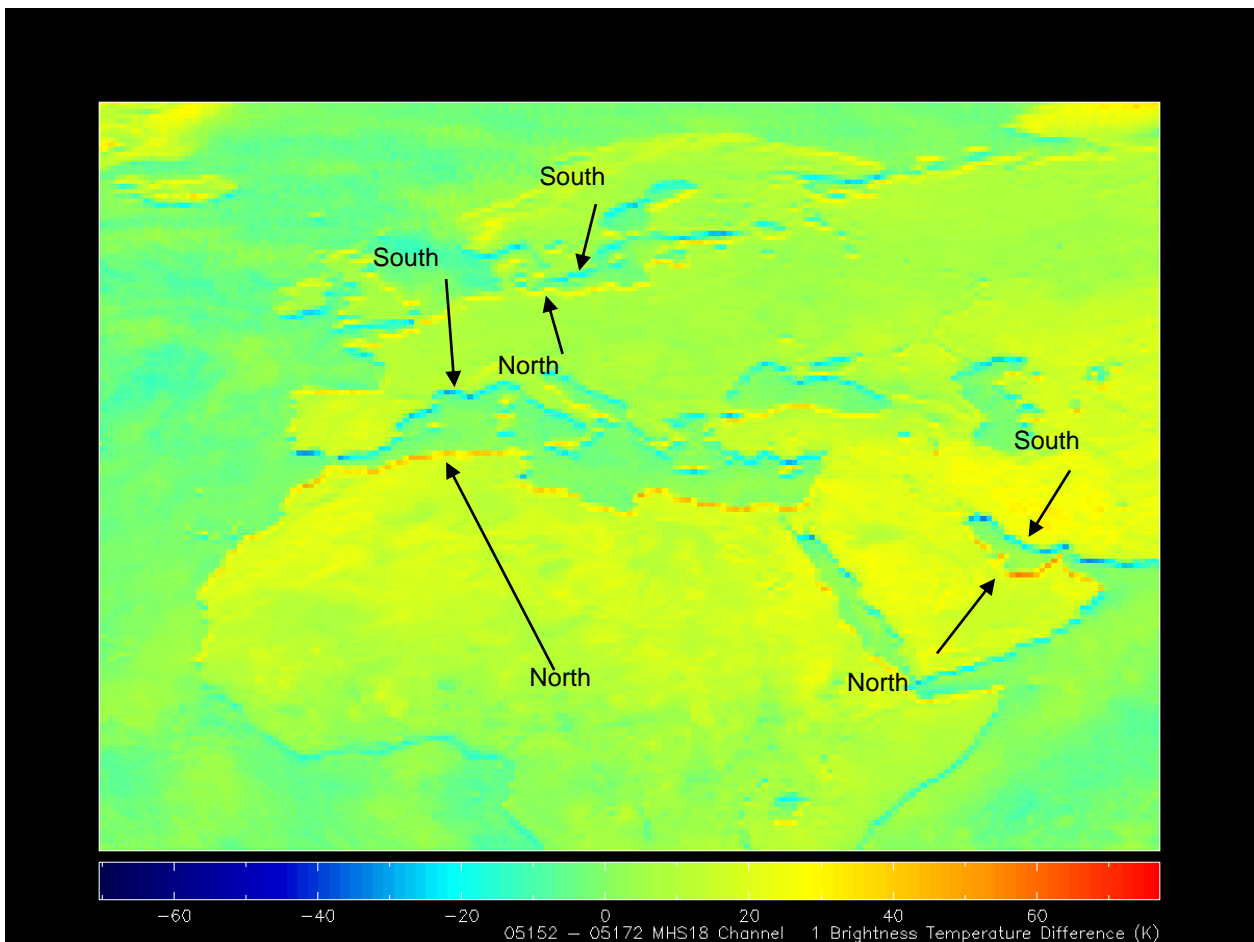


Figure 7. Ascending minus descending MHS channel 16 antenna temperatures for 2005 152-172.

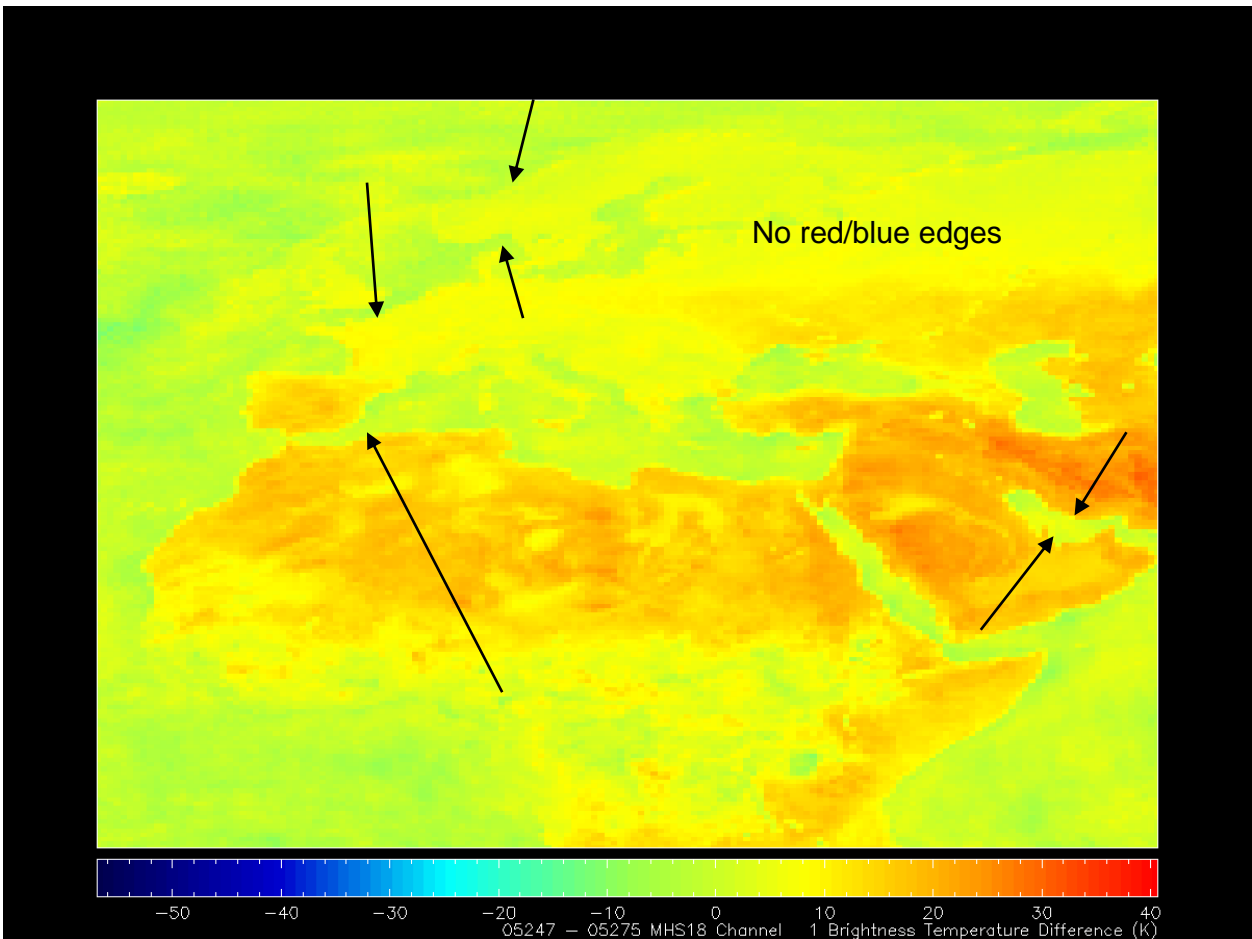


Figure 8. Ascending minus descending MHS channel 16 antenna temperatures for 2005 247-275.

6.7 MHS Scan Bias Evaluation

To determine if a cross scan bias is evident in the data, global 1B antenna temperatures are binned and averaged for each scan position. Data collected are from 40N-40S over ocean, with cloud and precipitation screening by an algorithm provided by Grody. Ascending and descending node data are plotted separately. A scan bias will be evident if one side is warmer or colder than the other.

Global level 1B data from days 152-181 in 2005 are used in this study. The test results (Figure 9) show that the window channels are ambiguous with ascending and descending portions of orbit have opposite signatures. Sounding channels show a slight bias (few tenth degree) with the right side being warmer.

As long as this bias is stable with time, the NWP analysis model can remove the bias and assimilate the data.

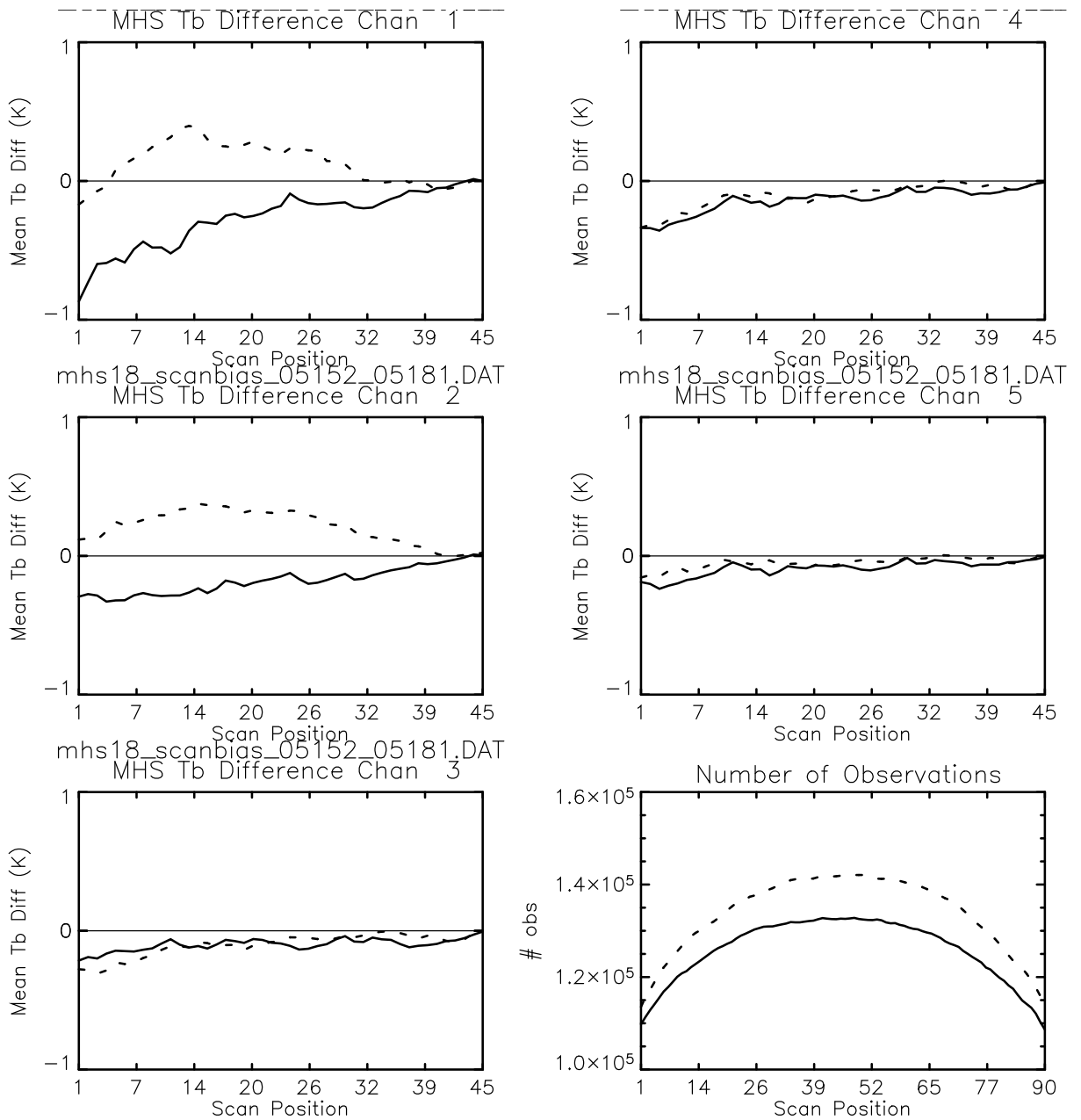


Figure 9: Pairwise Left-Right Side Antenna Temperature Difference. Solid is ascending and dashed is descending.

6.8 Absolute geo-reference of MHS

The absolute navigation accuracy can be derived by convoluting a high-resolution (550m) land-sea mask to the spatial resolution of the instrument. By varying the spatial position of the footprints and using knowledge of the sea surface temperature and homogeneous land temperatures near the coastline, the navigation accuracy can be determined and possible offsets can be identified via cross-correlation analysis.

MHS data from 12 passes over northern Europe and Indonesia over four days (2005/247-250) were used in this study. Test results show that the MHS exhibits about a 2 km cross-track and negligible along-track geo-location errors (see Table 4). The ‘Start time’ and ‘day’ identify the orbits according to NESDIS Level 1b file naming conventions. ‘Correlation’ gives the maximum correlation between land/sea-mask and observed antenna temperatures. The values for dx and dy are the corresponding navigation shifts in cross-track and along-track track direction. They are given in units of MHS instrument FOVS for the cross-track direction (i. e. a value of +1 means that the navigation has to be shifted by one MHS FOV in positive scan direction) and in units of MHS scan lines for the along track direction (i. e. a number of +1 means that the navigation has to be shifted by one MHS scan line in positive flight direction). The resulting average geo-referencing errors and standard deviations of the errors are also given in km for nadir observations in the last two rows.

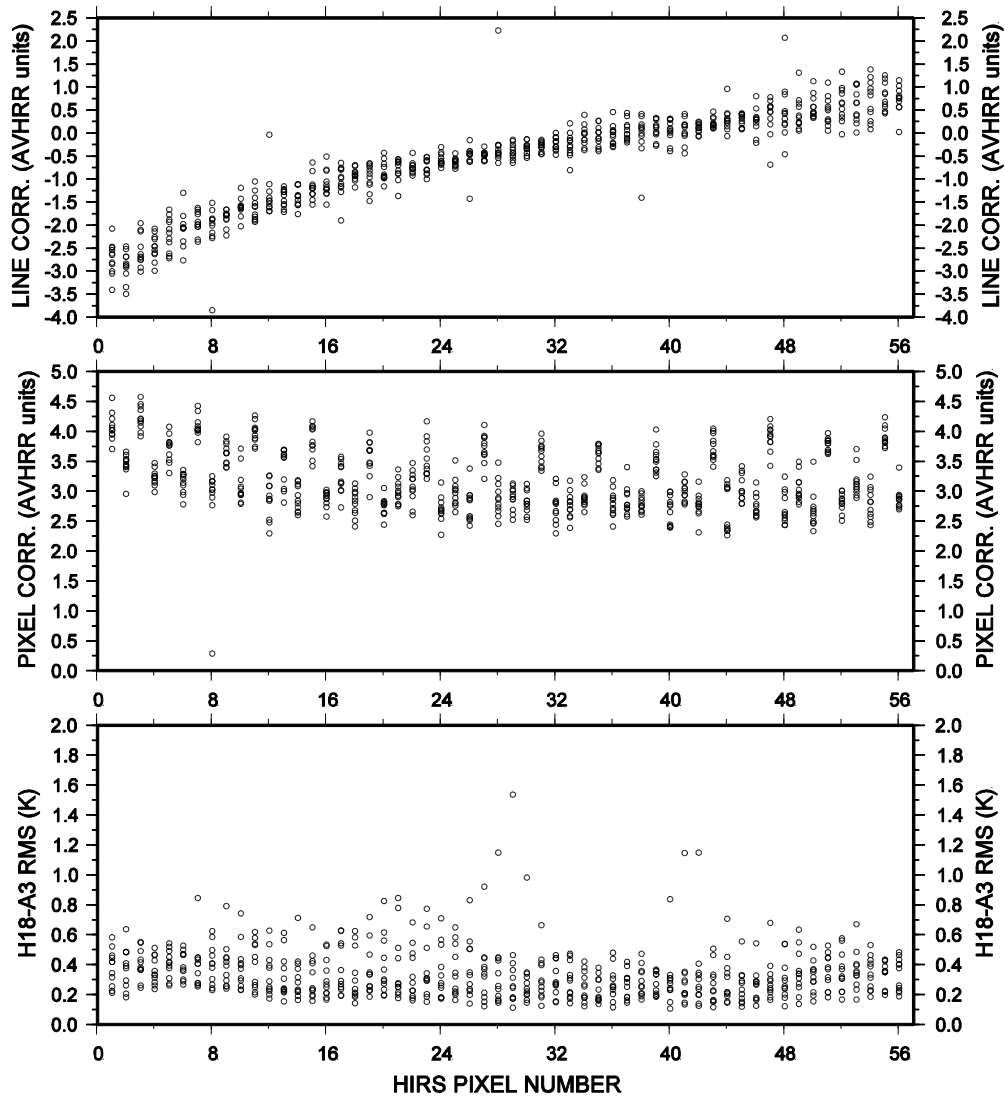
Table 4. Accuracy of MHS 89 GHz navigation for 12 different overpasses over northern Europe and Indonesia.

Day	Start	Correlation	DX	DY	Desc/Asc	Area
D05247	S0145	0.82	0.20	0.00	D	Baltic
D05247	S0334	0.68	0.20	0.40	A	Indo
D05247	S1023	0.88	0.00	0.00	A	Baltic
D05247	S1652	0.76	0.20	-0.40	D	Indo
D05248	S0134	0.84	0.20	0.00	D	Balic
D05248	S0513	0.65	0.20	0.40	A	Indo
D05248	S1013	0.88	0.00	0.00	A	Baltic
D05248	S1642	0.71	0.20	-0.40	D	Indo
D05249	S0119	0.84	0.20	0.00	D	Baltic
D05249	S0457	0.73	0.00	0.20	A	Indo
D05249	S1003	0.90	0.00	0.00	A	Baltic
D05250	S0120	0.86	0.20	0.00	D	Baltic
	Mean	Sdev	Mean[km]	Sdev[km]		
DX :	0.13	0.10	2.40	1.77		
DY :	0.02	0.25	0.30	4.46		

6.9 HIRS and AVHRR Co-registration

To verify pointing of the HIRS with respect to the AVHRR, a pseudo HIRS channel 18 is constructed from AVHRR channel 4. The fit of the pseudo channel to the real channel 18 is calculated. The location of the pseudo channel is varied until the antenna temperature difference is minimized. Any offset indicates a mis-registration between the AVHRR and the HIRS. Pascal Brunel of METEOFRENCE in Lannion performed this test. Data used in this study were collected over 39 direct readout passes at Lannion, France beginning 6/16/2005. The HIRS and the AVHRR are co-aligned to within a few AVHRR pixels (Figure 10).

Figure 10. HIRS 18 –AVHRR3 Mapping adjustment for NOAA-18



16 files From 20050621 Time 0119 Orbit 00446
 To 20050624 Time 0410 Orbit 00489

APPENDIX

**Presentations
at the ORA NOAA-18 Calibration and Validation Working Group Meeting**

August 9, 2005



Overview of ORA NOAA-18 Instrument Calibration and Validation Activities

Fuzhong Weng
Sensor Physics Branch
NOAA/NESDIS/Office of Research and Applications
September 8, 2005



Our Team

- Mitch Goldberg: ORA/SMCD Division Chief, - Management and Technical Oversight
- Fuzhong Weng: ORA/SMCD/Sensor Physics Branch Chief and NOAA-18 cal/val team leader, instrument asymmetry and microwave products and algorithms, radiance bias assessments for NWP model applications
- Changyong Cao: HIRS instrument calibration
- Fred Wu: AVHRR VIS/NIR instrument calibration
- Tsan Mo: AMSU/MHS instrument calibration
- Jerry Sullivan: AVHRR thermal channel calibration/ NDVI validation
- Tony Reale: HIRS/AMSU/MHS sounding channel/products validation
- Mike Chalfant: HIRS/AMSU/MHS sounding channel/products validation /geolocation
- Ralph Ferraro: AMSU/MHS window channels/MSPPS products validation
- Larry Flynn: SBUV product validation
- Tom Kleespies: AMSU on-orbit verification
- Hank Drahos: Sounding product validation
- Dan Tarpley: AVHRR product NDVI monitoring
- John LeMarshall (JCSDA): Impacts assessments of NOAA-18 data for NWP applications
- Stephen English (UK): tests of direct readout data and NWP impacts demonstration
- Alex Ignatov: AVHRR SST and aerosol products
- Ninghai Sun: Cal/val IT supports



Activities of the ORA NOAA-18 Cal/Val Team

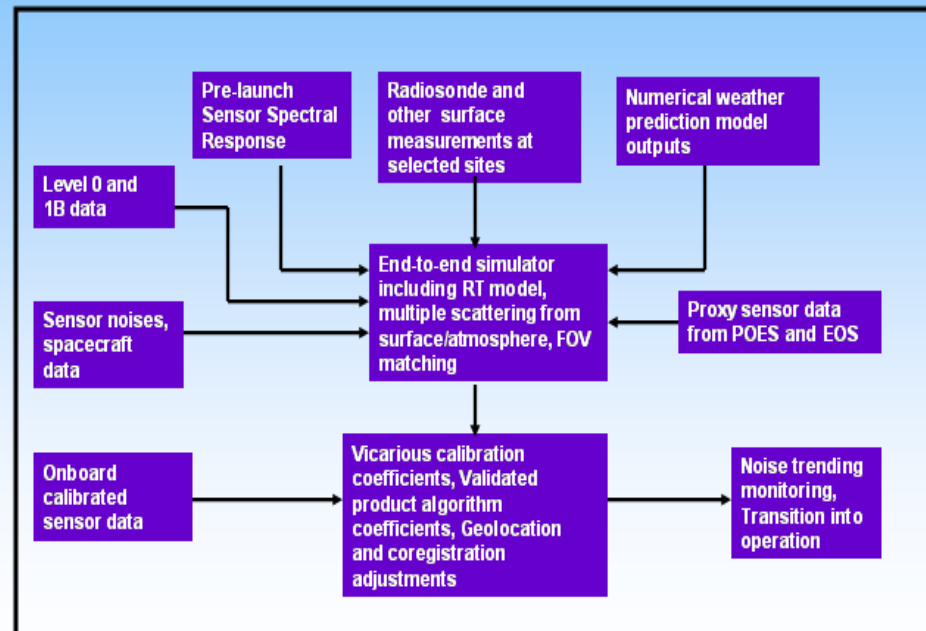
- Monitor and quantify instrument noises through analyzing calibration target counts and channel space view measurements
- Assess instrument geolocation biases and co-registration and provide recommended solutions for satellite roll and pitch adjustments
- Characterize other systematic biases in radiance through rigorous forward modeling and inter-satellite calibrations
- Provide initial demonstration and assessments of NOAA-18 data for improving numerical weather prediction
- Validate product algorithms (e.g. ATOVS and MSPPS, TOAST, UV index, NDVI, SST, AOD) for transition into operation
- Communicate with NOAA-18 OV team, instrument vendors and users with timeliness diagnostics of instrument performances and provide root cause analyses



Long-Term Goals of ORA's Cal/Val Program

- Develop an Integrated Cal/Val System Framework to enhance ORA's capability and efficiency to provide outstanding calibration and validation to METOP, NP, NPOESS, and GOES-R
- Outcome >>> Provide timely and accurate assessments of NOAA instrument's on-orbit performances and the impacts of noise and loss of channels on operational products and data assimilation

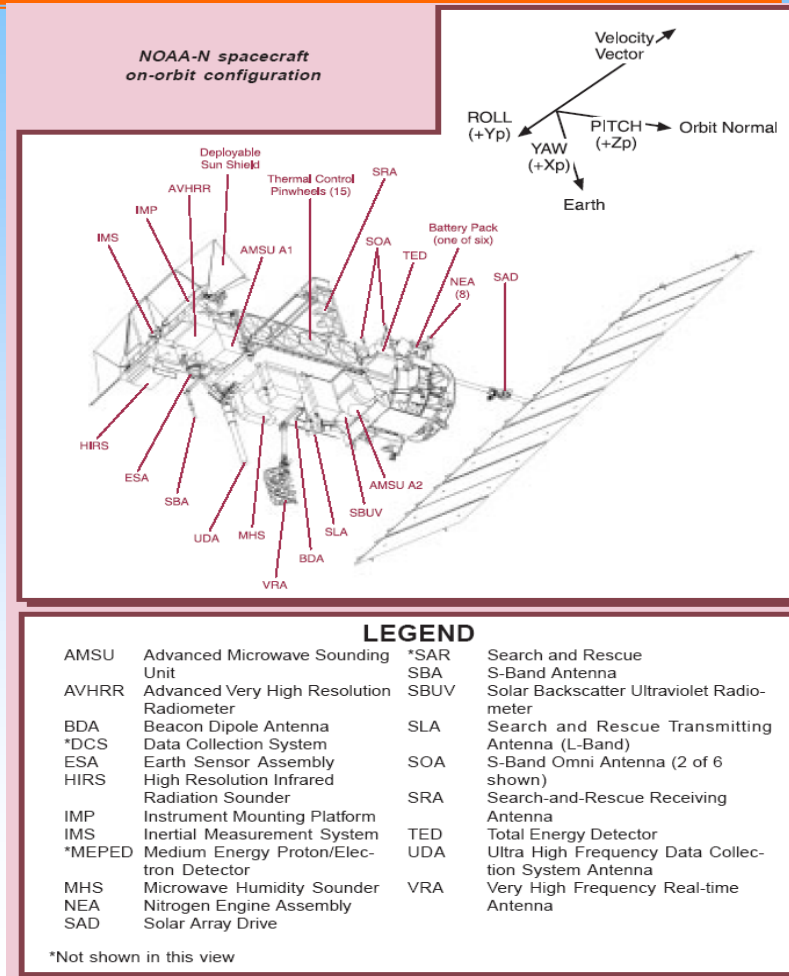
ORA Post-Launch Integrated Cal/Val System Framework





NOAA-18 Instrument Assessments

- AVHRR/3 Advanced Very High Resolution Radiometer
- HIRS/4 High Resolution Infrared Sounder
- AMSU-A Advanced Microwave Sounding Unit-A
- MHS Microwave Humidity Sounder
- SBUV/2 Solar Backscattered Ultraviolet Radiometer

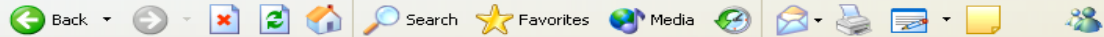




POES Cal/Val Website

NOAA-N Calibration and Validation - Microsoft Internet Explorer

File Edit View Favorites Tools Help

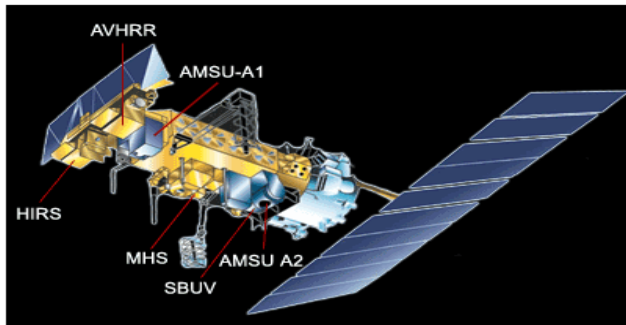


Address <http://www.orbit.nesdis.noaa.gov/smcd/spb/n18calval/index.html>

Go Links



NOAA-18 Instrument Calibration & Validation



What's New in NOAA-18 Instrument Cal/Val

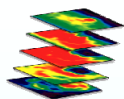
- ▶ [ORA NOAA-18 Cal/Val Group Meeting \(August 9, 2005, Agenda\)](#)
- ▶ [NOAA-18 SBUV/2 ozone products are compared with NOAA-16 and 17 derived products](#)
- ▶ [Optimized AMSU antenna pattern correction \(APC\) scheme for NOAA-18 AMSU with beam position 30 APC coeff.](#)
- ▶ [HIRS Intersatellite Calibration - SNO results using NOAA-17/18 HIRS data are shown through linkage](#)

[... More](#)

Background	Calibration & Validation Information					Archiving
Long-Term Goals	AMSU-A	MHS	HIRS/4	AVHRR/3	SBUV/2	Briefings
Cal/Val Activities	Instrument Noise Characterization	Meetings				
Sensor Summary	Geolocation & Co-registration					
Cal/Val Team	Products Demo & NWP Readiness	Products Demo				
Linkage	Spectrum Response					

NOAA-18 on-Orbit Verification Conducted by NOAA Scientists

Task #	Task Name	Status	Key Results	Principal Investigators
AM1005/2005	Instrument trending	Completed	stable	Mo
AM1007/2007	Determination of optimal space view	Completed	A1 @ SV1, A2 @SV2	Mo
AM1008/2008	noise measurements-all channels	Completed	Meet the spec	Mo
AM1009	satellite to satellite comparison	Completed	some difference	Mo
AM1010/2010	BB PRT temperature accuracy	Completed	meet spec	Mo
AM1011	Earth-scence bias characterization	Completed	A1 cross-track asymmetry	Weng, Kleespies
AM1012/2012	Channel co-registration	Completed	Along &cross track errors are quatified	Kleespies, Bennartz, Chalfant
MHS010	Lunar contamination in space view	on-going	Capture some signals	Mo
MHS011	Channel registration	Completed	Along &cross track errors are quatified	Chalfant, Kleespies
MHS013	MHS/AMSU-A 89 GHz comparison	Completed	Generally bias < 0.5K, nearly 1.0K in limb	Boukabara
MHS014	Earth-view bias characterizations	Completed	Small particular cross-track asymmetry	Kleespies
MHS016	MHS radiometric comparison with AMSU-B	Completed	noticeable difference at Ch17, 20	Reale, Ferraro, Kleespies
SBUA01	Range 3 Cathode/Anode	Completed	Consistent Change	SSAI
SBU012	Diffuser and Solar	Partially	Significant	SSAI
SBU007	Wavelength Scale	Completed	Small Shift	SSAI
SBUA05	OOBR estimation from position mode	Partially	Correction Needed	Flynn/SSAI
SBUA11	NOAA-16 Comparison	Partially	Differences noted	Kondragunta
AVH005	space clamp noise and stability	Completed	stable	Sullivan
AVH010	NEDT/Dynamic range - channel 3B,4,5	Completed	meet the spec	Sullivan
AVH011	instrument stability - channels 3B,4,5	Completed	stable	Sullivan
AVH014	operational calibration	Completed	ch1,2,3A	Wu/Sullivan
AVH018	Detection of land-sea boundary	Completed	nearly one pixel offset	Sullivan
AVH019	NOAA-18, 17, and 16 comparison	Completed	NDVI/SST/Aerosols	Tarpley/Ignatov
AVH022	striping evaluation	Completed	No striping	Wu/Sullivan
HIR011	NEDN - IR channels	Completed	More chs meet spec	Cao
HIR012	Instrument stability	Completed	noise fluctuated	Cao
HIR013	instrument trending	Completed	new website	Cao
HIR014	Detection of land-sea boundary	Completed	no geolocation errors	Chalfant/Cao
HIR015	Satellite-to-satellite comparsion	on-going	biase in some chs	Reale/Cao



NOAA-18/HIRS Noise Status Update

Channel	Req't (mW/m ² -sr-cm ⁻¹)	NEDN (orbital avg 9/2/05)	
		Blackbody	Spaceview
1	3.0	N/A	N/A
2	0.67	0.759	0.883
3	0.50	0.330	0.365
4	0.31	0.367	0.390
5	0.21	0.283	0.311
6	0.24	0.262	0.308
7	0.20	0.230	0.257
8	0.10	0.084	0.094
9	0.15	0.170	0.170
10	0.15	0.234	0.256

Channel	Req't (mW/m ² -sr-cm ⁻¹)	NEDN (orbital avg 9/2/05)	
		Blackbody	Spaceview
11	0.20	0.173	0.187
12	0.20	0.169	0.180
13	0.006	0.002	0.002
14	0.003	0.001	0.001
15	0.004	0.001	0.001
16	0.004	0.001	0.001
17	0.002	0.001	0.001
18	0.002	0.001	0.001
19	0.001	0.0004	0.0004



Channels fluctuating around the spec



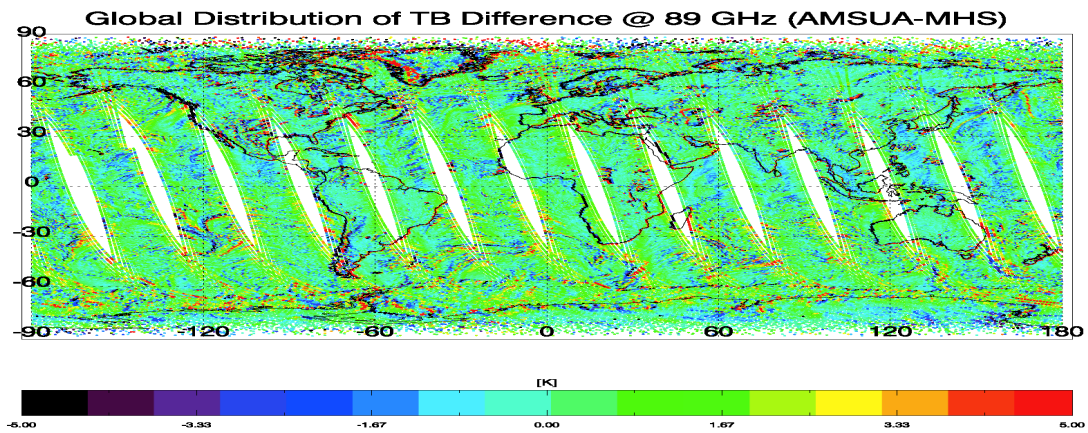
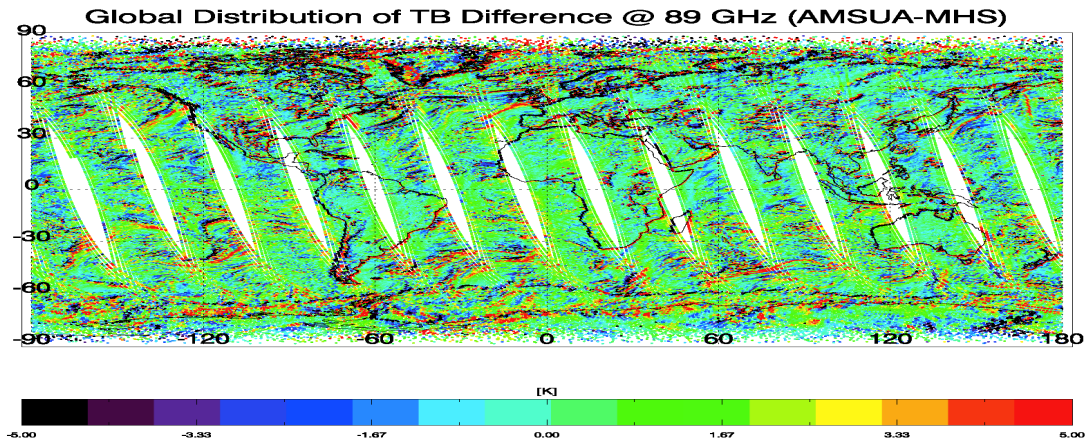
Channels meet spec



Ch1 cannot be calibrated



MHS013 – AMSU/MHS 89 GHz Comparison





ORA NOAA-18 OV Presentation

- HIRS/4 Calibration - Changyong Cao
- AVHRR/3 IR Calibration Overview - Jerry Sullivan
- AVHRR/3 VIS/NIR Calibration - Fred Wu
- AMSU Calibration Overview - Tsan Mo
- MHS Calibration Overview - Tsan Mo
- SBUV/2 OV - Larry Flynn
- AMSU and MHS Geolocation - Tom Kleespies



AMSU Cross-Track Asymmetry, Antenna Pattern Correction, Limb-Correction Algorithm Validation

Fuzhong Weng, Quanhua Liu and Tsan Mo
Office of Research and Applications

ORA NOAA-18 Cal/Val Meeting, August 9, 2005

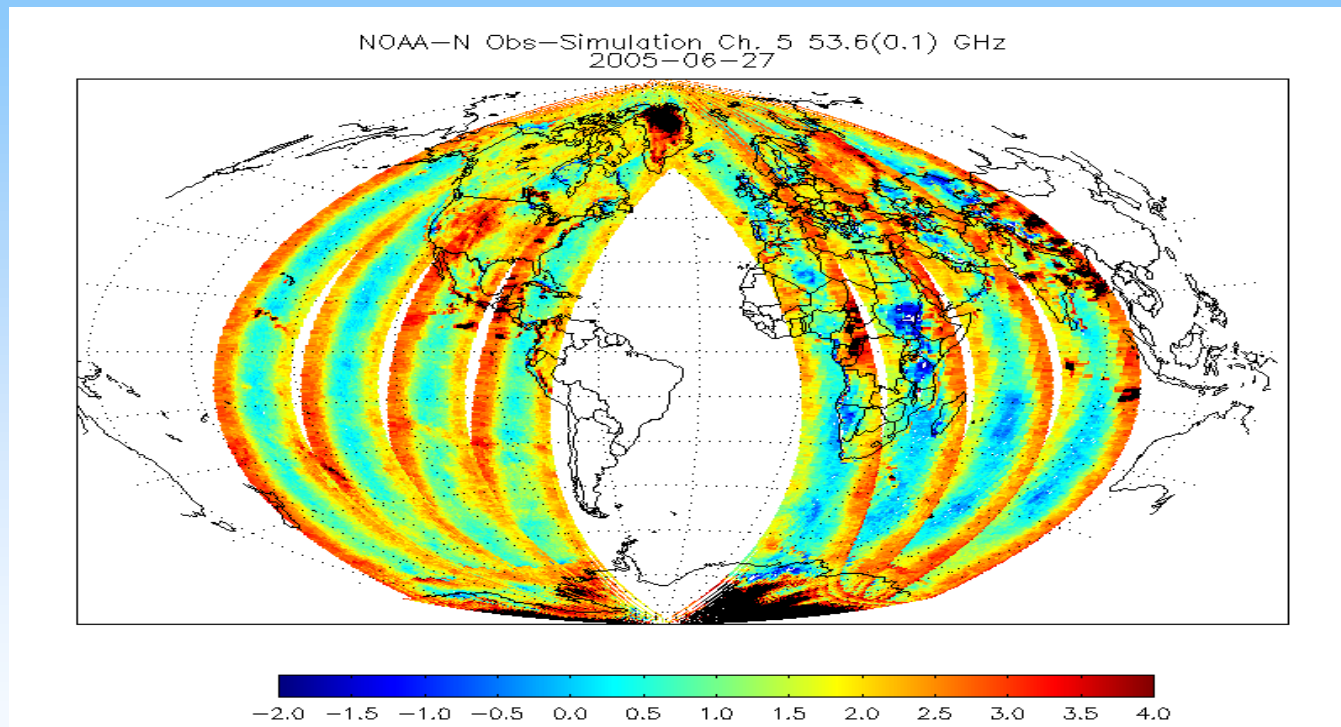


What is the Asymmetry?

- Definition:
 - Observed temperature difference for pairwise left and right scan positions assuming the same scene temperature
- How to Detect:
 - Observations under cloud-free conditions
 - Most evident from window channels
 - Relative asymmetry: mean brightness temperature difference
 - Absolute asymmetry: Mean difference between simulated and observed brightness temperatures
- How to Correct:
 - Optimized the antenna pattern correction reduces asymmetry
 - Curve-fitting to the mean absolute asymmetry



NOAA-18 AMSU-A1 Asymmetry

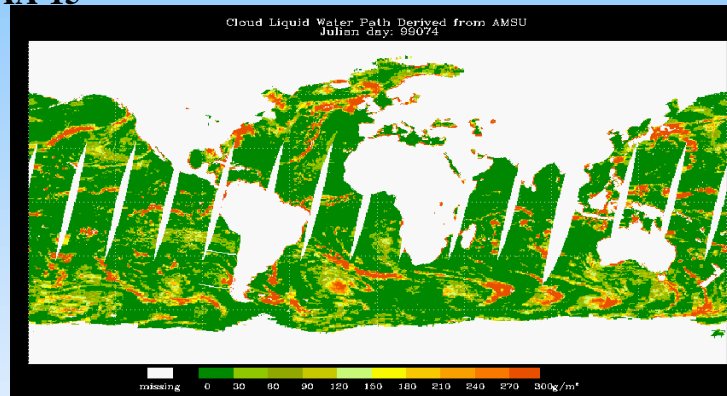
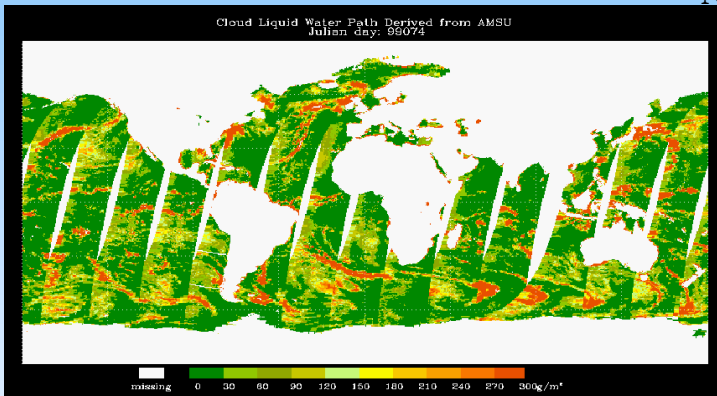


Global NWP analysis results (T,q, wind,sst...) are used as inputs to radiative transfer model.....

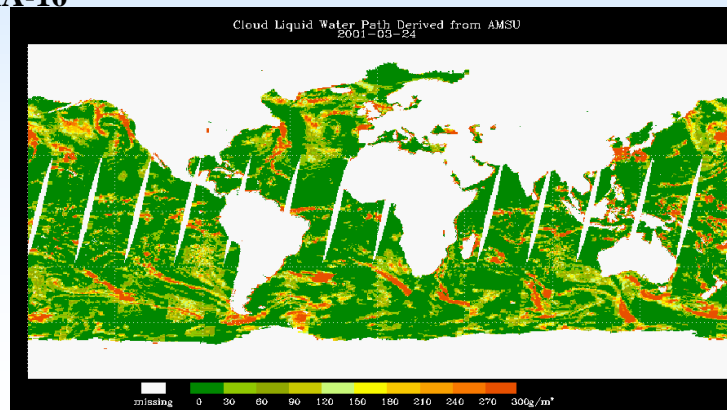
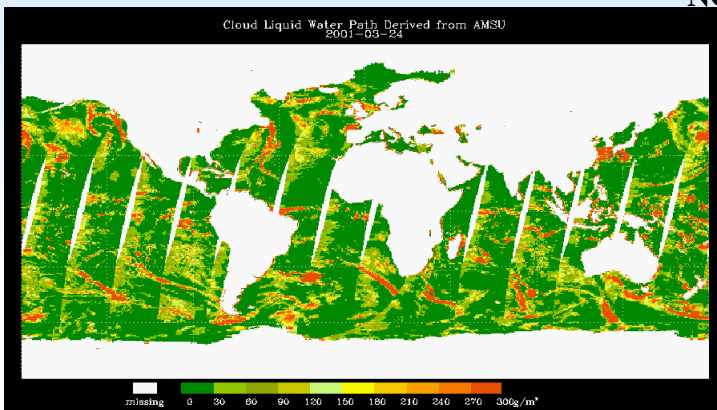


AMSU Cloud Liquid Water

Without Asymmetry Correction NOAA-15 With Asymmetry Correction

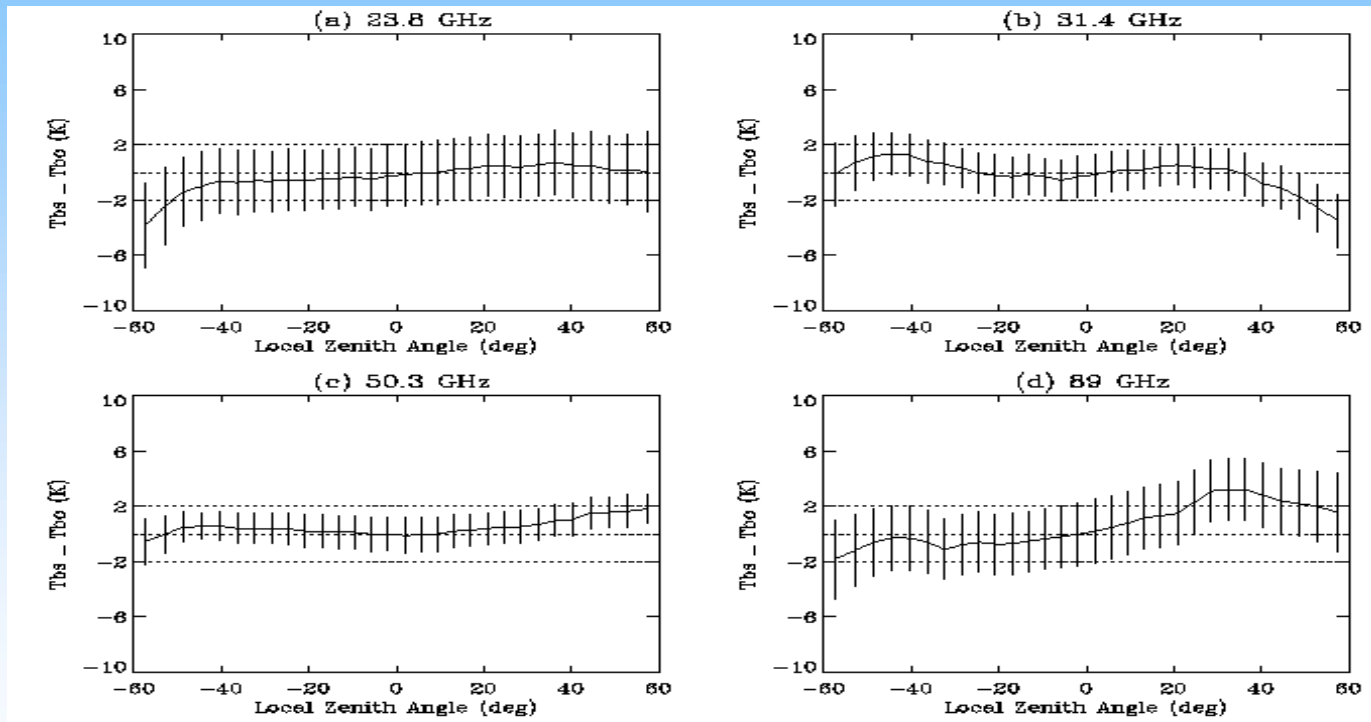


NOAA-16





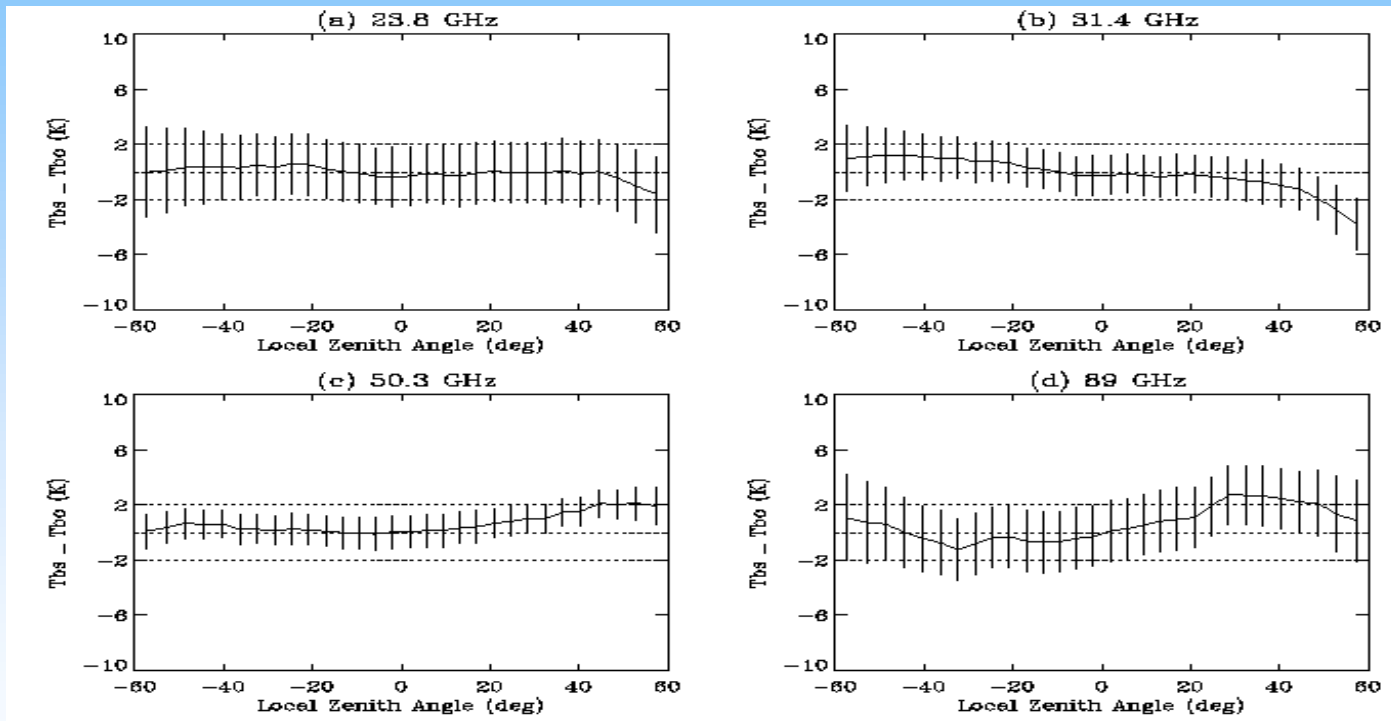
NOAA-15 AMSU-A Asymmetry Correction



$$\Delta T = A_0 \exp\{ -0.5[(\theta - A_1) / A_2]^2 \} + A_3 + A_4 \theta + A_5 \theta^2$$



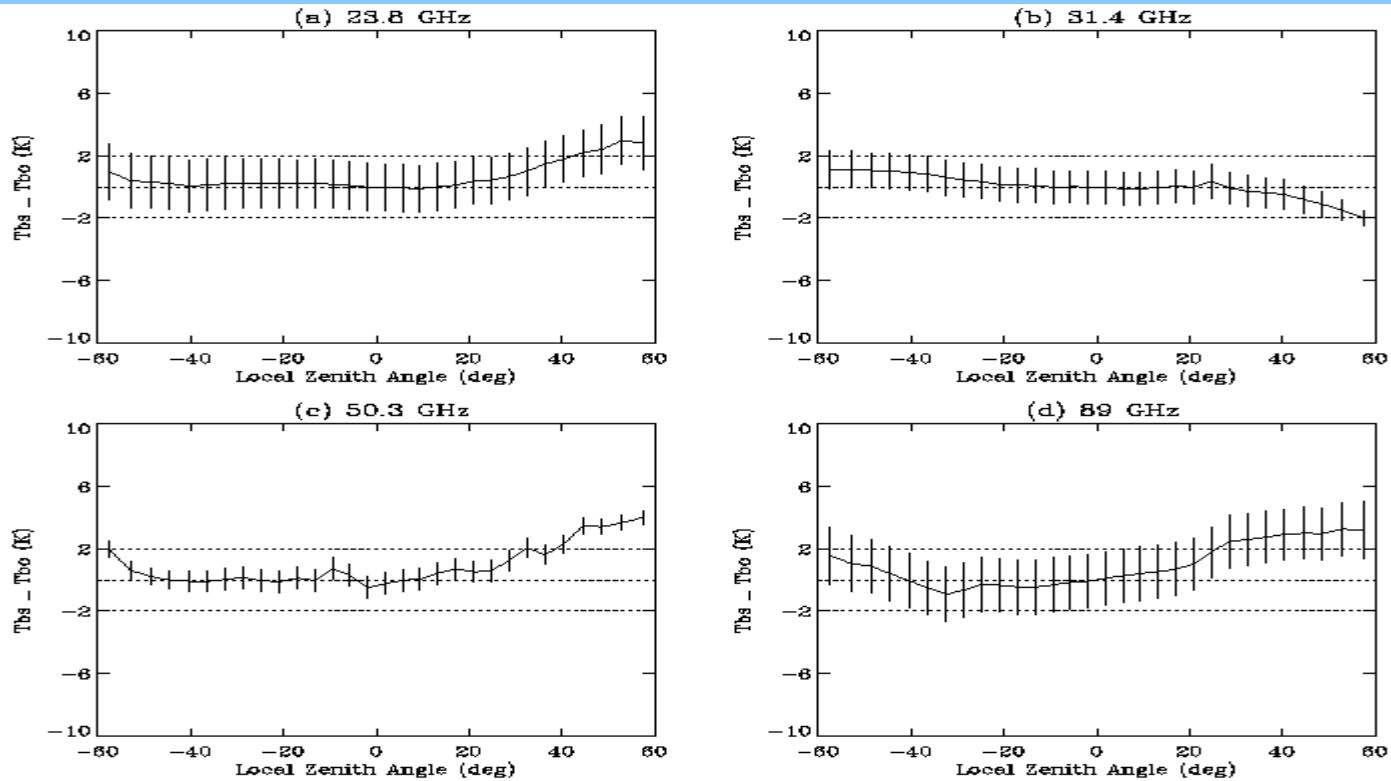
NOAA-16 AMSU-A Asymmetry Correction



$$\Delta T = A_0 \exp\{ -0.5[(\theta - A_1) / A_2]^2 \} + A_3 + A_4 \theta + A_5 \theta^2$$



NOAA-17 AMSU-A Asymmetry Correction



$$\Delta T = A_0 \exp\{ -0.5[(\theta - A_1) / A_2]^2 \} + A_3 + A_4 \theta + A_5 \theta^2$$



Possible Causes for AMSU Asymmetry

- A misalignment of AMSU polarization vector
 - Mostly noticeable at clean window channels
- Errors in Instrument pointing angle
 - It is unlikely because the cross-track pointing error (0.1 to 0.3 degree) is not large enough to produce this kind of asymmetry.
- Side lobe intrusion to the solar array
 - There should be some latitudinal dependence
 - The response would occur at multiple channels

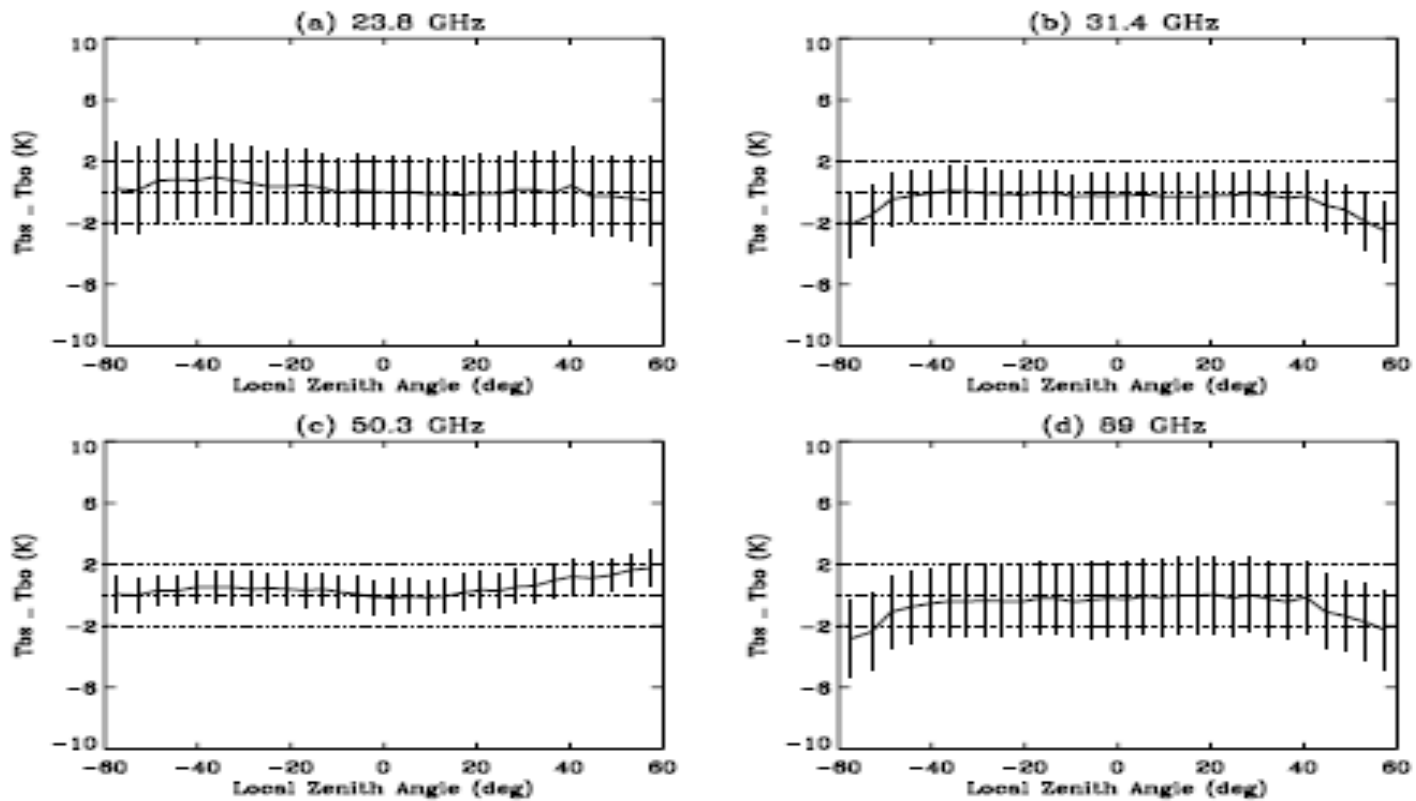


NOAA-18 Asymmetry Correction

- New Process:
 - Apply the antenna pattern correction scheme (APC) which converts T_a to T_b
 - Optimization from three APC (OAPC) schemes (BP 1, 15 and 30) tends to reduce symmetry
 - Deliver OAPC to user community (e.g. AAPP)
- How to Correct:
 - Curve-fitting to the mean absolute TB asymmetry after the OAPC is applied.



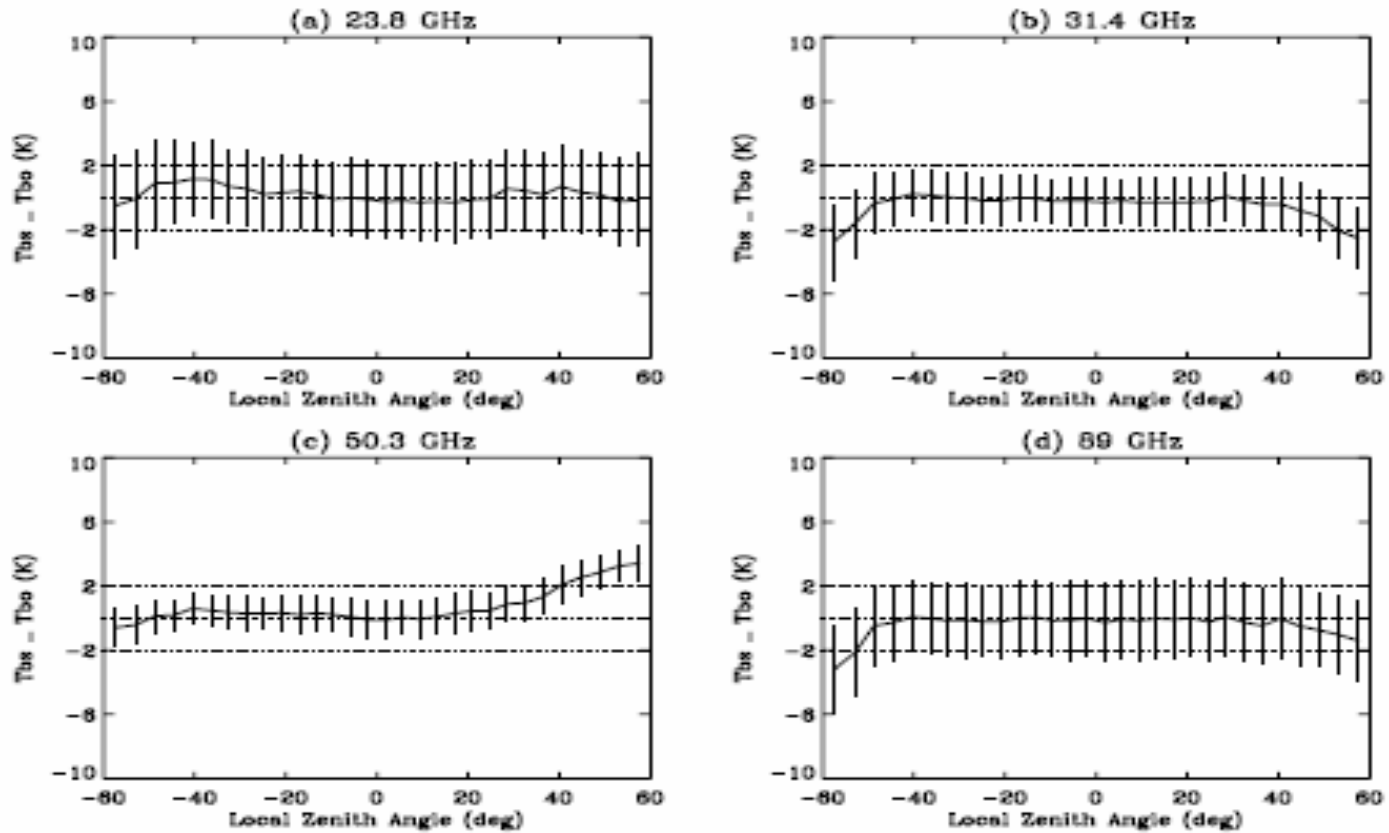
Antenna Pattern Correction from BP30



AMSU-A1-2 module (50 GHz) are best corrected with the antenna pattern correction coefficients from beam position 30



Antenna Pattern Correction from BP1



AMSU-A1-2 module (50 GHz) are corrected with the antenna pattern correction coefficients from beam position 1



What is the Limb Effect?

- The variation in the cross-track measurements due to the change of the scanning angle is called a limb effect
- The effect can be as much as 30 K for the 23.8 GHz water vapor channel, and 15 K for troposphere sounding channels (Goldberg et al., 2001)
- The limb effect is a darkening brightness temperature for infrared sounding channels. This effect can be either limb-darkening or brightening
- Unadjusted measurements prevent the objective analysis of weather system from channel measurements and also make the retrieval algorithm complicated
- Climate study requires that the data are limb adjusted prior to averaging.



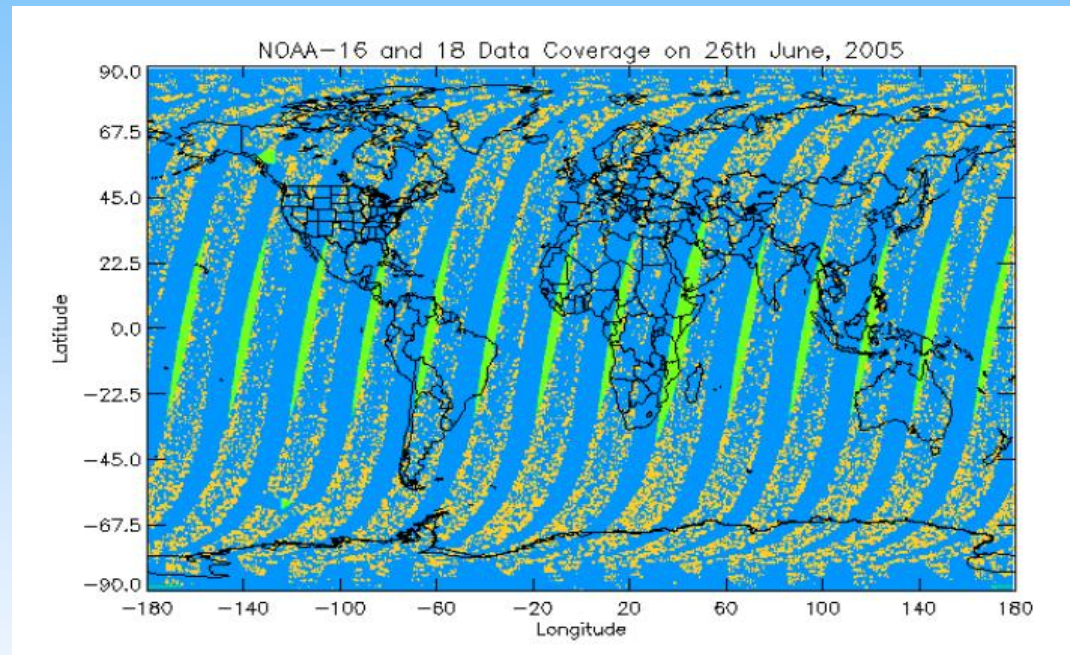
Limb-Correction Algorithm

- Limb-correction algorithm adjusts the off-nadir brightness temperature to the nadir-like brightness temperature
- The effect may be corrected from a multi-channel approach (Goldberg's approach)



NOAA-16 and 18 Orbit Coverage

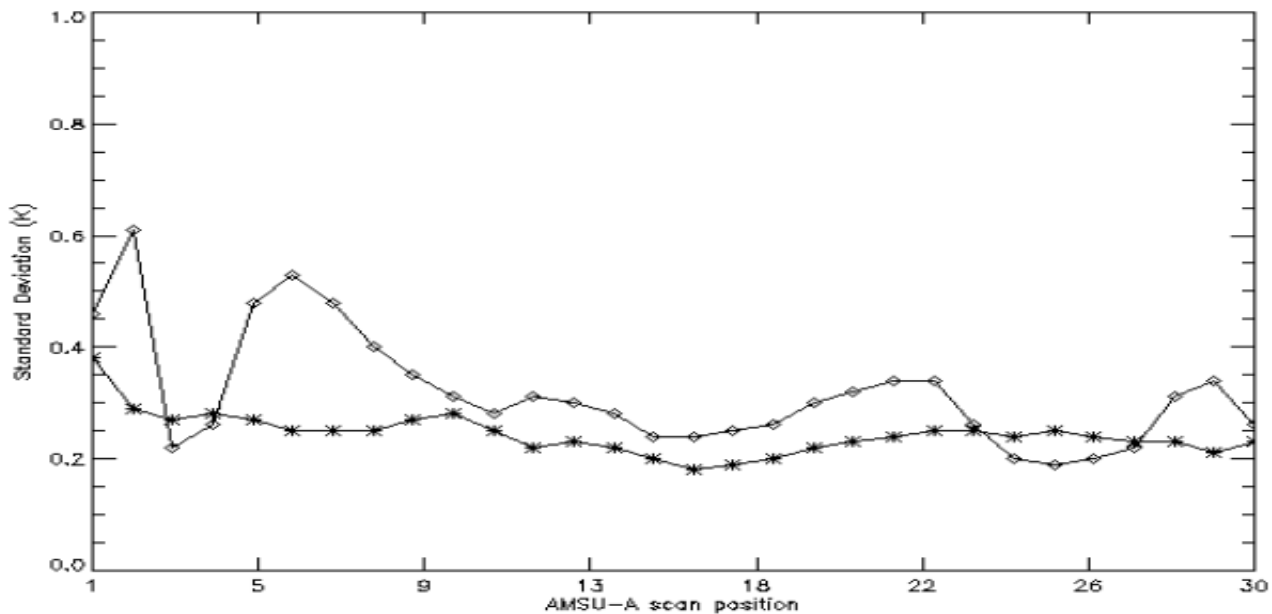
- The same storm is viewed from two different viewing angles (a lot of operational information, testing limb-correction with real time data)



Global coverage and overlap of the NOAA-16 and 18 orbit data. The cyan color represents NOAA-16 orbit data. The green represents NOAA-18 data appearing at the gap of the NOAA-16 orbits. The orange is for the overlap of the NOAA-16 and 18 orbit data within a spatial difference of 10 km



Validation of Limb-Correction Algorithms



The standard deviation the nadir measured (NOAA-18) and limb-corrected (NOAA-16) brightness temperatures at channel 6 of NOAA AMSU-A. The symbol star is for over ocean and the symbol diamond is for over land



Summary

- NOAA-18 AMSU instrument cross-track biases are quantified and A1 module displays the largest asymmetry
- The A1 cross-track asymmetry can be significantly reduced with the optimized antenna pattern correction scheme (beam position 30)
- The quality of AMSU products (e.g. cloud liquid water and precipitable water) is significantly improved
- The nadir observations from NOAA-18 and the off-nadir ones from NOAA-16 AMSU are used to verify the limb-correction algorithm which is vital in NESDIS sounding product system. The Goldberg's algorithm works well.

Microwave Surface and Precipitation Products Systems (MSPPS) Update

Ralph Ferraro and Fuzhong Weng

5 August 2005

9 August 2005

N18 Cal/Val Working Group Meeting



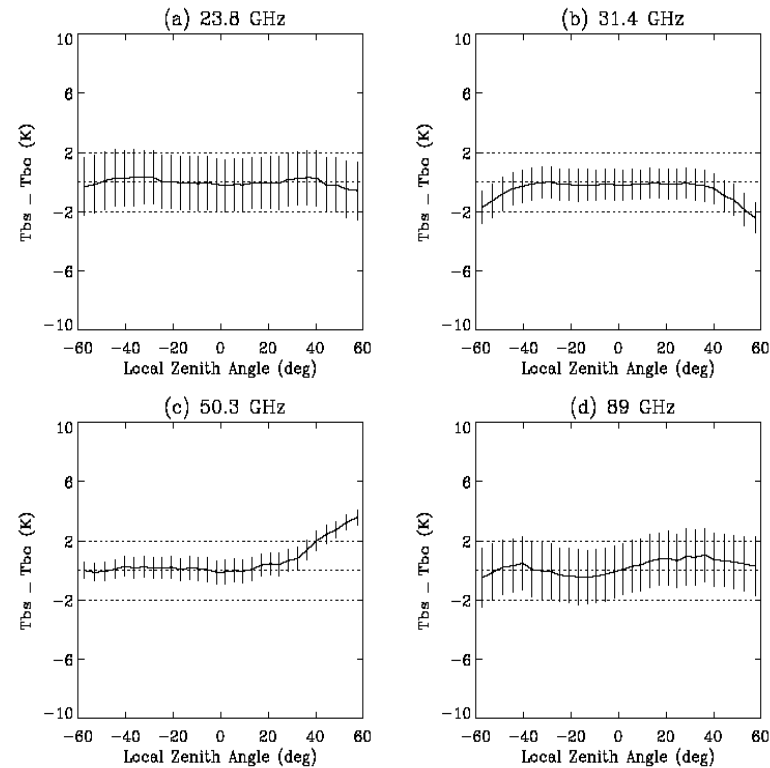
Topics

- AMSU-A Asymmetry
 - Impacts on CLW and TPW
 - Monitoring
- MHS vs. AMSU-B
 - Impacts on IWP, precipitation rate, SWE
- Overall product quality
 - Intercomparisons with N-15, N-16, N-17, DMSP

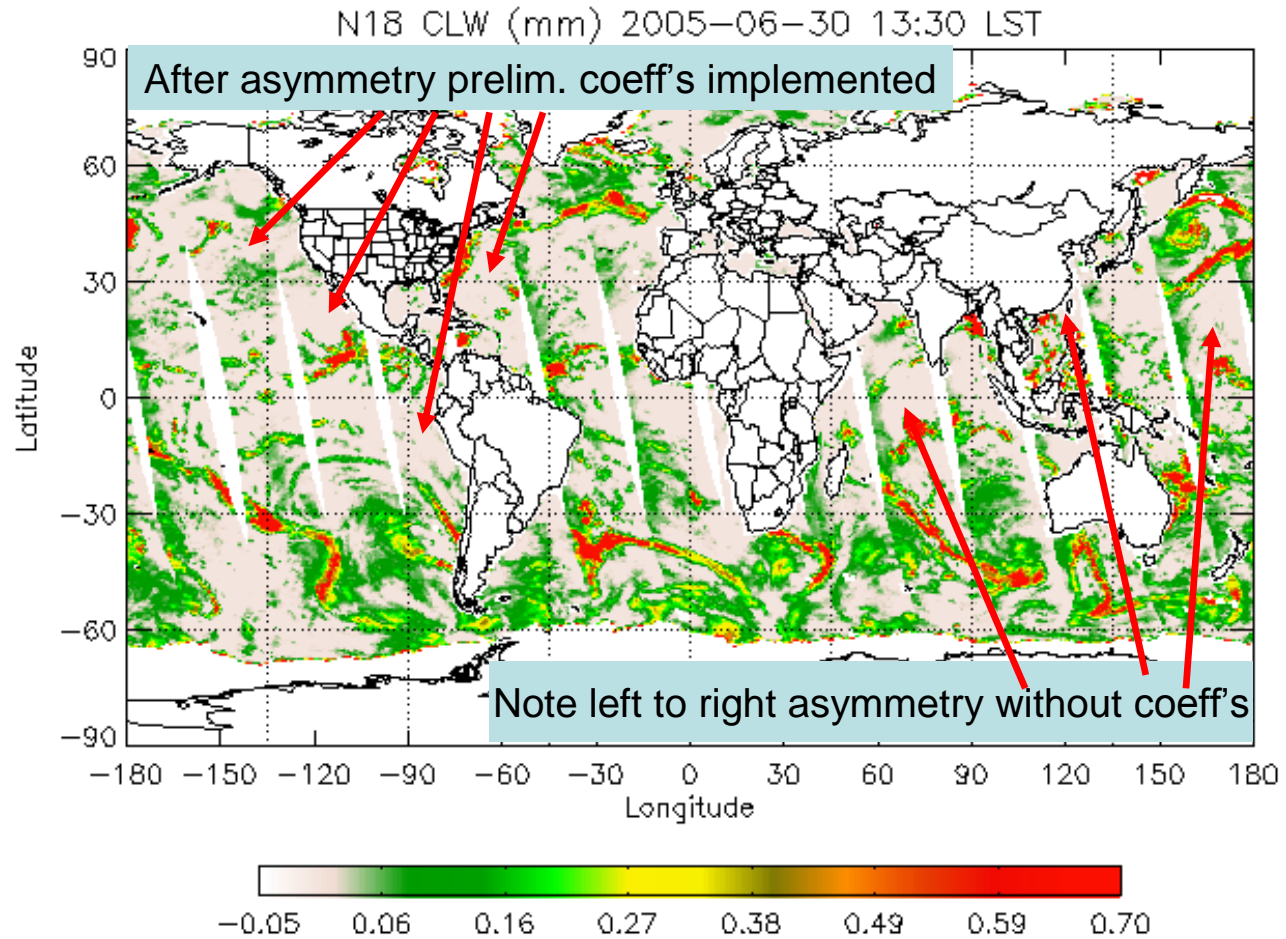


AMSU-A Asymmetry

- Coefficients derived using 30 days of AVHRR, GDAS and AMSU-A data
 - Clear sky
 - RT calculations
 - APC at BP 1
- Asc/Dsc (example is Asc)
- Vastly improves MSPPS ocean products, in particular, TPW and CLW
- 5-day mean asymmetry monitoring
- Coefficients delivered to OSDPD for implementation



Product Impacts - CLW

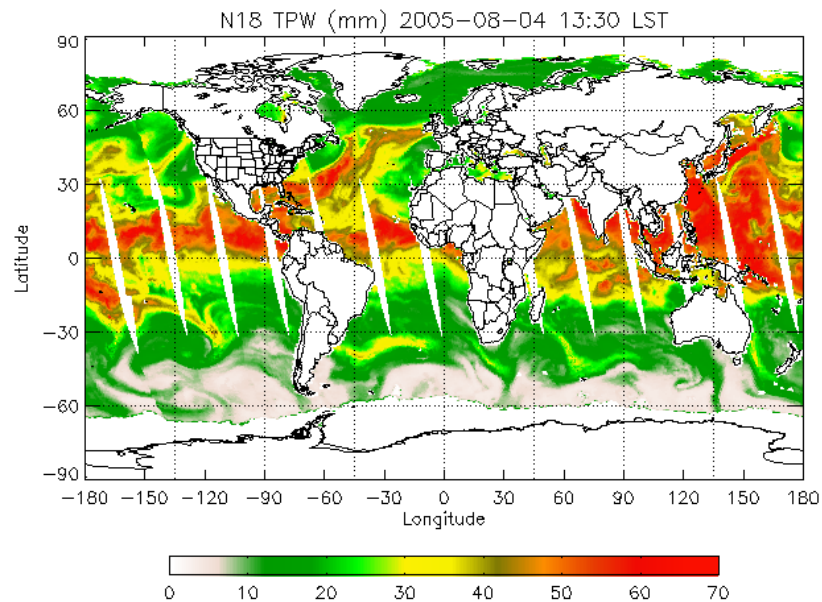
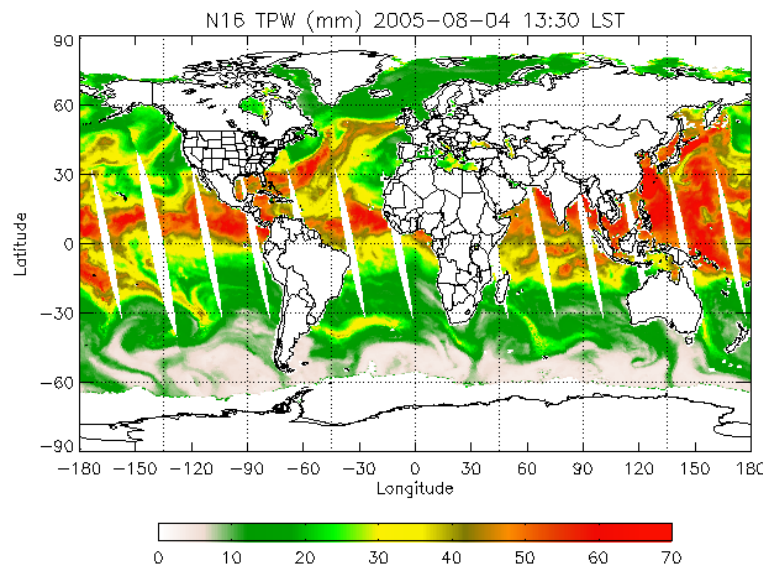


9 August 2005

N18 Cal/Val Working Group Meeting



N16 and N18 TPW Comparisons

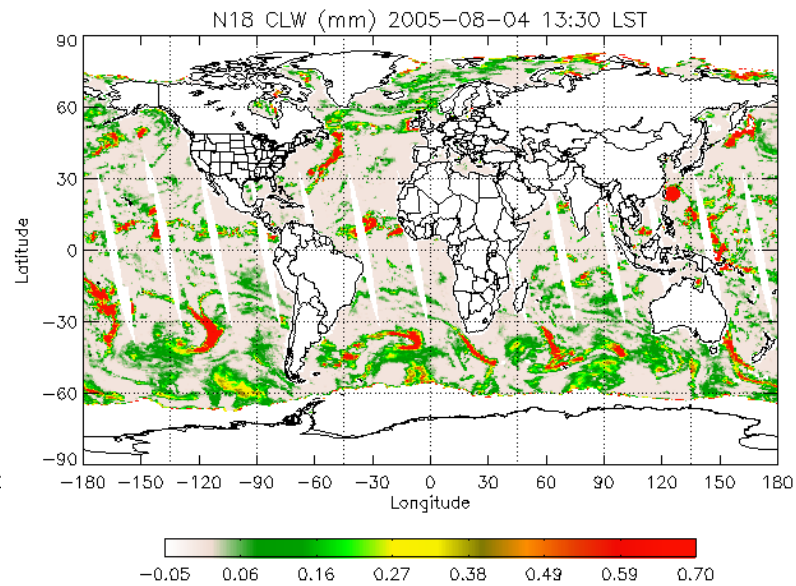
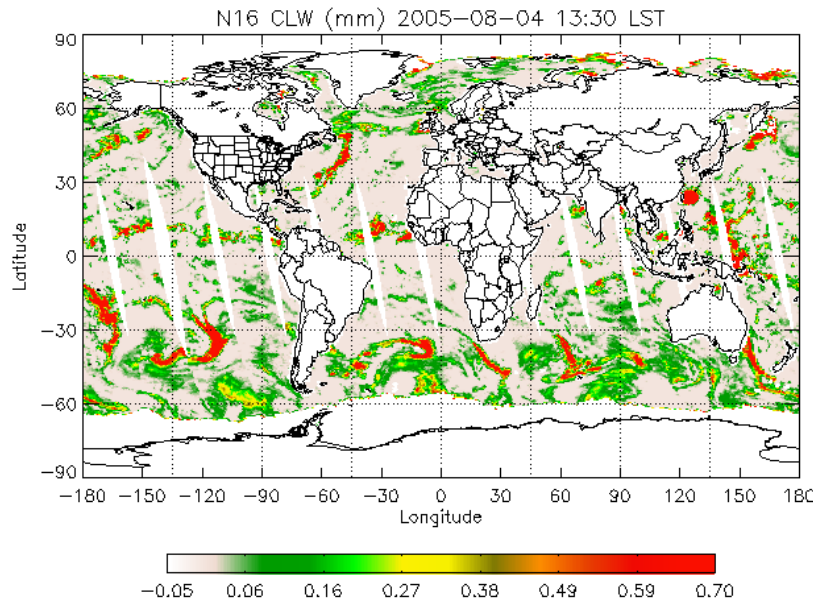


9 August 2005

N18 Cal/Val Working Group Meeting



N16 and N18 CLW Comparisons



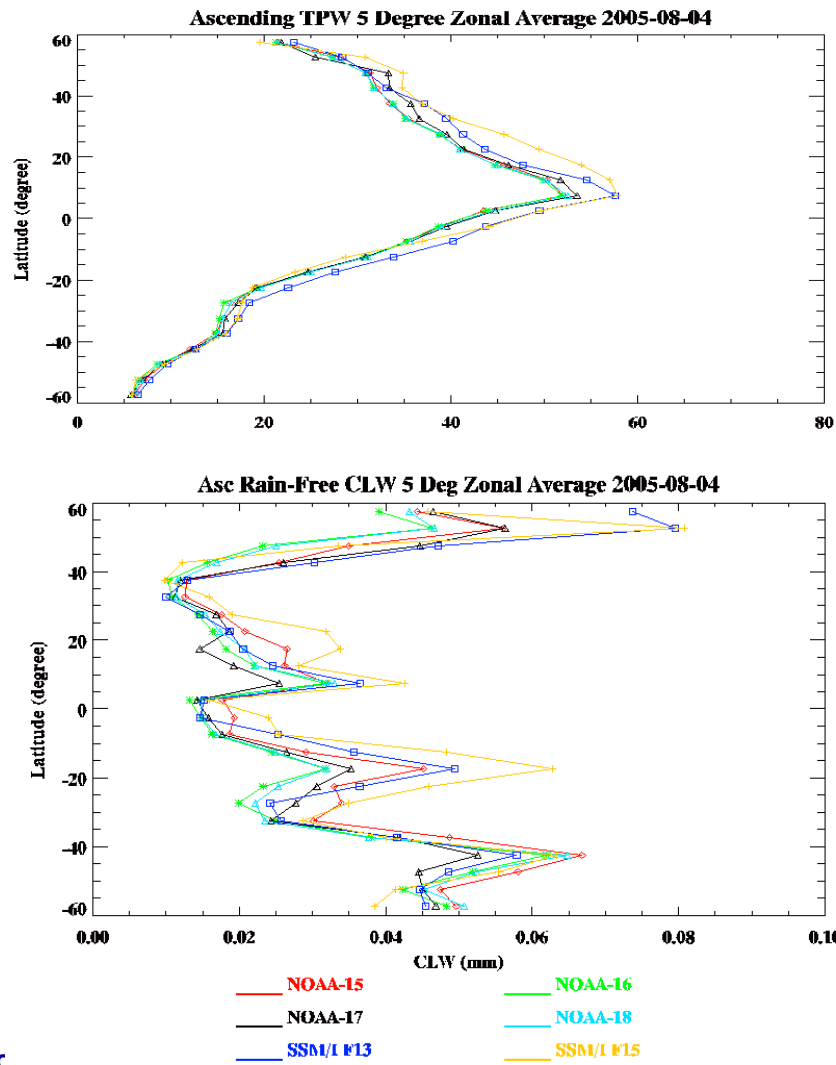
9 August 2005

N18 Cal/Val Working Group Meeting

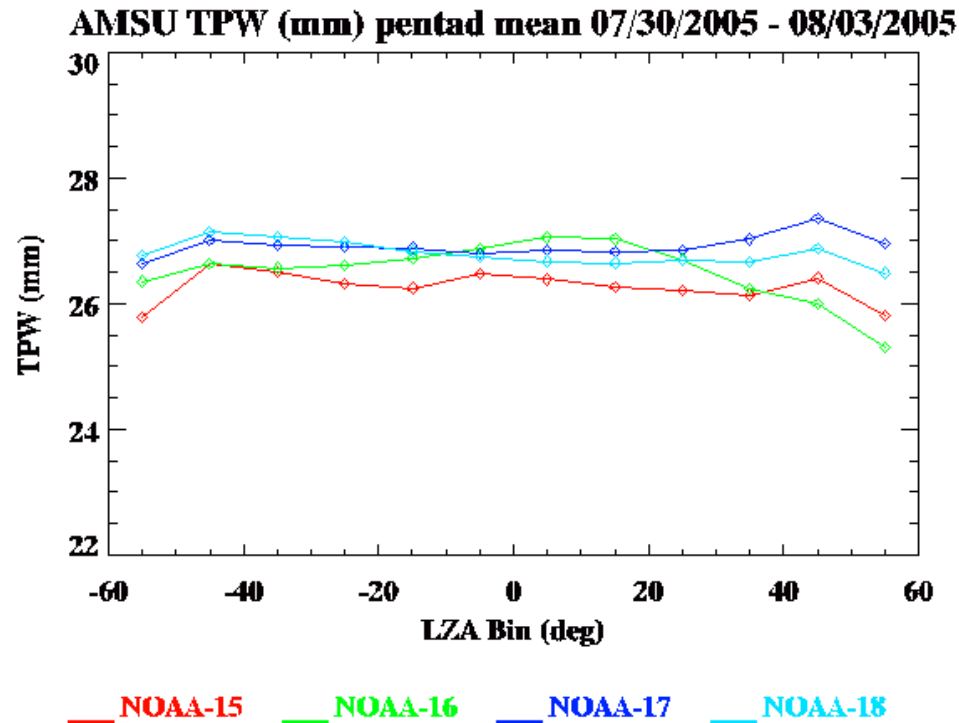


Intercomparisons – TPW & CLW

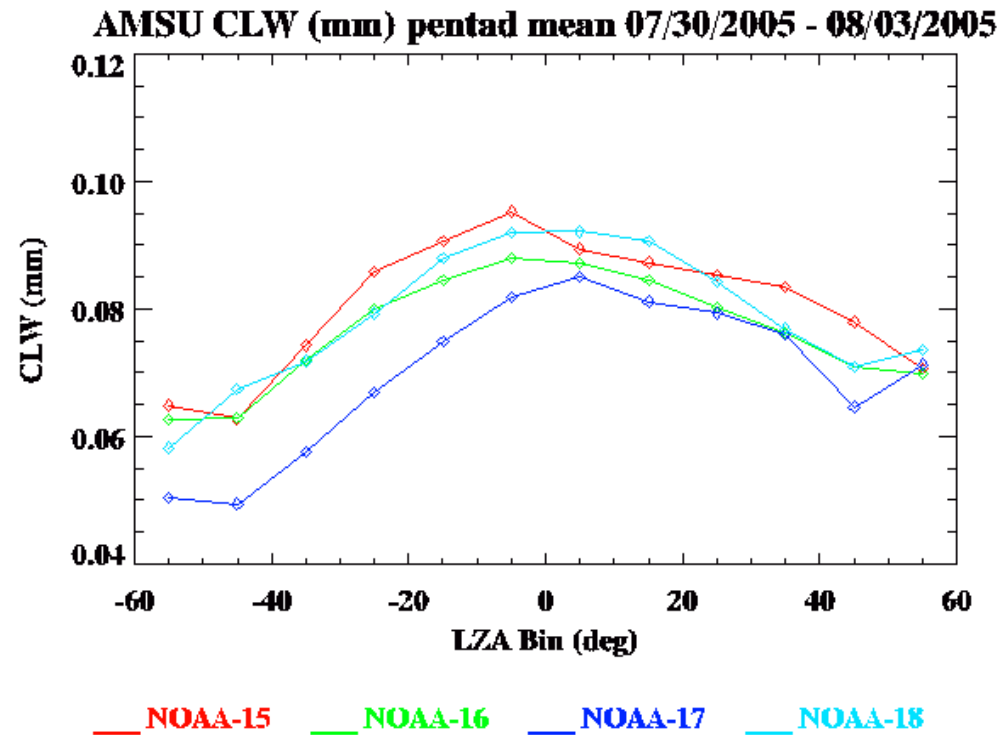
- Expect close agreement between N16 and N18
- Zonal TPW between all AMSU's in very close agreement (SSM/I is outlier – SDR bias)
- Zonal CLW in close agreement (SSM/I higher due to better sensitivity to CLW)
- Evaluations continuing



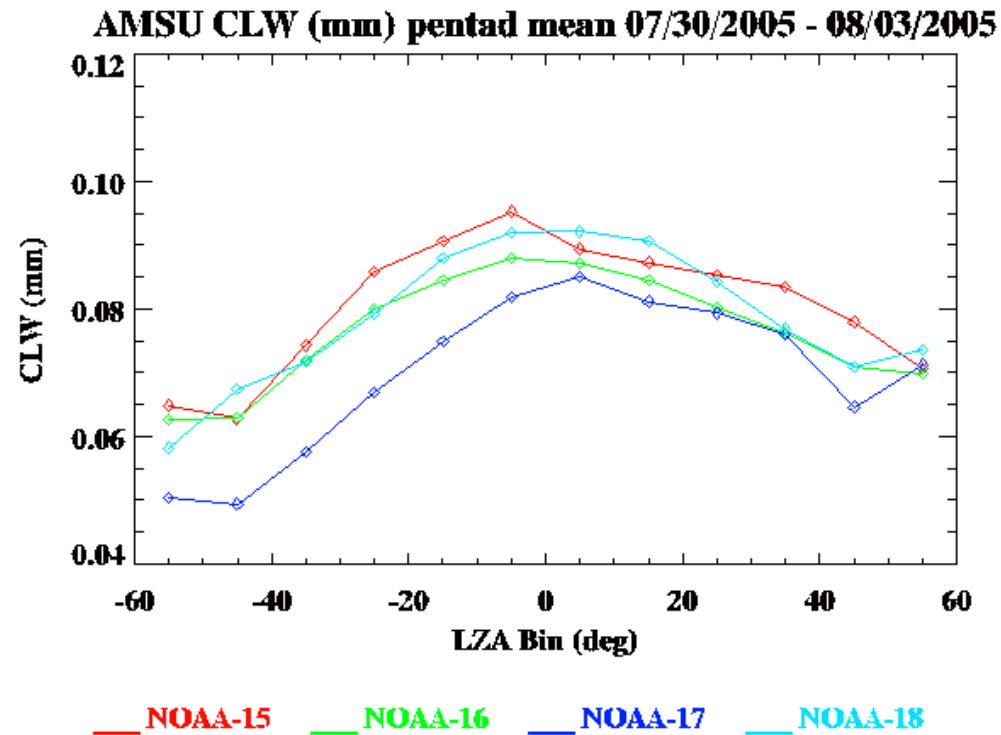
Asymmetry Monitoring - TPW



Asymmetry Monitoring - CLW

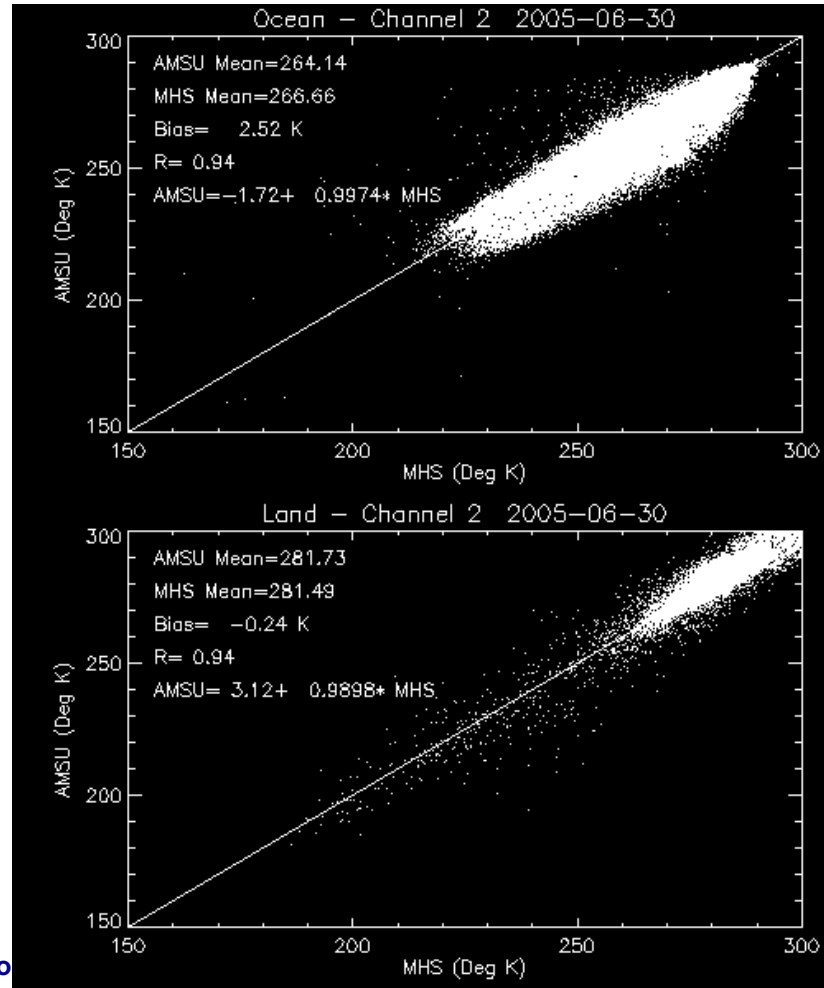


Asymmetry Monitoring - CLW



MHS vs. AMSU-B

- MSPPS particularly concerned with differences between CH 2 (157 vs. 150 GHz) and CH 5 (183+/-7 vs. 190 GHz)
 - Product impacts on IWP, RR, Snow/SWE
- Approach
 - Generate synthetic AMSU-B based on MHS and not alter retrieval algorithms
 - Pre-launch simulations support this approach
 - Preliminary post-launch product evaluations indicate that this approach will work
 - Generating daily match ups between N-16 and N-18
 - Develop regression relationships
 - Stratify by land, ocean, etc.
 - Determine stability of these relationships

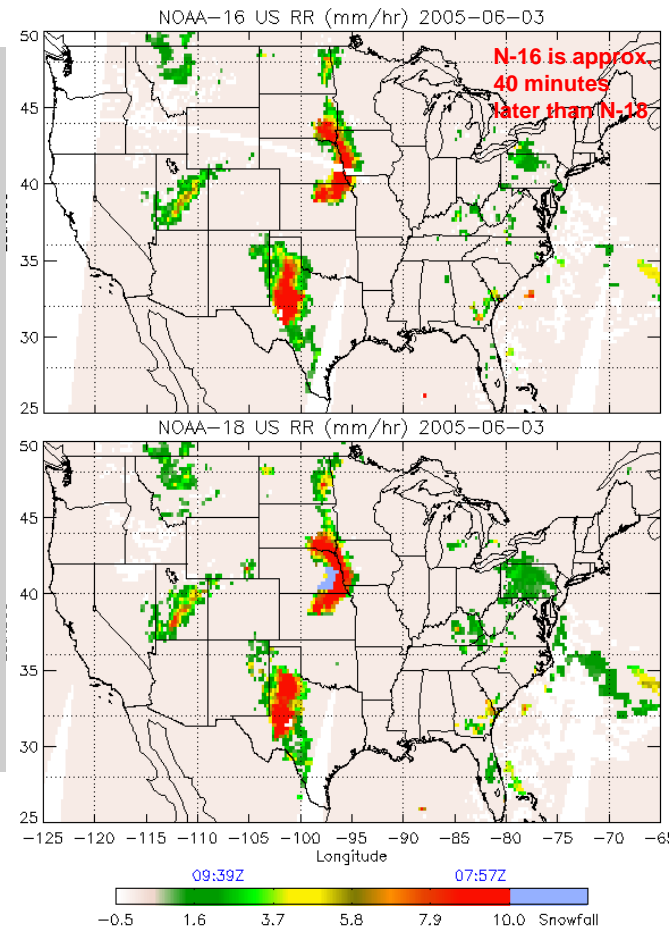
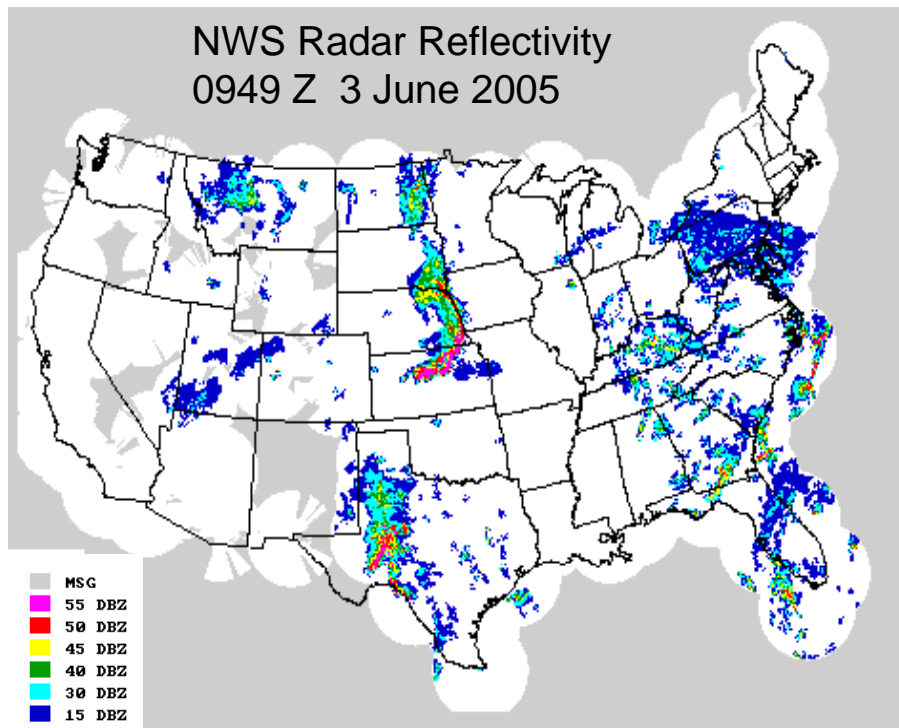


9 August 2005

N18 Cal/Val Wo

Comparison of N-16 AMSU-B and N-18 MHS derived rain rates

3 June 2005



9 August 2005

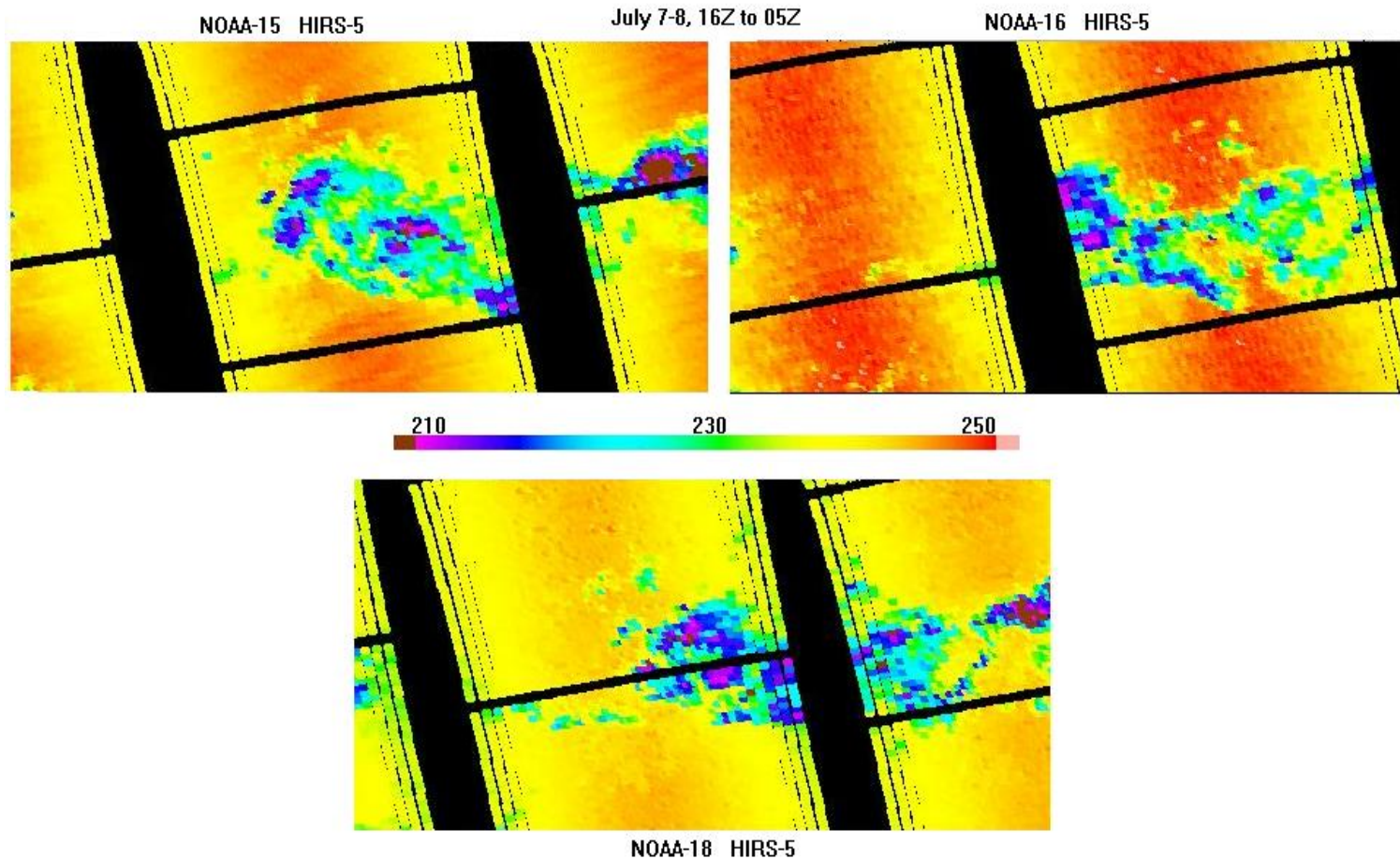
N18 Cal/Val Working Group

NOAA-18 ATOVS Status

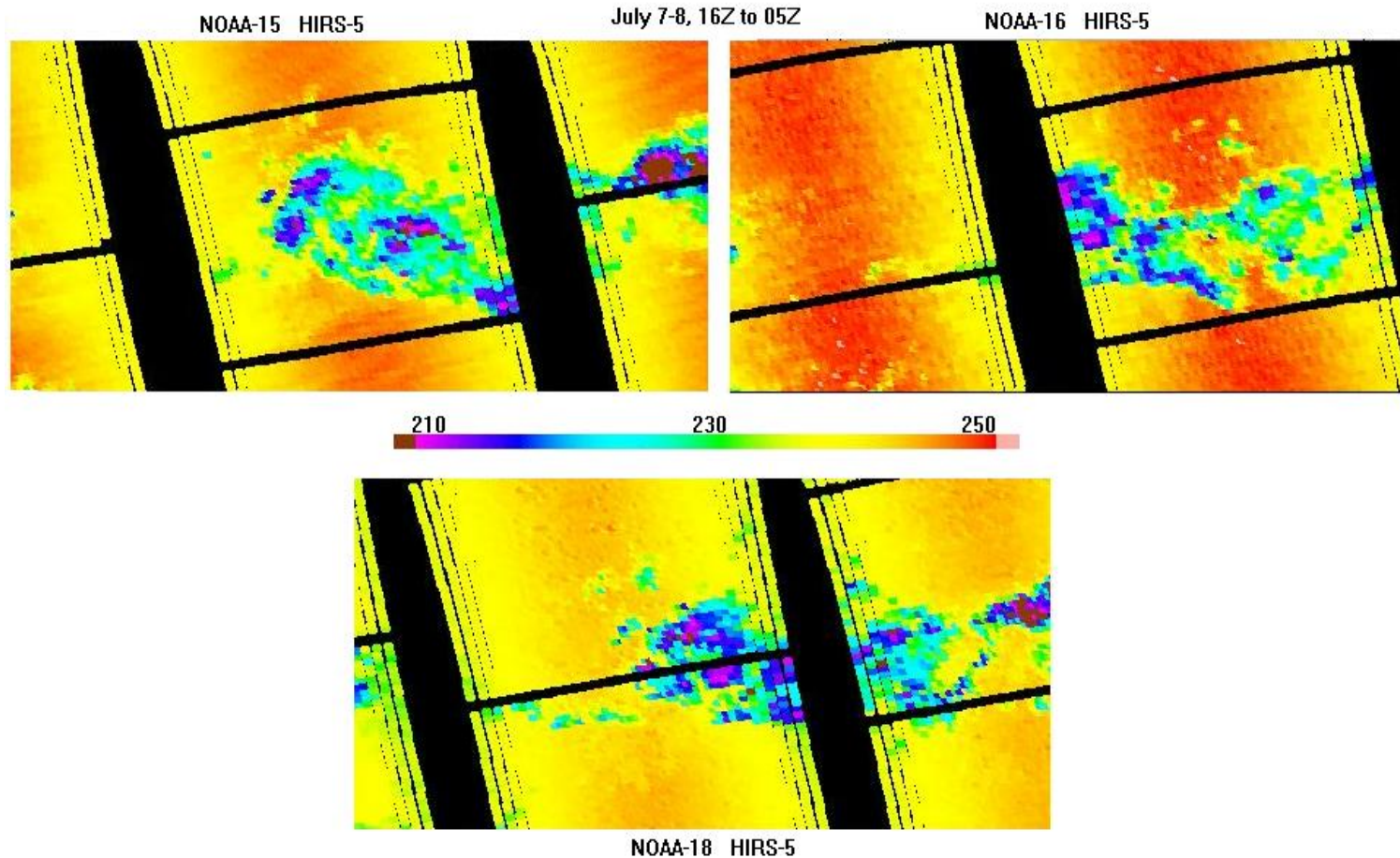
Tony Reale
ORA/FPDT
Aug 9, 2005

Summary

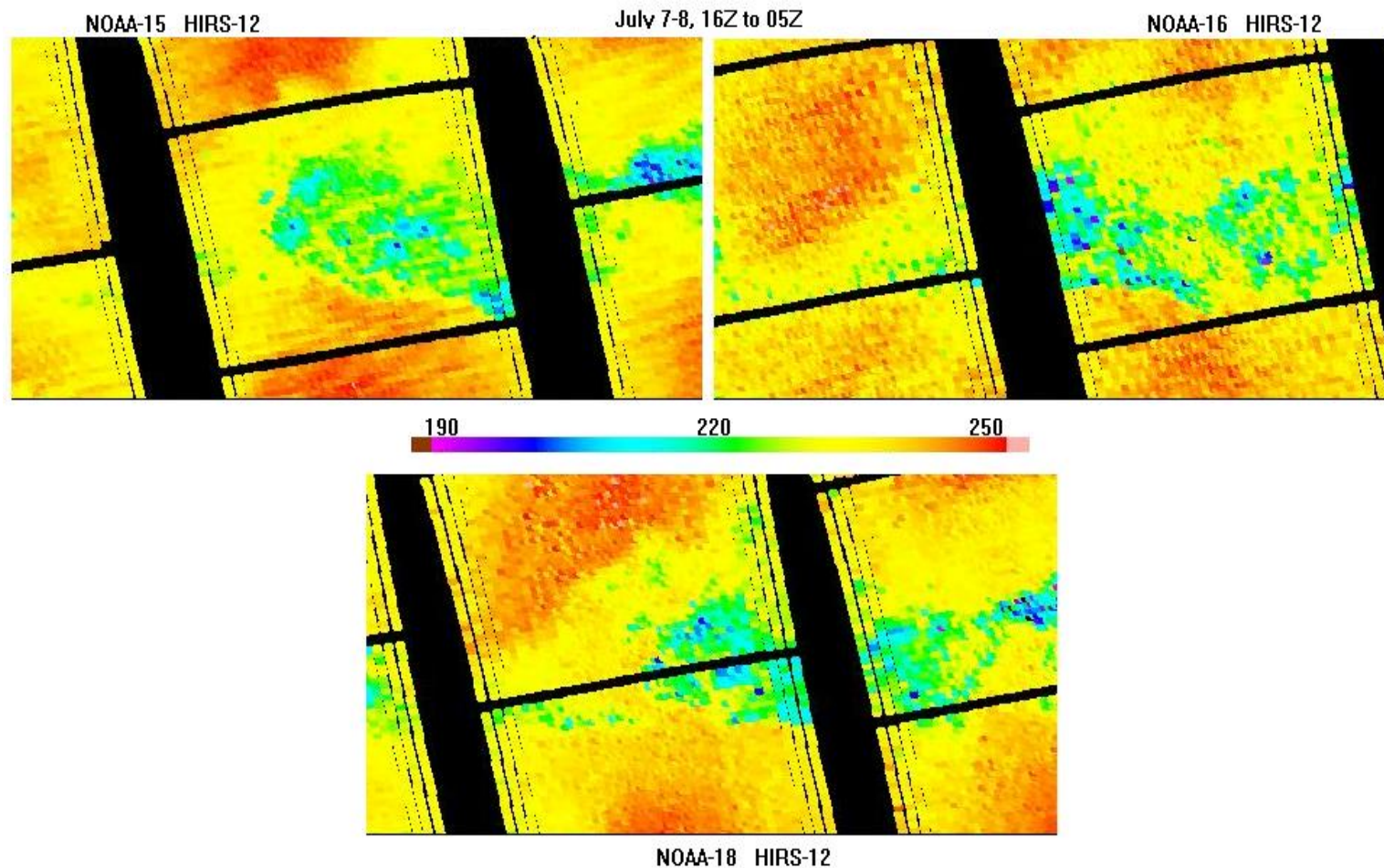
- HIRS channels 1 through 4, and channel 12 are not (yet) suitable for products
- AMSU and MHS are performing nominal for products; MHS pixel mis-location
- Examples using selected channels from each from each sounder are shown



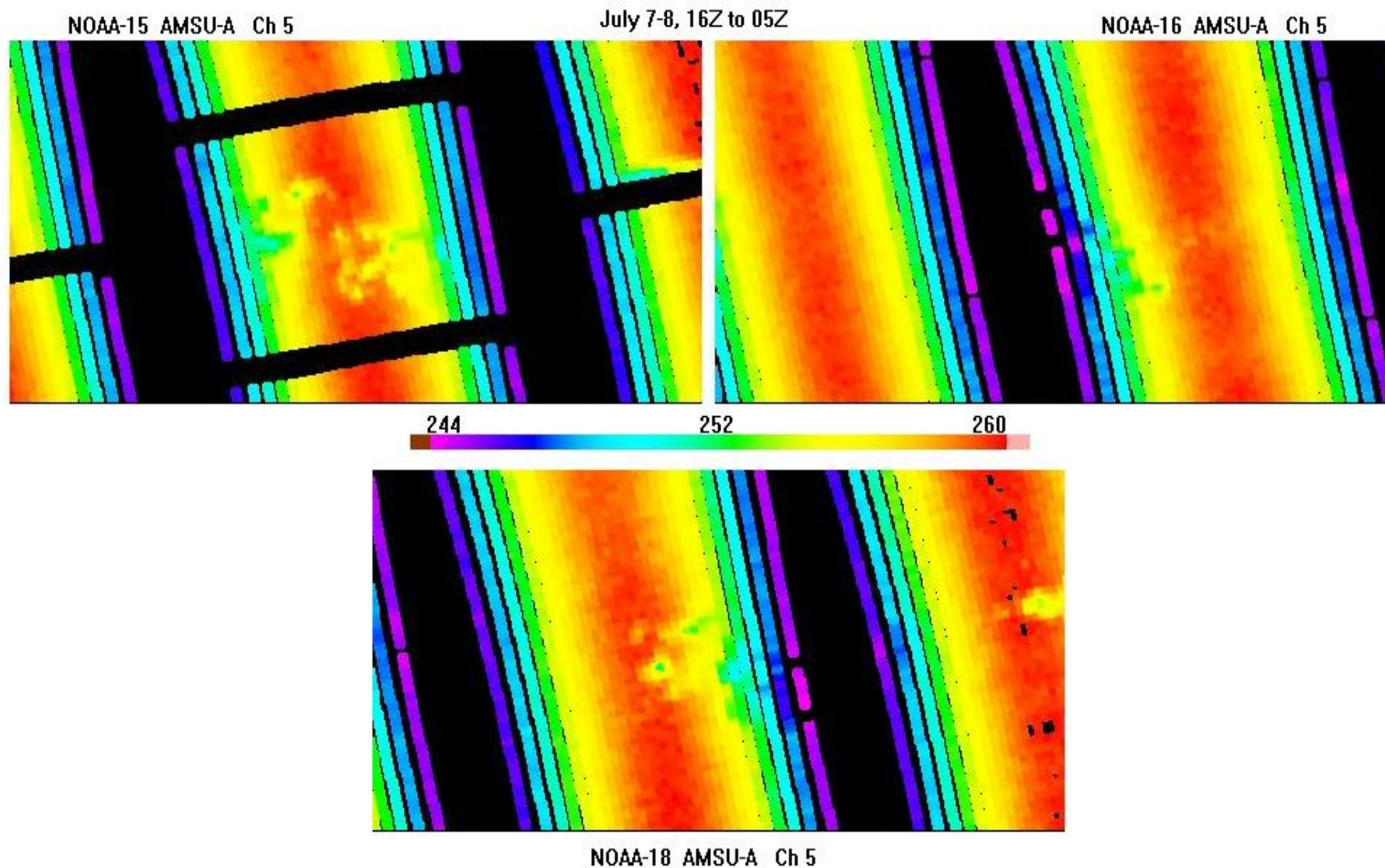
HIRS Channel 5 calibrated radiance temperatures (K) are compared for N15 (upper left), N16 (upper right) and NOAA-18; each panel is scaled identically allowing direct color comparison of differences. The region of coverage is an approximately 5000 km² region in the remote west tropical pacific. Random noise characteristics for N18 are now comparable to N16; a cool bias (less red) on the order of 5K is observed for N18 measurements relative to N16.



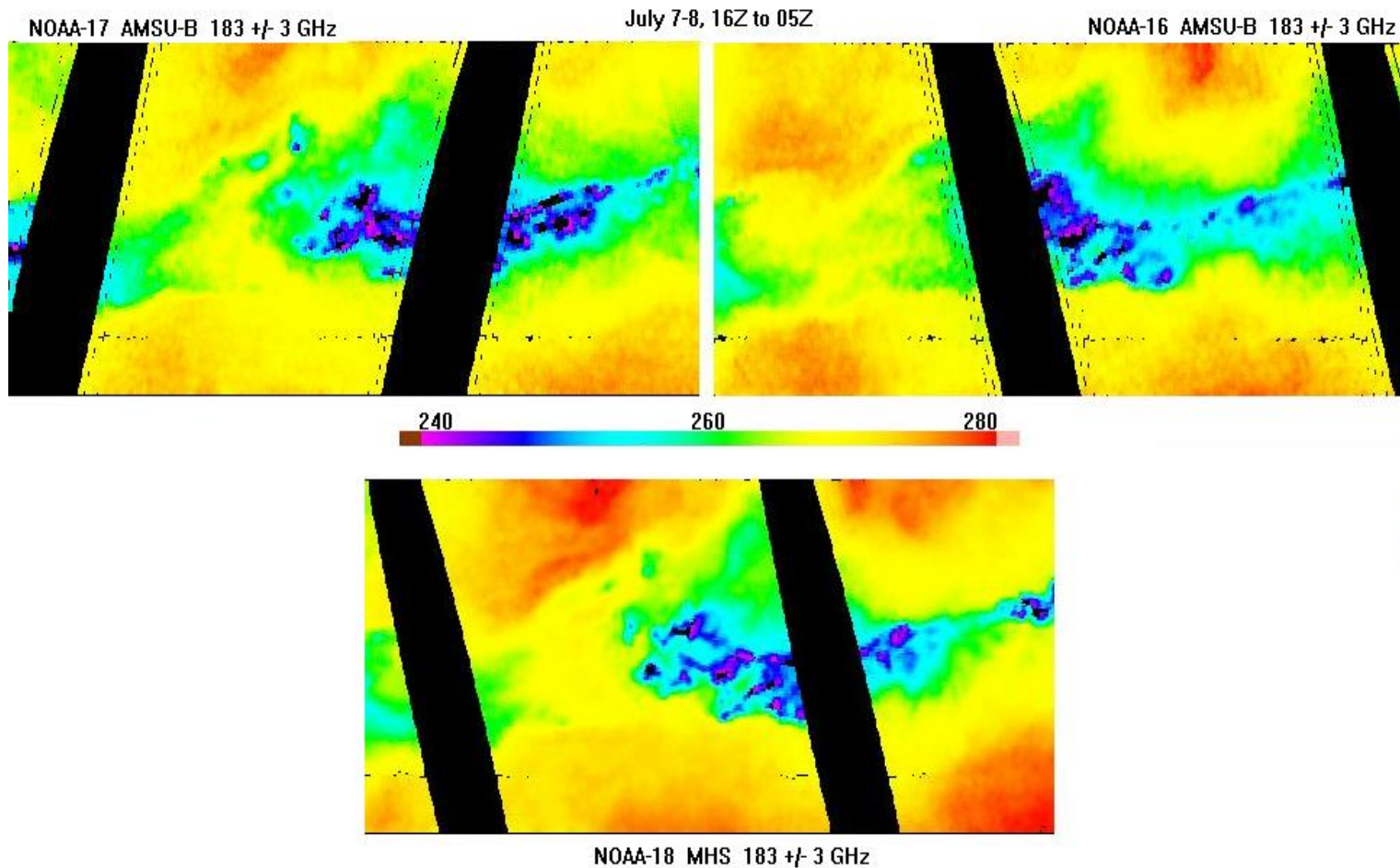
HIRS Channel 5 calibrated radiance temperatures (K) are compared for N15 (upper left), N16 (upper right) and NOAA-18; each panel is scaled identically allowing direct color comparison of differences. The region of coverage is an approximately 5000 km² region in the remote west tropical pacific. Random noise characteristics for N18 are now comparable to N16; a cool bias (less red) on the order of 5K is observed for N18 measurements relative to N16.



HIRS Channel 12 calibrated radiance temperatures (K) are compared for N15 (upper left), N16 (upper right) and NOAA-18; each panel is scaled identically allowing direct color comparison of differences. The region of coverage is an approximately 5000 km² region in the remote west tropical pacific. Random noise characteristics for N18 are now comparable to N16 but still unsuitable for products generation.



AMSU-A channel 5 calibrated radiance temperatures (K) are compared for N15 (upper left), N16 (upper right) and NOAA-18; each panel is scaled identically allowing direct color comparison of differences. The region of coverage is an approximately 5000 km² region in the remote west tropical pacific. The performance of NOAA-18 AMSU sounder is nominal for products generations, although some asymmetry across the scan is observed, manifested as cooler values (more purple) along the right side of the orbit track compared to the left (also seen for NOAA-15).



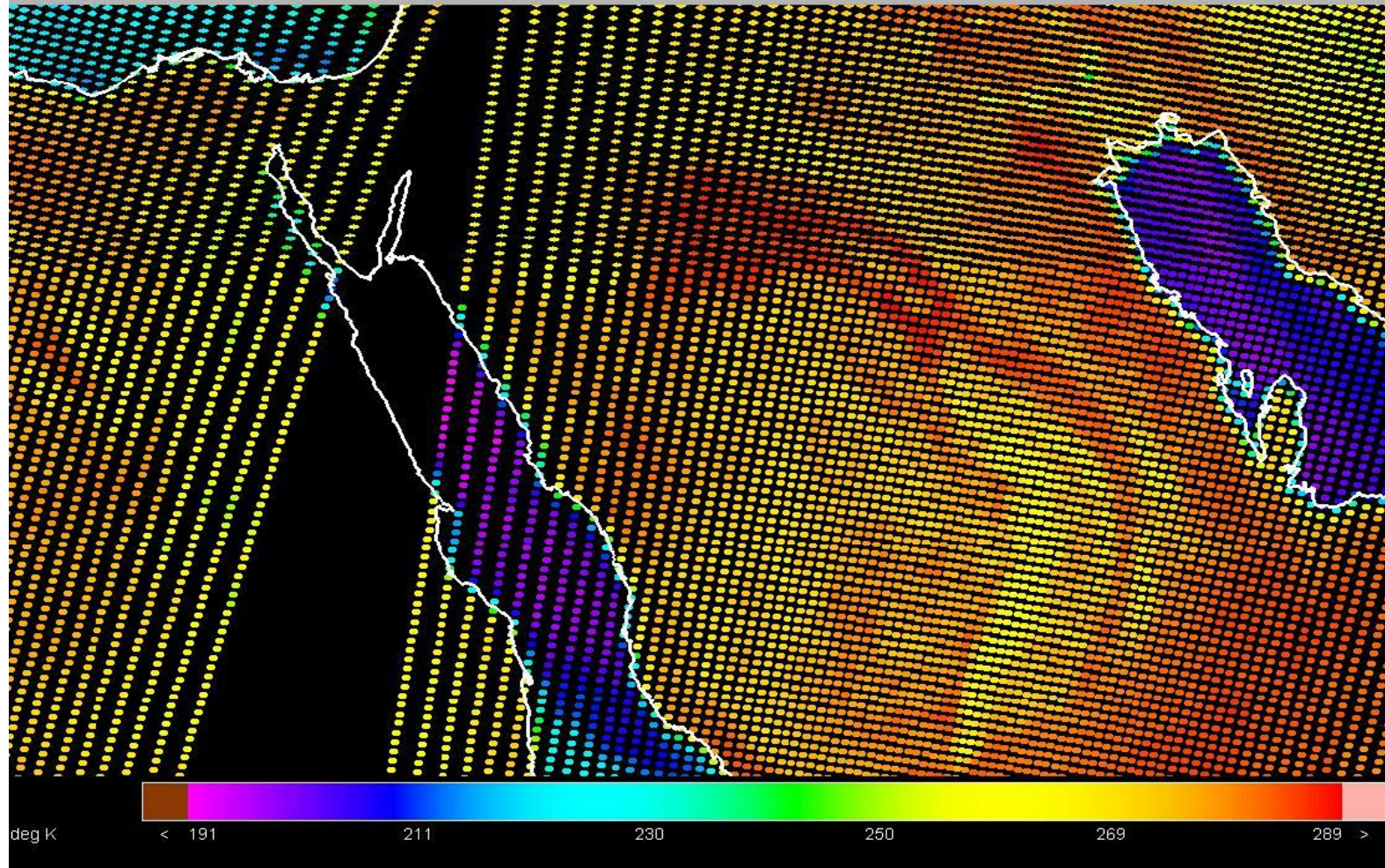
AMSU-B 183 +/- 3 GHz channel (4) calibrated radiance temperatures (K) for N17 (upper left) and N16 (upper right) are compared to MHS 183 +/-3GHz channel (4) on NOAA-18; each panel is scaled identically allowing direct color comparison of differences. The region of coverage is an approximately 5000 km² region in the remote west tropical pacific. The performance of NOAA-18 MHS is nominal for products generations, although it appears to be measuring slightly warmer (more red) on the order of 1.5 K than its counterparts on NOAA-17 and 16.

NOAA-18 Develop MODF (X1)

Aug 3, 2005 16Z to Aug 4, 2005 5Z

Limb Corr MHS Temp (89 GHz)

Center Point: 25.9N/40.4E (zoom: 14x)



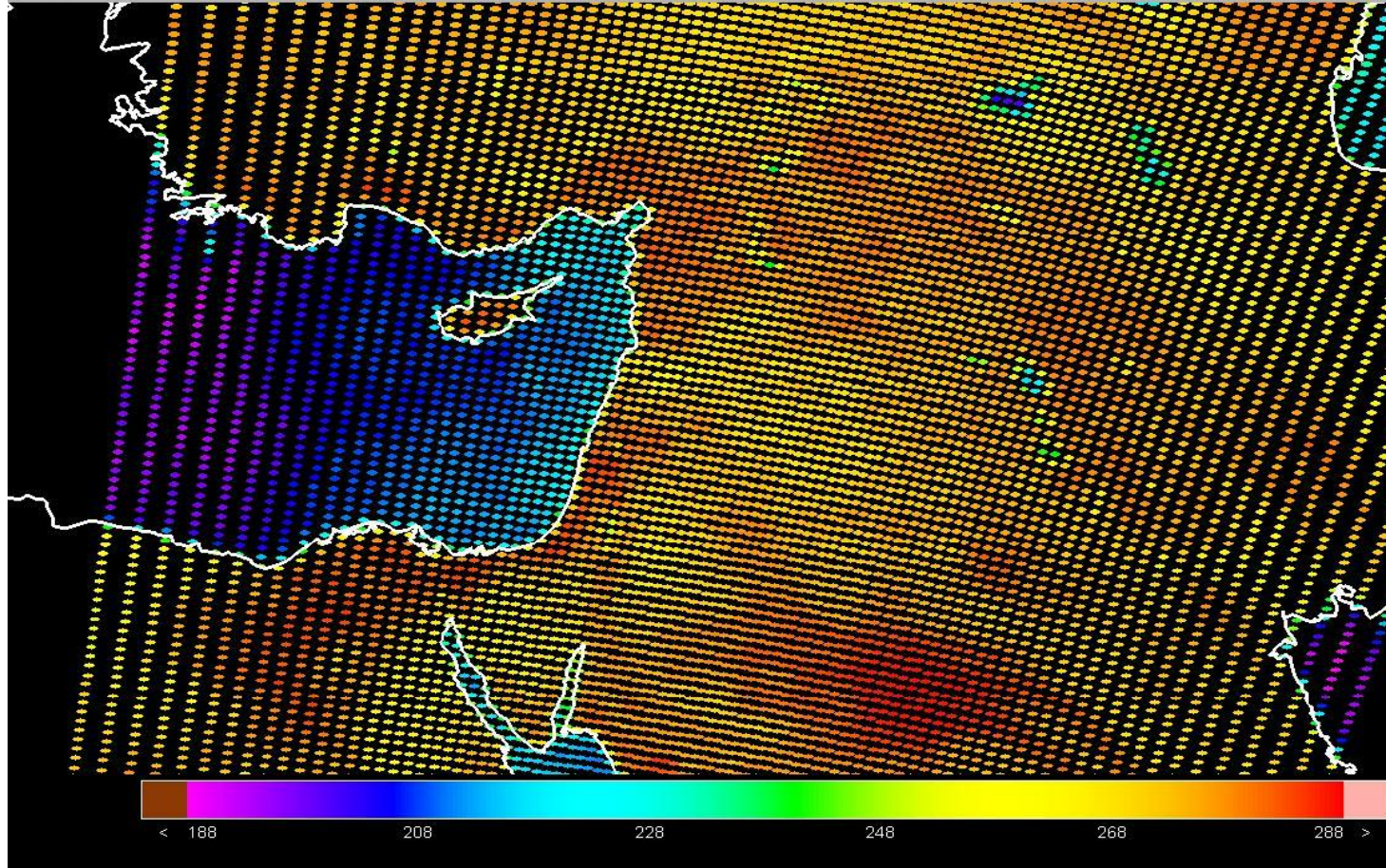
MHS mis-located by one pixel in direction of orbit track

N18 TEST BODF

Jul 20, 2005 23Z to Jul 21, 2005 1Z

LC MHS CH 1

Center Point: 33.8N/37.1E (zoom: 14x)



Corrected in test mode

Plans

- Demonstrate IOC using NOAA-18 HIRS, AMSU-A and MHS in operational sounding products generation:
 - Phase-1, implement in AMSU-only mode, late August
 - Develop contingencies for removing selected HIRS channels (i.e., channels 1, 2, 3, 4, and 12)
 - Phase-2, implement HIRS/AMSU-A mode, September
 - Phase-3, implement ATOVS-200X approach (HIRS, AMSU-A, MHS), October/November ...
- Demonstrate impacts of reduced FOV size for HIRS onboard NOAA-18 from 17km to 10km:
 - Cloud detection
 - Sounding products
 - Cloud products

New ATOVS System-200X Science

- *Incorporate AMSU-B*
- Regression Guess replaces Library Search
 - Calculate First Guess Radiance (OPTRAN)
- Measurement (Radiance) Bias Adjustment
 - AMSU-A
 - AMSU-B
 - HIRS
- Analytical Retrieval Solution (OPTRAN) per sounding (Paul Van-delst, Tom Kleespies, Yong Han)
 - based on Guess Temp and Moisture
- Peripheral Upgrades
 - Limb-adjustment
 - MSPPS Products
 - Expanded Validation

ATOVS Limb Correction Status

Tony Reale
ORA/FPDT
Aug 9, 2005

Orbital Processing

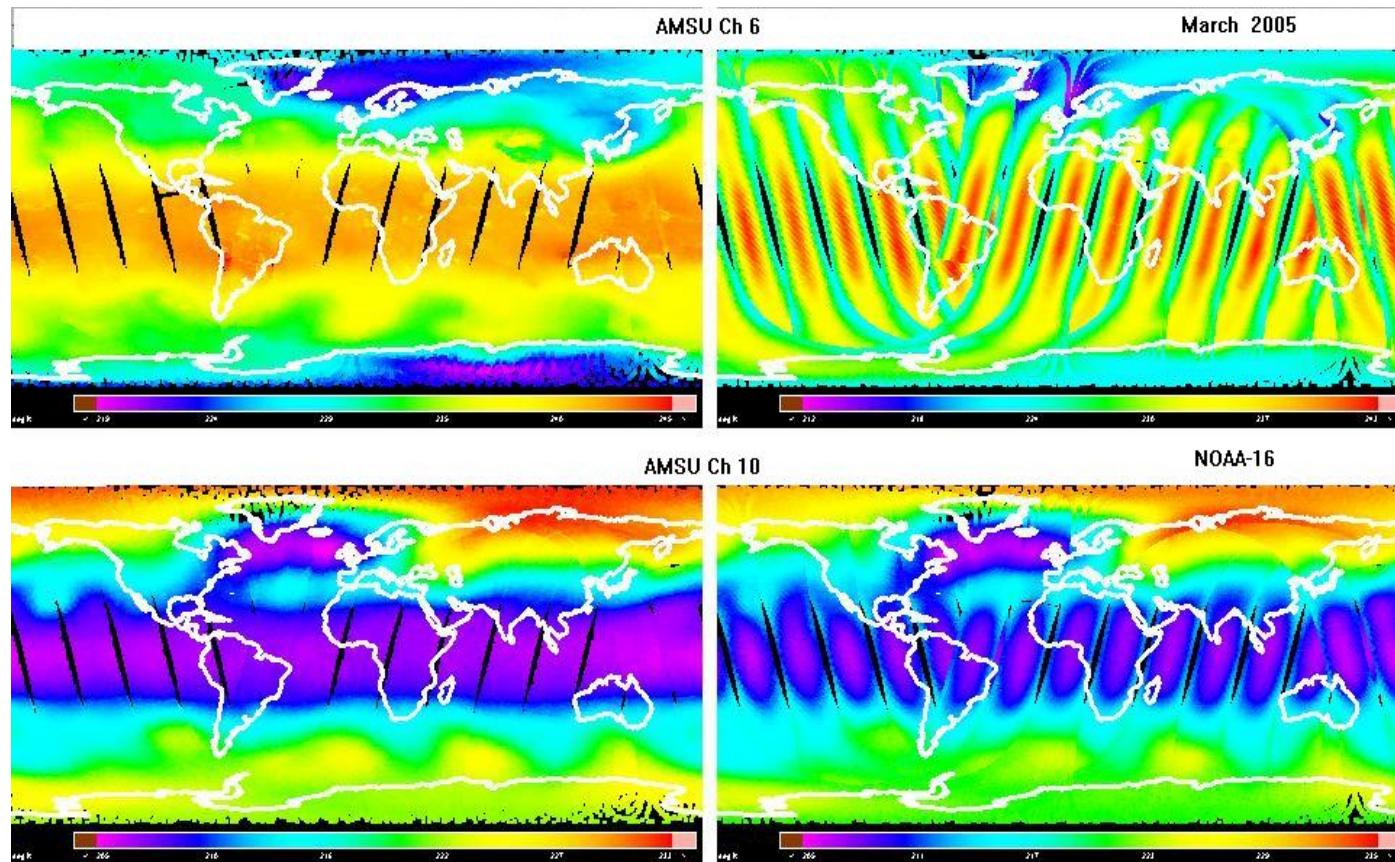
- Earth-location/Calibration
- Append SST, Terrain, Ice/Snow, NWP
- **Limb Adjustment**
- Interpolate to HIRS
- Microwave Products (CLW, TPW ... MSPPS)
- Contamination Detection
 - Precipitation
 - Cloud
- First Guess
- Retrieval

Limb Adjustments

- Dave Wark; NOAA Tech Re NESDIS 64, 1993
- 5-day Level 1b (per sounder) samples in Radiance Temperature
- 2-degree latitude belts (82), Sea vs. Nonsea, and Scan L
- 3 predictors least square regression (i=channel, j=scan)
 - $T_{i,0} = a_{i,j} + a_{i-1,j} T_{i-1,j} + a_{i,j} T_{i,j} + a_{i+1,j} T_{i+1,j}$
- Symmetric vs. Asymmetric; Smoothing option (?)
- Update as Necessary

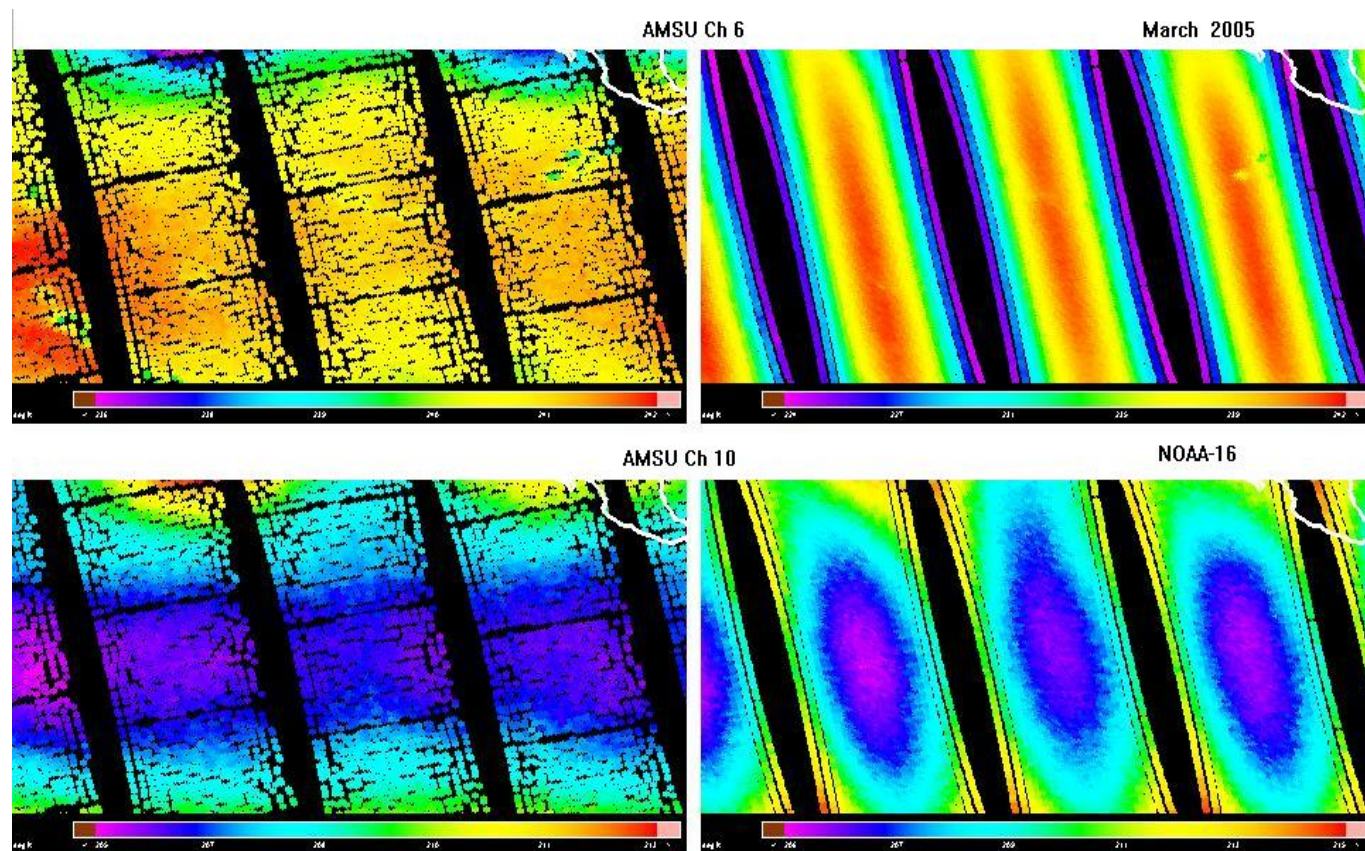
Limb Adjustment

(Wark, NOAA Tech Re. NESDIS 64' 1993)

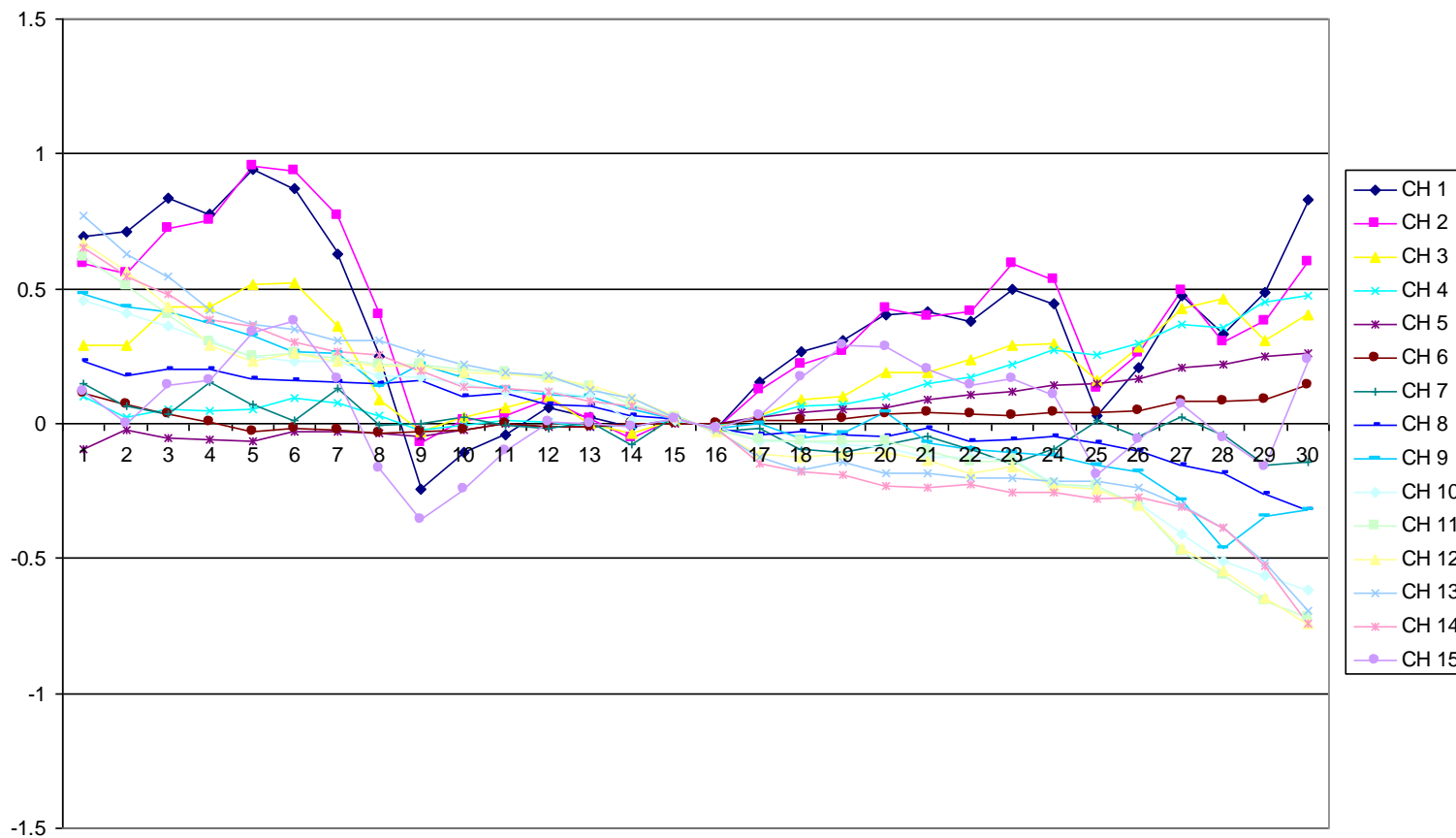


Limb Adjustment

(Wark, NOAA Tech Re. NESDIS 64' 1993)



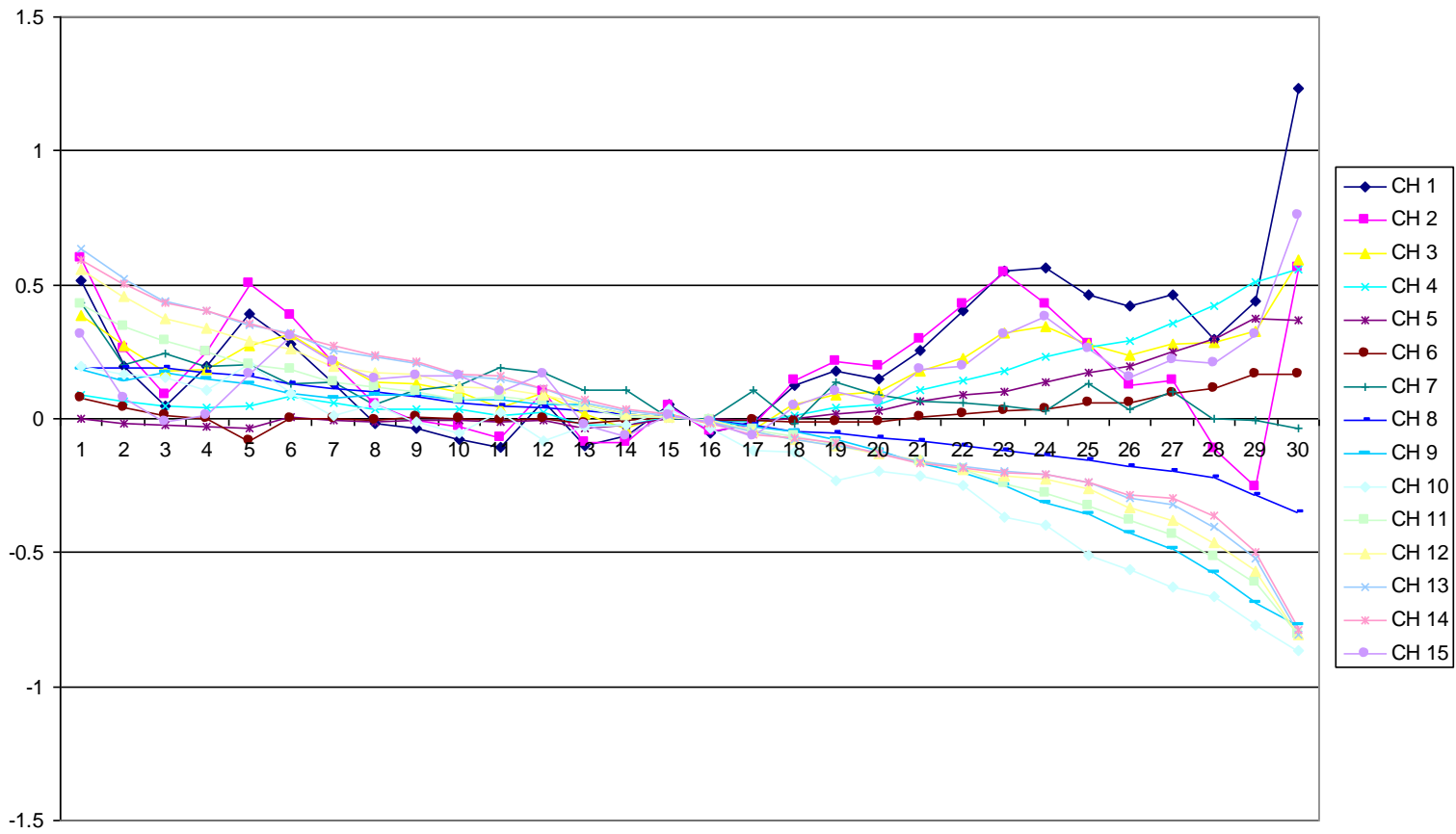
A2 AMSU-A Sea Residuals Nov 25-29, 2004



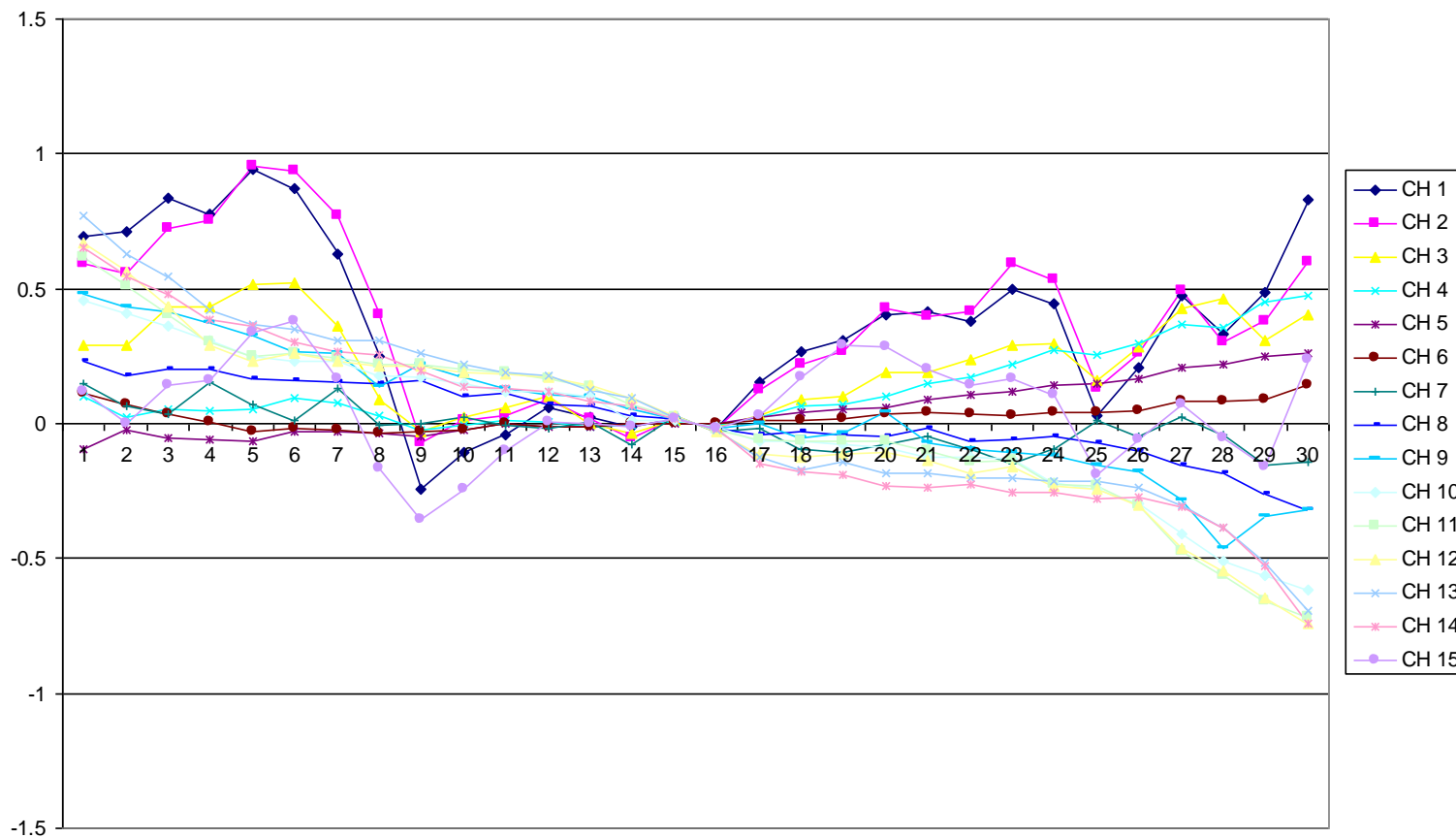
Proposed Changes to Limb Adjustment (New System-2005)

- Retain the basic Wark approach, but:
 - Replace 5-day with 30-day files for generating coefficients
 - Routinely collect radiance temperature samples (daily)
 - Store covariance matrices of measurements for 30-day periods over operational satellite lifetime
 - may have to retain matrices consistent with Wark approach, (i.e., per latitude band?)
 - Routinely arbitrate based on residual plots (weekly, monthly?)
 - May include NWP based residual
 - Archive

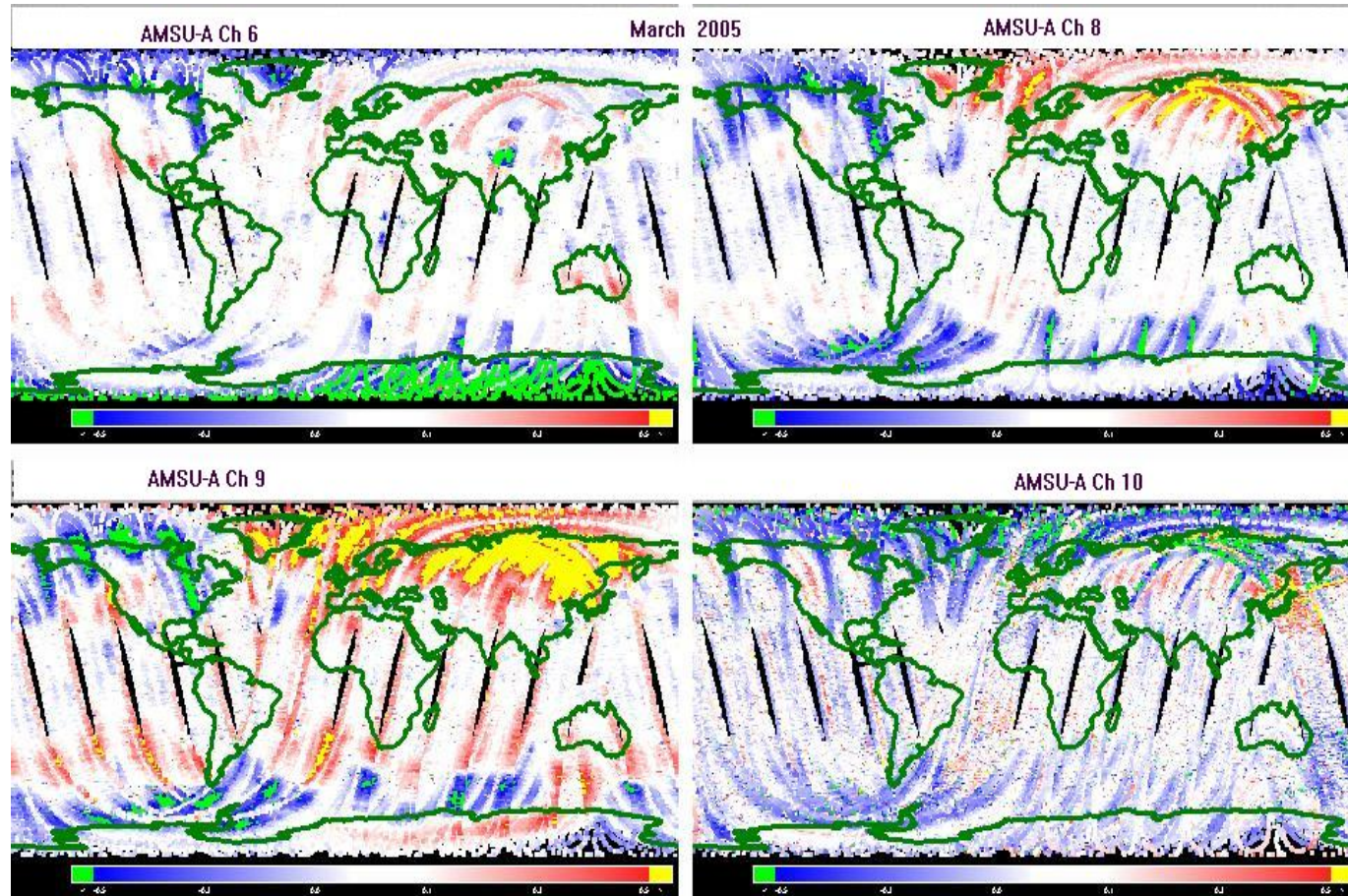
A4 AMSU-A Sea Residuals (30 day coeffs) Nov 25-29, 2004



A2 AMSU-A Sea Residuals Nov 25-29, 2004



Limb Adjustment (Comparison of 5-day vs 30-day coefficients)



NESDIS Converged Approach

- Data Collection
- Regression Computation
- Validation and Monitoring (use NWP?)
- Update (and Archive)



NOAA-18 AVHRR SST and Aerosol Products

Alexander Ignatov, John Sapper,
William Pichel, Xiaofeng Li, Yury Kihai

11/11/2005

N18 Cal/Val Workshop 9 Aug 2005:
SST and Aerosol Status

1



AVHRR products over ocean



Solar Reflectance Bands (Aerosol) (*No onboard calibration*)

- 1: 0.63 μm τ_1 : *Single-channel LUT*
- 2: 0.83 μm τ_2 : *Single-channel LUT*
- 3A: 1.61 μm τ_3 : *Single-channel LUT (N18: disabled 8-16 Jun 05)*

Earth Emission Bands (SST) (*Onboard calibration*)

- 3B: 3.7 μm (*Daytime: not used due to solar reflectance*)
- 4: 11 μm
- 5: 12 μm

Day SST derived using split-window NLSST

$$T_s = \alpha_1 T_{11} + \gamma(T_{11} - T_{12}) + \alpha_o \quad \text{where } \gamma = \gamma_o(T_c) + \gamma_1(\sec\theta - 1)$$

Night SST derived using triple-window MCSST

$$T_s = \alpha_1 T_{3.7} + \alpha_2 T_{11} + \alpha_3 T_{12} + \alpha_4 (T_{3.7} - T_{11}) \times (\sec\theta - 1) + \alpha_5 (\sec\theta - 1)$$



Status of N18 Algorithms

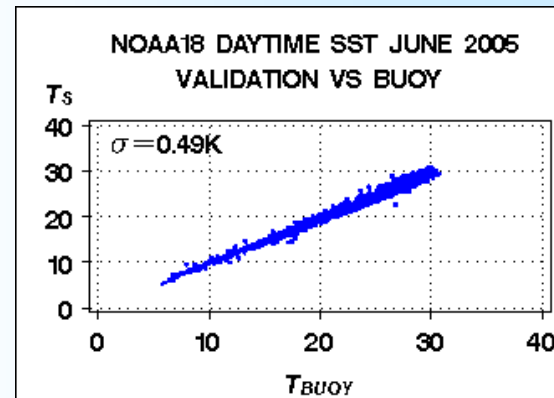


Aerosol Algorithm:

- Sensor-filter specific LUTs calculated using RTM
- Retrieval algorithm delivered to OSDPD Dec 2004

SST Algorithm:

- Coefficients derived vs. buoy post-launch
- OSDPD delivered match-up to ORA 7 Jul 2005
- ORA delivered algorithms to OSDPD 13 Jul 2005
- OSDPD implemented 2 Aug 2005
- 2 technical issues (resolved by John Sapper):
 - Match-up files filled up for NOAA-17 and -18
 - Delays w/implementation (hard-coded pointers in OSDPD code and personnel changes/contractor vacation)



11/11/2005

N18 Cal/Val Workshop 9 Aug 2005:
SST and Aerosol Status

3



Data



Operational NESDIS SST and Aerosol over global ocean 8-16 Jun 2005 from 3 AVHRR/3 NOAA-18, NOAA-17, and NOAA-16



SST/AEROBS 8-day rotating files CEMSCS
(N18: started on 7 June 2005 with N16 coeff)
 τ_1 , τ_2 , τ_3 , NLSST, MCSST, Climate T_s
8km (2×2 GAC pixels) × daily
AEROBS: Day only/40° glint/anti-solar side
SSTOBS: Day/Night + glint/solar side

NOAA-16/L (Sep 2000; 3 PM)
NOAA-17/M (Jun 2002; 10 AM)
NOAA-18/N (May 2005; 2 PM)

11/11/2005

N18 Cal/Val Workshop 9 Aug 2005:
SST and Aerosol Status

4

Sea Surface Temperature

NB:

- *N18 SST in these analyses use N16 coefficients*
- *New coefficients were implemented on 2 August 2005*
- *The SST/AEROBS 8-day rotating files will be fully refreshed by 11 Aug 2005*
- *Comprehensive evaluation of SST will be completed after that date*
- *SST coefficients might be adjusted based on evaluation before 31 Aug 2005*

11/11/2005

N18 Cal/Val Workshop 9 Aug 2005:
SST and Aerosol Status

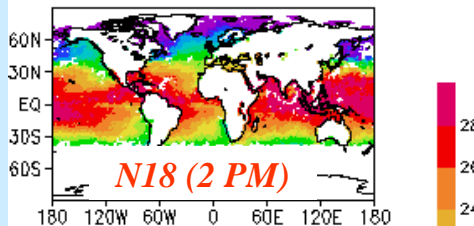
5



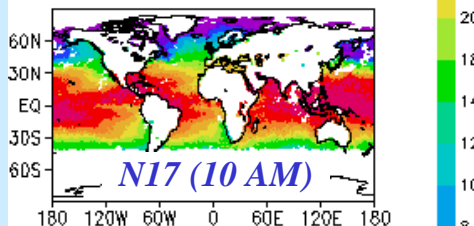
NLSST June 2005



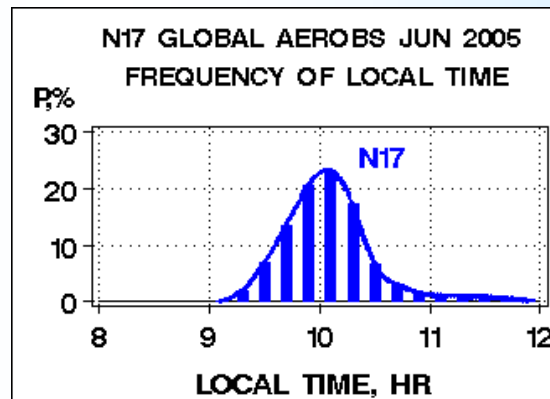
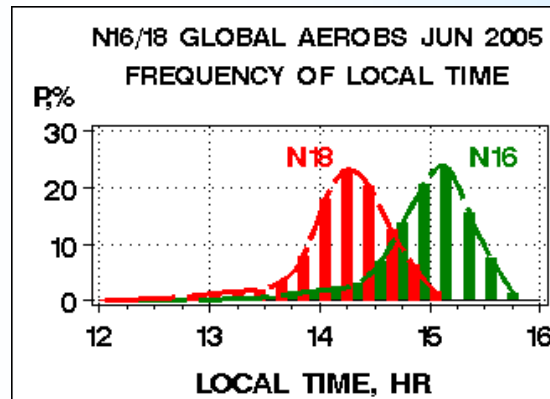
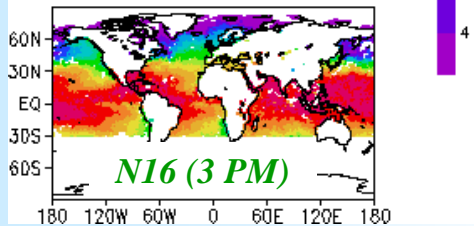
N18 NLSST 8-16 JUN 2005



N17 NLSST 8-16 JUN 2005



N16 NLSST 8-16 JUN 2005



*N16 is ~3pm
N18 is ~2pm
N17 is ~10am*

11/11/2005

N18 Cal/Val Workshop 9 Aug 2005:
SST and Aerosol Status

6

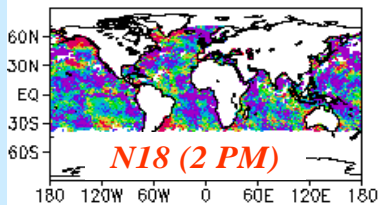


NLSST Anomalies June 2005

(Bauer-Robinson 1985 climatology subtracted)

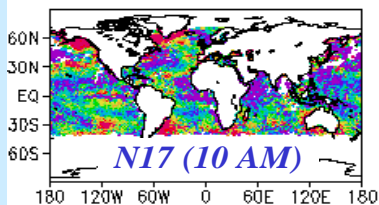


N18 NLSST ANOMALY JUN 05



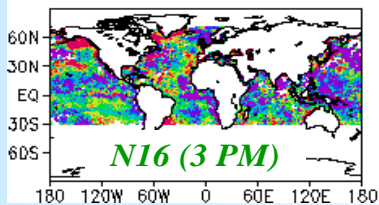
N18 (2 PM)

N17 NLSST ANOMALY JUN 05

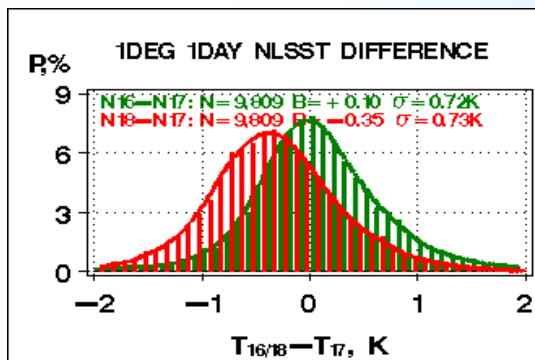


N17 (10 AM)

N16 NLSST ANOMALY JUN 05



N16 (3 PM)



N16/17/18 data have been merged by Day/Lat/Lon, and normalized to N17. N16 is +0.10K warmer than N17, N18 is -0.35K cooler than N17 (N18 uses N16 coeffs)

11/11/2005

N18 Cal/Val Workshop 9 Aug 2005:
SST and Aerosol Status

7



Conclusion to SST



- ORA calculated SST coefficients from buoy match ups
- OSDPD implemented 2 August 2005
- Analyzed daytime NLSST (11/12 μm) derived w/N16 coefficients
- No excessive noise found in N18 daytime NLSST
- N16/17 SSTs remain globally consistent within $\sim 0.1\text{K}$

Work underway

- Do global analyses w/correct N18 coefficients (after 11 Aug 2005)
- Include night-time SST in consistency analyses (3.7 μm)
- Document at the AMS'06 Conf on Satellite Meteorology & Oceanography

Aerosol

11/11/2005

N18 Cal/Val Workshop 9 Aug 2005:
SST and Aerosol Status

9



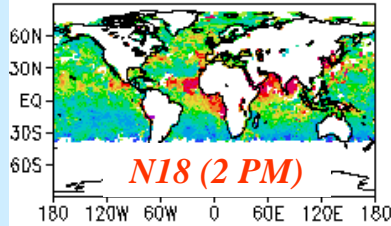
Aerosol June 2005: ☺₁

τ-errors: due to AVHRR calibration

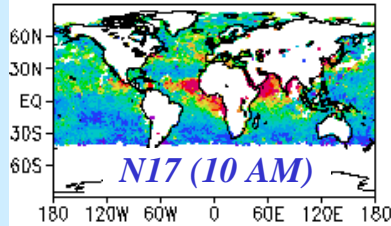


τ₁ (0.63 μm)

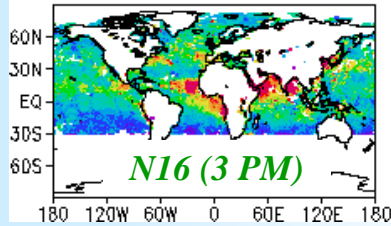
N18 AOD1 8-16 JUN 2005



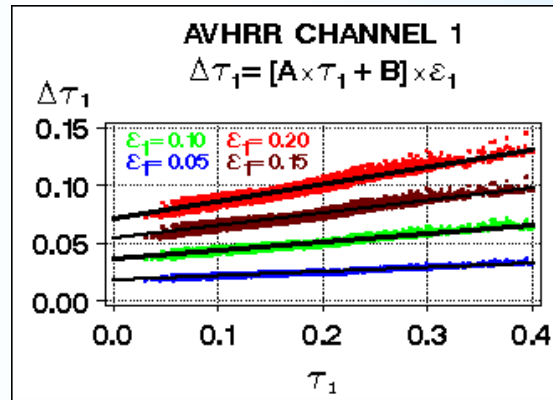
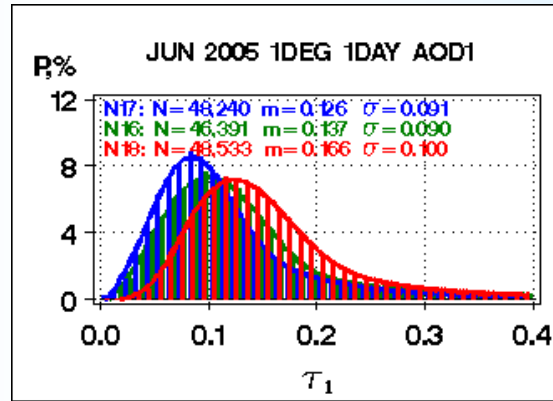
N17 AOD1 8-16 JUN 2005



N16 AOD1 8-16 JUN 2005



11/11/2005



AVHRR band 1:
N18 biased high by ~+9% with respect to N17 and by ~+6% with respect to N16.

Sensitivity charts show error in AOD1 as a function of AOD1, for 4 levels of cal error from 5% to 20%.

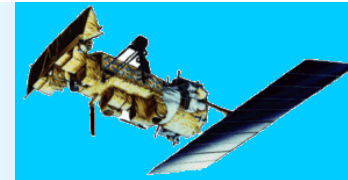
N18 Cal/Val Workshop 9 Aug 2005:
 SST and Aerosol Status

10



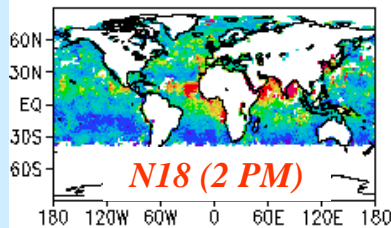
Aerosol Jun 2005: ☺₂

τ-errors: due to AVHRR calibration

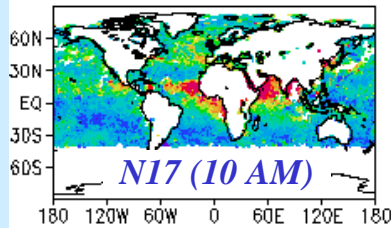


τ₂ (0.83 μm)

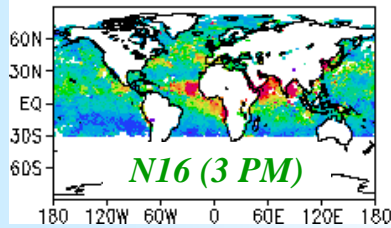
N18 AOD2 8-16 JUN 2005



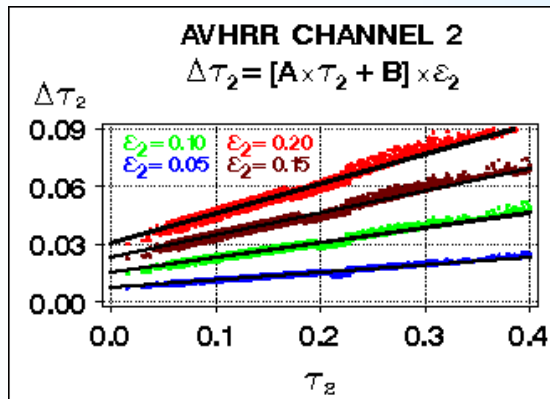
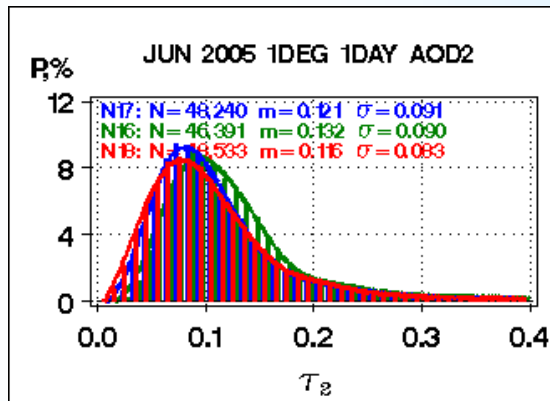
N17 AOD2 8-16 JUN 2005



N16 AOD2 8-16 JUN 2005



11/11/2005



AVHRR band 2:
 N18 biased high by
 ~-1% with respect to
 N17 and by ~-4% with
 respect to N16.

Sensitivity charts show
 error in AOD2 as a
 function of AOD2, for
 4 levels of cal error
 from 5% to 20%.

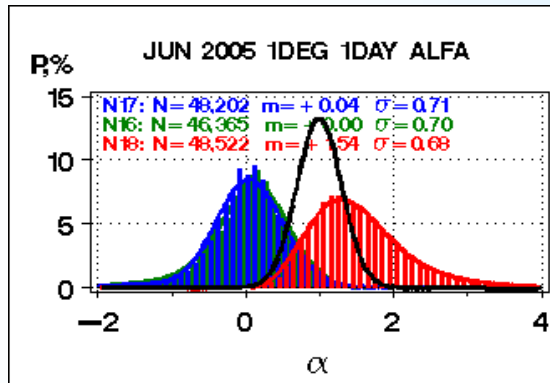
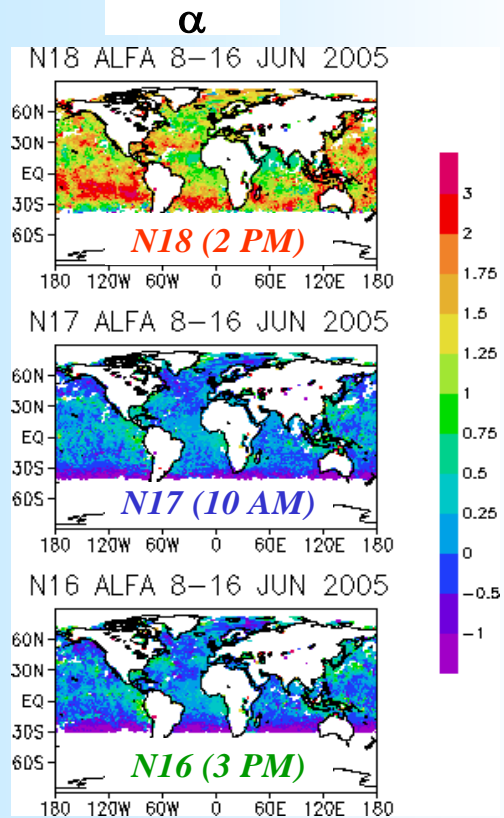
N18 Cal/Val Workshop 9 Aug 2005:
 SST and Aerosol Status

11

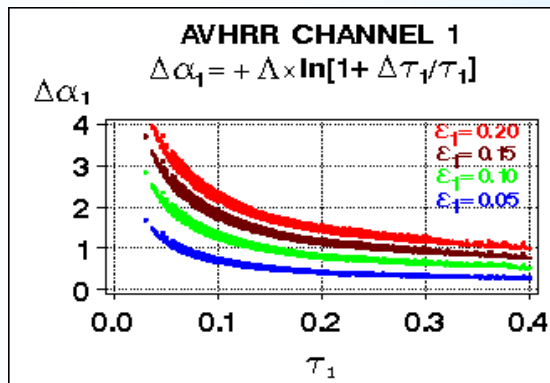


Aerosol Dec 2003: α

α -errors: due to AVHRR calibration



Black curve shows the expected distribution of Angstrom exponent. High bias in N18 band 1 and low bias in band 2 work in the same direction and amplified in Angstrom exponent.



Angstrom exponent (related to a ratio of two AODs in bands 1 and 2) is a very sensitive indicator of AVHRR cal (shows unresolved combination of bands).

11/11/2005

N18 Cal/Val Workshop 9 Aug 2005:
SST and Aerosol Status

12



Conclusion to Aerosol



- N18 AVHRR channel 1 is biased high by +6..9%
- N18 AVHRR channel 2 is biased low by -1..-4%
- Vis Cal should be fixed for the quality aerosol product
- Channel 3A was not available for analyses from 8-16 June 2005
- No “unusual” anomalies in solar reflectance bands observed

Work underway

- Re-examine aerosol product after Vis Cal adjustments
- Do global analyses of SST/Aerosol correlations (after 11 Aug 2005)
- Document at the AMS'06 Conf on Satellite Meteorology & Oceanography



Conclusion to SST/Aerosol:

Recommend declaring N18 operational by end August

11/11/2005

N18 Cal/Val Workshop 9 Aug 2005:
SST and Aerosol Status

14



Impact of NOAA18 in the Met Office Global Model

Brett Candy, Steve English and Fiona Hilton

- Monitoring of NOAA18 AMSU data shows that the data is of comparable quality to other NOAA platforms
- Currently operational global model assimilates AMSU data from N15, N16, Aqua
- The time for processing ATOVS data cannot increase therefore we intend to *withdraw* Aqua and *replace* it with NOAA-18
- Prior to assimilation we thin data to 1 ATOVS observation per analysis gridpoint. Intention is to give NOAA-18 the priority in the thinning
- A near real time trial of duration 1 month has been run to test this strategy

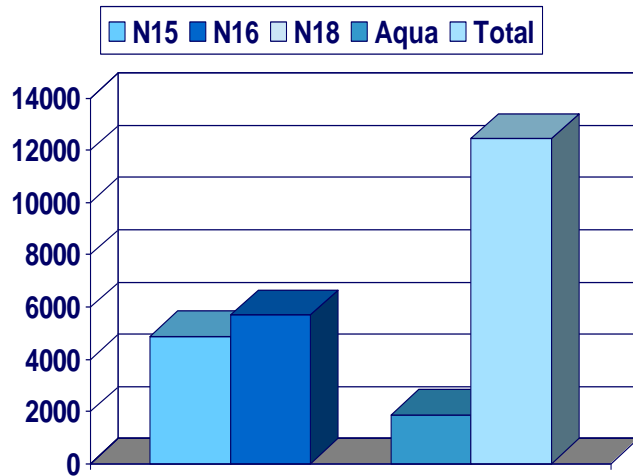
- Trial consists of two runs
 - a) Control as operations (N15, N16, Aqua) + N18 in passive mode to collect bias correction stats
 - b) Experiment Aqua withdrawn, N18 assimilated

- The experiment was switched on after the control had completed 10 days in order to accumulate enough stats for bias correction.

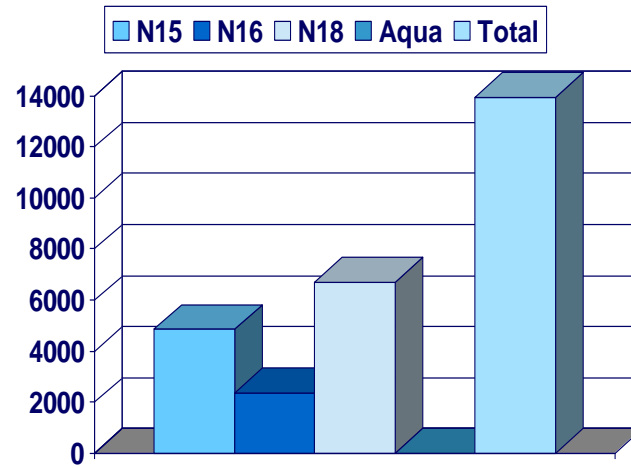
Average Data Assimilated for a Main forecast Run



Control



Experiment



Main forecast Run Plot

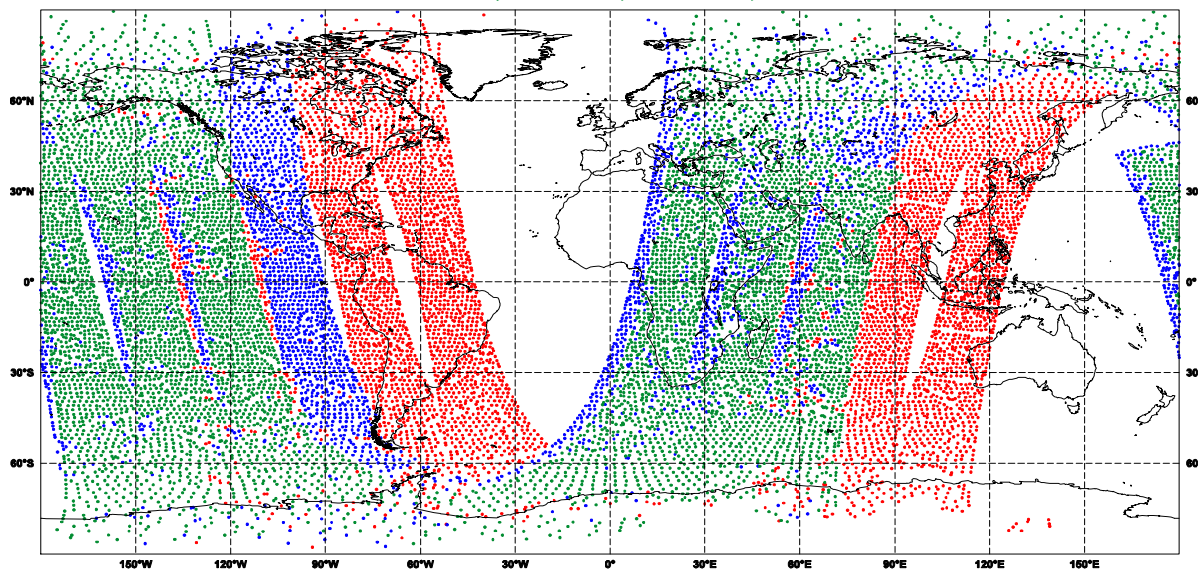


Data Coverage: SatRad ATOVS (27/7/2005, 0 UTC, qg00)
Total number of observations assimilated: 15750

5231 NOAA-15, Min: 206, Max: 206, Mean: 206

3185 NOAA-16, Min: 207, Max: 207, Mean: 207

7334 NOAA-18, Min: 209, Max: 209, Mean: 209

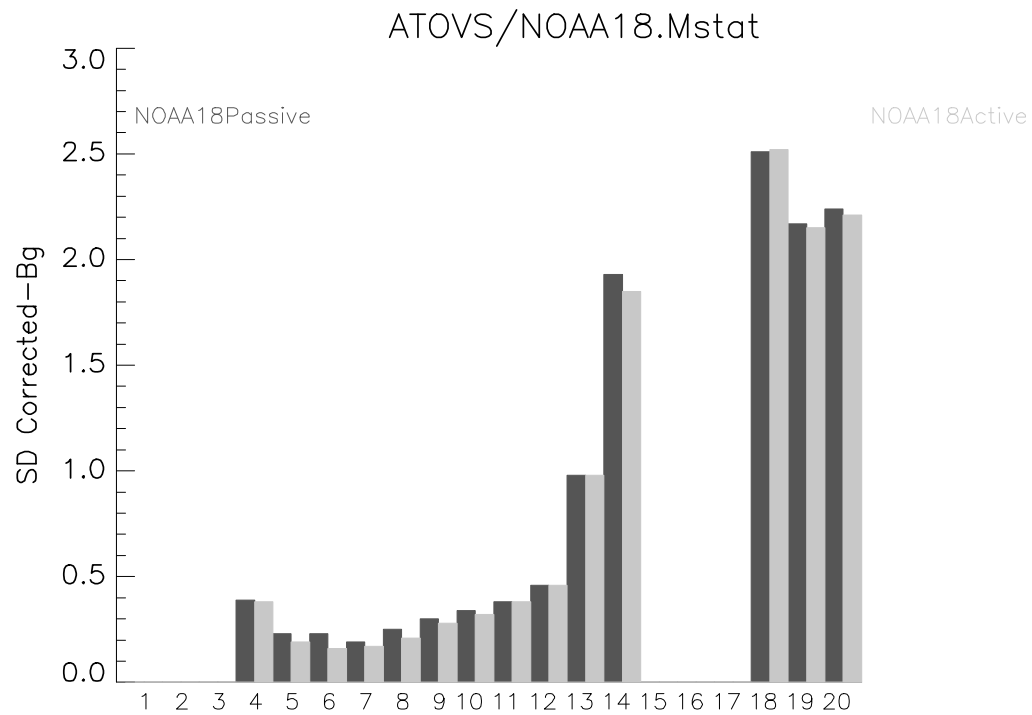


NOAA18 fit to short range forecast



Black – Control run

Grey – NOAA18 assimilated

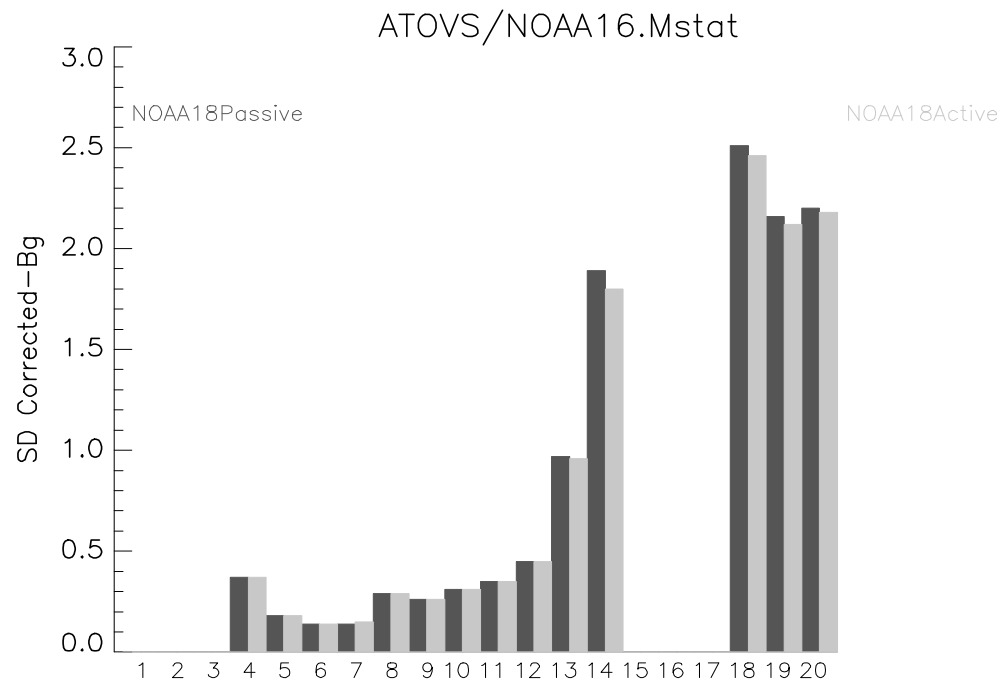


NOAA16 fit to short range forecast



Black – Control run

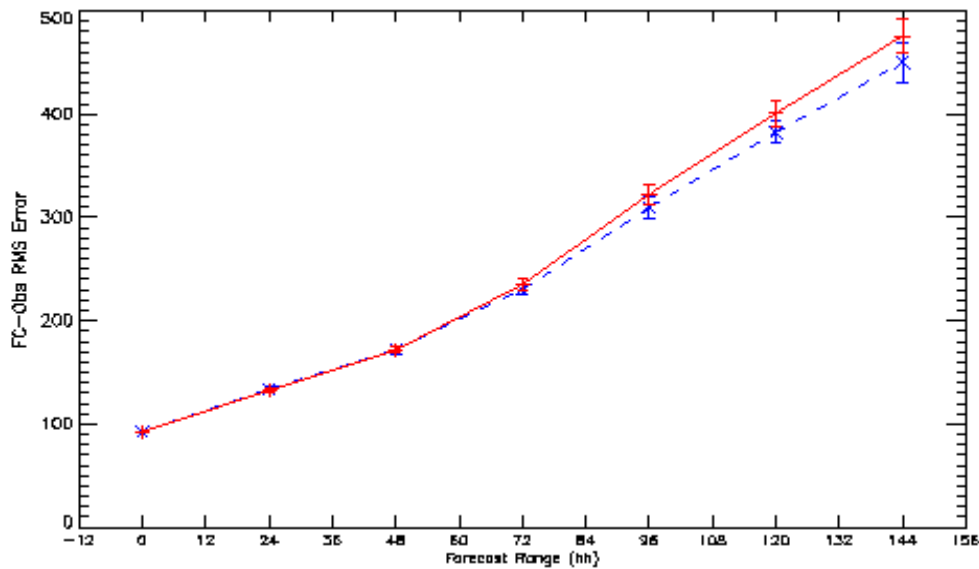
Grey – NOAA18 assimilated



Northern Hemisphere: Main impact is in PMSL



Red: Control Blue: Exp

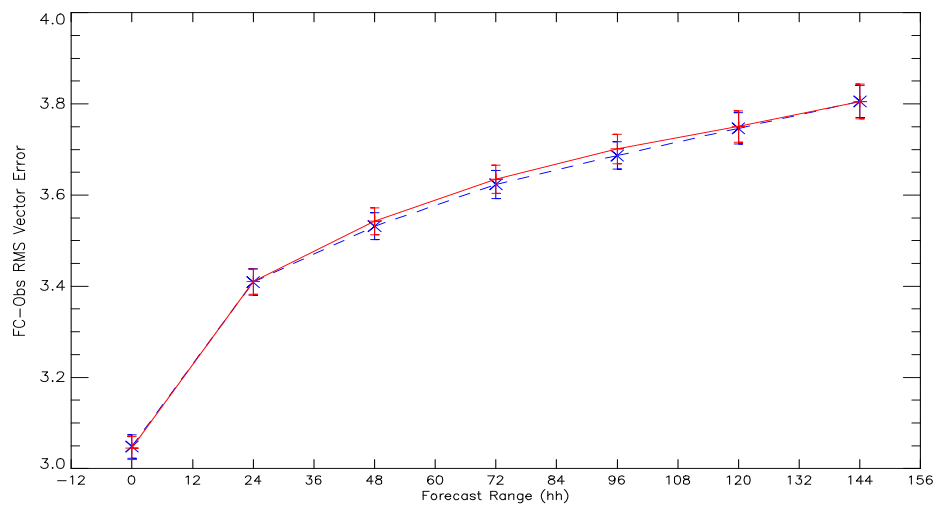


Overall: 16 parameters improved, 101 neutral, 6 worsened

Tropics: ~Neutral for surface winds



Red: Control Blue: Exp

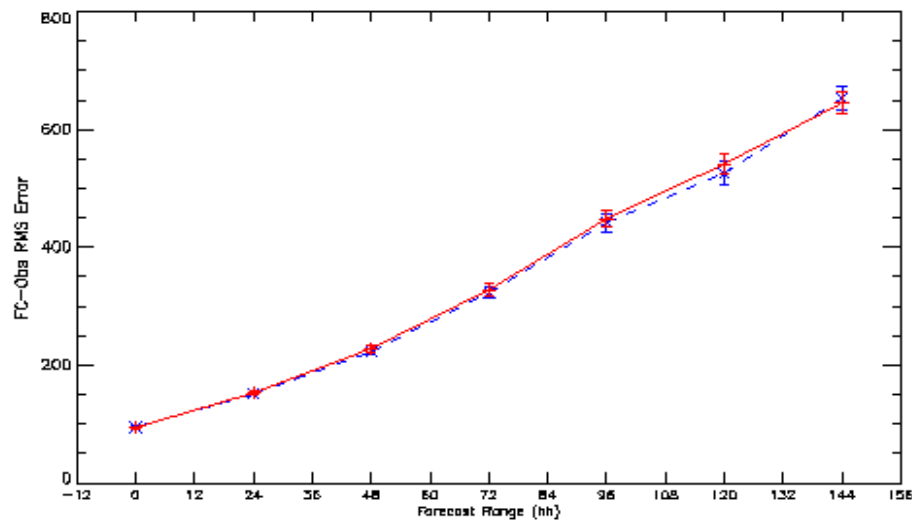


Overall: 14 parameters improved, 106 neutral, 3 worsened

Southern Hemisphere: Main impact is again in PMSL



Red: Control Blue: Exp

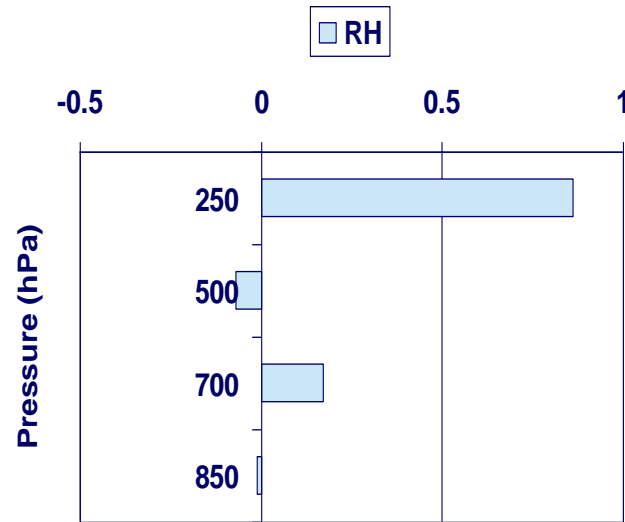
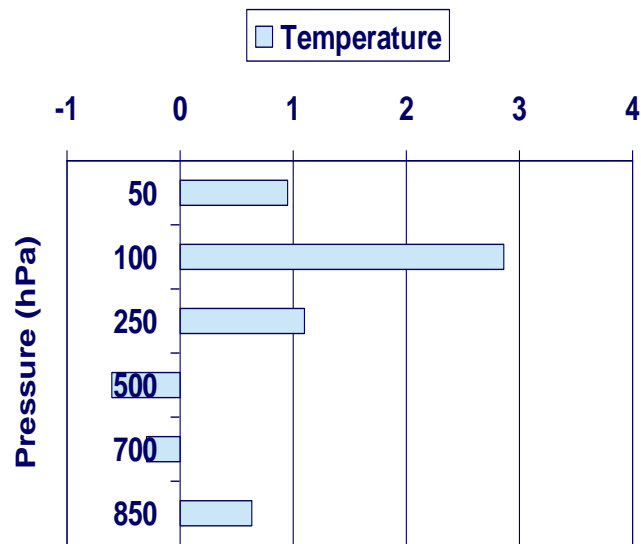


Overall: 26 parameters improved, 83 neutral, 14 worsened

Global T+6 fit comparisons using Sondes



% Improvement to RMS fit

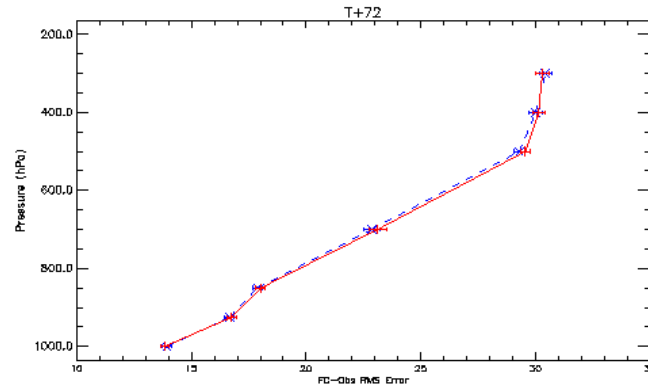


Verification of the moisture forecasts

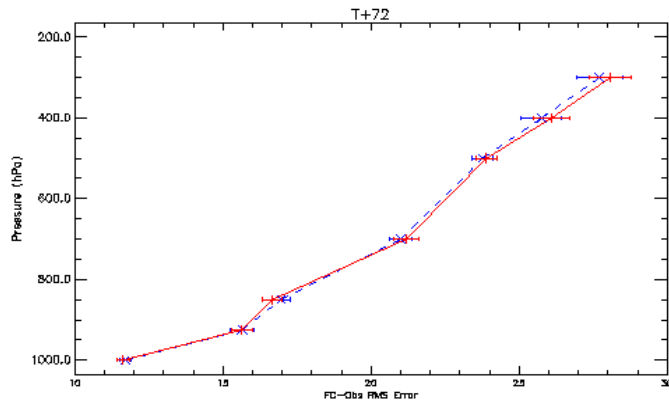
Red: Control Blue: Exp



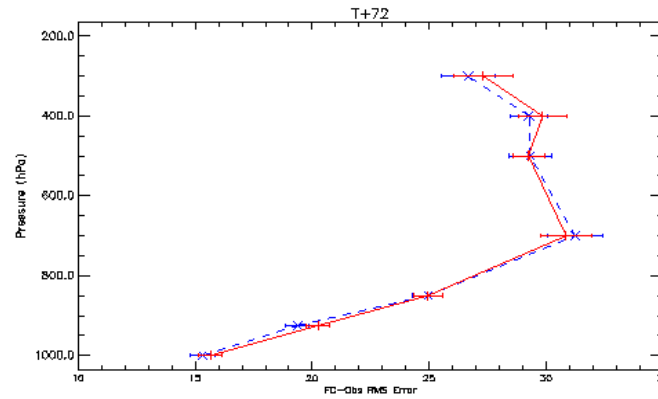
NH



Tropics



SH



Conclusions



- Forecast impacts due to the switch over from Aqua to Noaa18 are very encouraging. Part of this improvement is probably due to more data arriving in time for the main runs
- NOAA18 is now in our parallel suite with the expectation of operational assimilation from 9th August
- Use of N18 data in regional models expected from Autumn

- NESDIS 98 NOAA-L and NOAA-M AMSU-A Antenna Pattern Corrections. Tsan Mo, August 2000.**
- NESDIS 99 The Use of Water Vapor for Detecting Environments that Lead to Convectively Produced Heavy Precipitation and Flash Floods. Rod Scofield, Gilberto Vicente, and Mike Hodges, September 2000.**
- NESDIS 100 The Resolving Power of a Single Exact-Repeat Altimetric Satellite or a Coordinated Constellation of Satellites: The Definitive Answer and Data Compression. Chang-Kou Tai, April 2001.**
- NESDIS 101 Evolution of the Weather Satellite Program in the U.S. Department of Commerce - A Brief Outline. P. Krishna Rao, July 2001.**
- NESDIS 102 NOAA Operational Sounding Products From Advanced-TOVS Polar Orbiting Environmental Satellites. Anthony L. Reale, August 2001.**
- NESDIS 103 GOES-11 Imager and Sounder Radiance and Product Validations for the GOES-11 Science Test. Jaime M. Daniels and Timothy J. Schmit, August 2001.**
- NESDIS 104 Summary of the NOAA/NESDIS Workshop on Development of a Coordinated Coral Reef Research and Monitoring Program. Jill E. Meyer and H. Lee Dantzler, August 2001.**
- NESDIS 105 Validation of SSM/I and AMSU Derived Tropical Rainfall Potential (TRaP) During the 2001 Atlantic Hurricane Season. Ralph Ferraro, Paul Pellegrino, Sheldon Kusselson, Michael Turk, and Stan Kidder, August 2002.**
- NESDIS 106 Calibration of the Advanced Microwave Sounding Unit-A Radiometers for NOAA-N and NOAA-N=. Tsan Mo, September 2002.**
- NESDIS 107 NOAA Operational Sounding Products for Advanced-TOVS: 2002. Anthony L. Reale, Micheal W. Chalfant, Americo S. Allergrino, Franklin H. Tilley, Michael P. Ferguson, and Michael E. Pettey, December 2002.**
- NESDIS 108 Analytic Formulas for the Aliasing of Sea Level Sampled by a Single Exact-Repeat Altimetric Satellite or a Coordinated Constellation of Satellites. Chang-Kou Tai, November 2002.**
- NESDIS 109 Description of the System to Nowcast Salinity, Temperature and Sea nettle (*Chrysaora quinquecirrha*) Presence in Chesapeake Bay Using the Curvilinear Hydrodynamics in 3-Dimensions (CH3D) Model. Zhen Li, Thomas F. Gross, and Christopher W. Brown, December 2002.**
- NESDIS 110 An Algorithm for Correction of Navigation Errors in AMSU-A Data. Seiichiro Kigawa and Michael P. Weinreb, December 2002.**
- NESDIS 111 An Algorithm for Correction of Lunar Contamination in AMSU-A Data. Seiichiro Kigawa and Tsan Mo, December 2002.**
- NESDIS 112 Sampling Errors of the Global Mean Sea Level Derived from Topex/Poseidon Altimetry. Chang-Kou Tai and Carl Wagner, December 2002.**
- NESDIS 113 Proceedings of the International GODAR Review Meeting: Abstracts. Sponsors: Intergovernmental Oceanographic Commission, U.S. National Oceanic and Atmospheric Administration, and the European Community, May 2003.**
- NESDIS 114 Satellite Rainfall Estimation Over South America: Evaluation of Two Major Events. Daniel A. Vila, Roderick A. Scofield, Robert J. Kuligowski, and J. Clay Davenport, May 2003.**
- NESDIS 115 Imager and Sounder Radiance and Product Validations for the GOES-12 Science Test. Donald W. Hillger, Timothy J. Schmit, and Jamie M. Daniels, September 2003.**
- NESDIS 116 Microwave Humidity Sounder Calibration Algorithm. Tsan Mo and Kenneth Jarva,**

October 2004.

NOAA SCIENTIFIC AND TECHNICAL PUBLICATIONS

The National Oceanic and Atmospheric Administration was established as part of the Department of Commerce on October 3, 1970. The mission responsibilities of NOAA are to assess the socioeconomic impact of natural and technological changes in the environment and to monitor and predict the state of the solid Earth, the oceans and their living resources, the atmosphere, and the space environment of the Earth.

The major components of NOAA regularly produce various types of scientific and technical information in the following types of publications

PROFESSIONAL PAPERS - Important definitive research results, major techniques, and special investigations.

CONTRACT AND GRANT REPORTS - Reports prepared by contractors or grantees under NOAA sponsorship.

ATLAS - Presentation of analyzed data generally in the form of maps showing distribution of rainfall, chemical and physical conditions of oceans and atmosphere, distribution of fishes and marine mammals, ionospheric conditions, etc.

TECHNICAL SERVICE PUBLICATIONS - Reports containing data, observations, instructions, etc. A partial listing includes data serials; prediction and outlook periodicals; technical manuals, training papers, planning reports, and information serials; and miscellaneous technical publications.

TECHNICAL REPORTS - Journal quality with extensive details, mathematical developments, or data listings.

TECHNICAL MEMORANDUMS - Reports of preliminary, partial, or negative research or technology results, interim instructions, and the like.



**U.S. DEPARTMENT OF COMMERCE
National Oceanic and Atmospheric Administration
National Environmental Satellite, Data, and Information Service
Washington, D.C. 20233**